PNNL-14898

Pacific Northwest
National Laboratory
Operated by Battelle for the
U.S. Department of Energy

Results of Groundwater Modeling for Tritium Tracking at the Hanford Site 200 Area State-Approved Land Disposal Site – 2004

D. B. Barnett
M. P. Bergeron
E. J. Freeman

September 2004

Prepared for the U.S. Department of Energy
under Contract DE-AC06-76RL01830

PACIFIC NORTHWEST NATIONAL LABORATORY
operated by
BATTELLE
for the
UNITED STATES DEPARTMENT OF ENERGY
under Contract DE-AC06-76RL01830

PNNL-14898

Results of Groundwater Modeling for Tritium Tracking at the Hanford Site 200 Area State-Approved Land Disposal Site – 2004

D. B. Barnett
M. P. Bergeron
E. J. Freeman

September 2004

Prepared for
the U.S. Department of Energy
under Contract DE-AC06-76RL01830

Pacific Northwest National Laboratory
Richland, Washington 99352

Summary

The purpose of this report is to present the results of the latest assessment of the impacts of treated water from the Hanford Site 200 Area Effluent Treatment Facility (ETF) that is currently being discharged and predicted to be discharged in the future to the drain field named the State-Approved Land Disposal Site (SALDS). The SALDS facility is located immediately north of 200-West Area in the Central Plateau of the Hanford Site in southeast Washington.

The objectives of this updated assessment are to:

- Incorporate up-to-date historical discharge and groundwater monitoring data (hydraulic head) into the current Hanford Site-Wide groundwater flow and transport model (from SALDS and adjoining areas).
- Incorporate the most recent and accurate projections of future tritium disposal and water discharge volume to the SALDS.
- Predict the lateral and vertical extent of travel in the subsurface of the tritium plume emanating from the SALDS
- Predict the activities of tritium at various locations within the plume.
- Provide improved sequential illustrations of predicted tritium plume behavior from present through the year 2140.
- Recommend strategies for future monitoring based on model results.

The numerical model used for this effort is revised from that used by Barnett et al. (1997) to reflect recent refinements in the Hanford Site-Wide Groundwater Model (SGM) and to incorporate actual water volume and tritium activity release information reported through June 2004. Simulations made in this assessment consider the hydraulic effect of past historical waste water discharges in the unconfined aquifer but only evaluates the potential impacts of tritium loading from past and projected future tritium discharges at the SALDS facility. Potential impacts of other sources of groundwater contamination for other nearby source areas are not considered in this analysis.

This report presents a comparison of updated treated water discharges and tritium inventory values based on discharge records to the SALDS from its startup in 1995 through 2004 with projected values used in previous modeling summarized Barnett et al. (1997). This comparison shows that while actual discharge volumes through June 2004 exceeded projections made in previous modeling efforts, actual cumulative tritium inventories contained in discharges to the facility have been about one-half of inventories projected in previous analysis through the current year (2004).

The model results presented in this report incorporate the reported data through June 2004, and then uses projected discharge and tritium inventory values through 2034 that have been updated with more current information. Simulation results show that the tritium concentration in the aquifer reaching a maximum of 1.6 million pCi/L in 1996. After that time, predicted concentration levels at the water table were variable ranging from just over 1 million to several hundred thousand pCi/L and on a downward trend by the year 2004. These simulated results generally reflect the changes in simulated monthly effluent discharges and tritium inventories discharged to the aquifer in the model analysis. These results are also generally consistent with tritium concentration levels and trends that have been observed in well 699-48-77A, the well south of the SALDS facility that is the first well impacted by SALDS operations.

Accounting for the differences between the smaller actual facility discharges and those projected in previous modeling, the updated 2004 model was generally consistent with previous estimates made with the 1997 model with regard to plume behavior. Concentrations for the updated model did not reach levels projected in the 1997 model and the plume did not extend as far out as was estimated in previous modeling. However because of the increase in tritium inventory in the updated projections from effluents originating from the Waste Treatment Plant and supplemental low-level treatment facilities, estimated tritium concentration levels beyond the year 2004 were projected to be much larger and to remain longer in the aquifer than was estimated in previous modeling efforts. Concentration levels resulting from increased tritium inventories starting in the year 2009 will increase from about 300,000 to 400,000 pCi/L before reaching maximum concentrations of just over 3 million pCi/L at the end of operation. Previous modeling had suggested that tritium concentration levels would drop below 500 pCi/L by the 2090. With updated increase in future tritium inventories in the current projections, modeled results suggest that tritium concentration levels would not drop below the 500 pCi/L level until about the year 2140.

Modeling results suggest that the current network, which consists of 3 proximal monitoring wells and (currently) 12 tritium tracking wells, will continue to provide adequate coverage for tracking the impacts from tritium in effluent from the SALDS facility. Current predictions suggest that concentration levels of 500 pCi/L may potentially arrive at well 699-51-75P within the next 5 to 10 years. Once discharges cease on 2034, simulations show that the plume will not likely grow much beyond the area of the this observation well as a result of continued plume dispersion and tritium decay.

Current recommendations are to continue groundwater level monitoring and tritium sampling at the current level of effort. Current monitoring and predictions of future plume migration with past and projected estimates of effluent volumes and tritium inventory suggest that adding additional monitoring wells at this time will not necessarily improve the effectiveness of the existing monitoring network to monitor the effect of current and projected effluents at the SALDS facility.

Estimated water table projections also suggest that careful monitoring of some of the current monitoring wells is needed as the water table continues to decline to more natural conditions. Wells that may be particularly vulnerable include those along the northern boundary of 200-West Area. Another well that could be vulnerable is one of the proximal observation wells, 699-48-77A. This well should continue to be functional through the end of facility operations but could be vulnerable if effluent discharges are less than volumes in current projects. Both wells in question are located south of the SALDS.

Acronyms and Abbreviations

AFPM	Aquifer Porous Media
BHI	Bechtel Hanford, Inc.
CFEST	Coupled Fluid, Energy, and Solute Transport
Ci	curie
DGI	Dynamic Graphics Inc.
DMR	Discharge Monitoring Report
DWS	Drinking Water Standard
ETF	Hanford Site 200 Area Effluent Treatment Facility
FY	fiscal year
K/Ar	Potassium/Argon isotope ratios
Ka	thousand years before present
LLBG	low-level burial ground
Ma	million years before present
MDA	minimum detectable activity
MDL	method detection limit
SAC	System Assessment Capability
SALDS	200 Area State-Approved Land Disposal Site
SGM	Sitewide Groundwater Model
SOLTR	Solute Transport
STOMP	Subsurface Transport Over Multiple Phases
TDS	total dissolved solids
UCODE	Universal Inverse-Modeling Code
VZDROP	Vadose Zone Data Restructure for Other Programs
WIDS	Waste Information Data System

Contents

Figures

Tables

1.0 Introduction

Treated water from the Hanford Site 200 Area Effluent Treatment Facility (ETF) is discharged to a drain field as allowed by State Waste Discharge Permit ST-4500 (ST-4500; Ecology 2000). The permit allows disposal of tritium to the drain field, named the State-Approved Land Disposal Site (SALDS), which is located immediately north of the 200-West Area of the Hanford Site on the Central Plateau (Figure 1). Tritium is discharged to the ground at SALDS because no known, economically reasonable method of removal has been identified. A relatively benign radionuclide, tritium has a half life of only 12.3 years.

As a condition of Permit ST-4500, a numerical groundwater model is applied to the SALDS at least once every permit cycle (5 years). The primary reason for modeling is to determine if tritium discharges from SALDS could reach the Columbia River and therefore pose a possible threat to human and ecological health in the region. Earlier models (see Section 4.1) suggested that some tritium from SALDS could reach the Columbia River in quantifiable amounts, but the most recent model (Barnett et al. 1997) showed that tritium did not leave the immediate vicinity of the SALDS. The most recent groundwater monitoring results (Barnett et al. 2003) support this prediction.

1.1 Objectives and Scope

The purpose of this report is to present the results of the latest application of a refined groundwater model to the SALDS based on the updated Systems Assessment Capability (SAC) tool (Bryce et al. 2002). Within this intent are the additional objectives to:

- Incorporate the most recent and accurate projections of future tritium disposal and water discharge volume to the SALDS.
- Incorporate up-to-date historical discharge and groundwater monitoring data (hydraulic head) into the model (from SALDS and adjoining areas).
- Predict the lateral and vertical extent of travel in the subsurface of the tritium plume emanating from the SALDS.
- Predict the activities of tritium at various locations within the plume.
- Provide improved sequential illustrations of predicted tritium plume behavior from present through the year 2140.
- Recommend strategies for future monitoring based on model results.

Along with continued groundwater monitoring at SALDS, accomplishment of these tasks will enhance the protection of groundwater and the Columbia River where the SALDS is concerned. The model run provided here is focused on the SALDS facility and its affect on the surrounding subsurface.

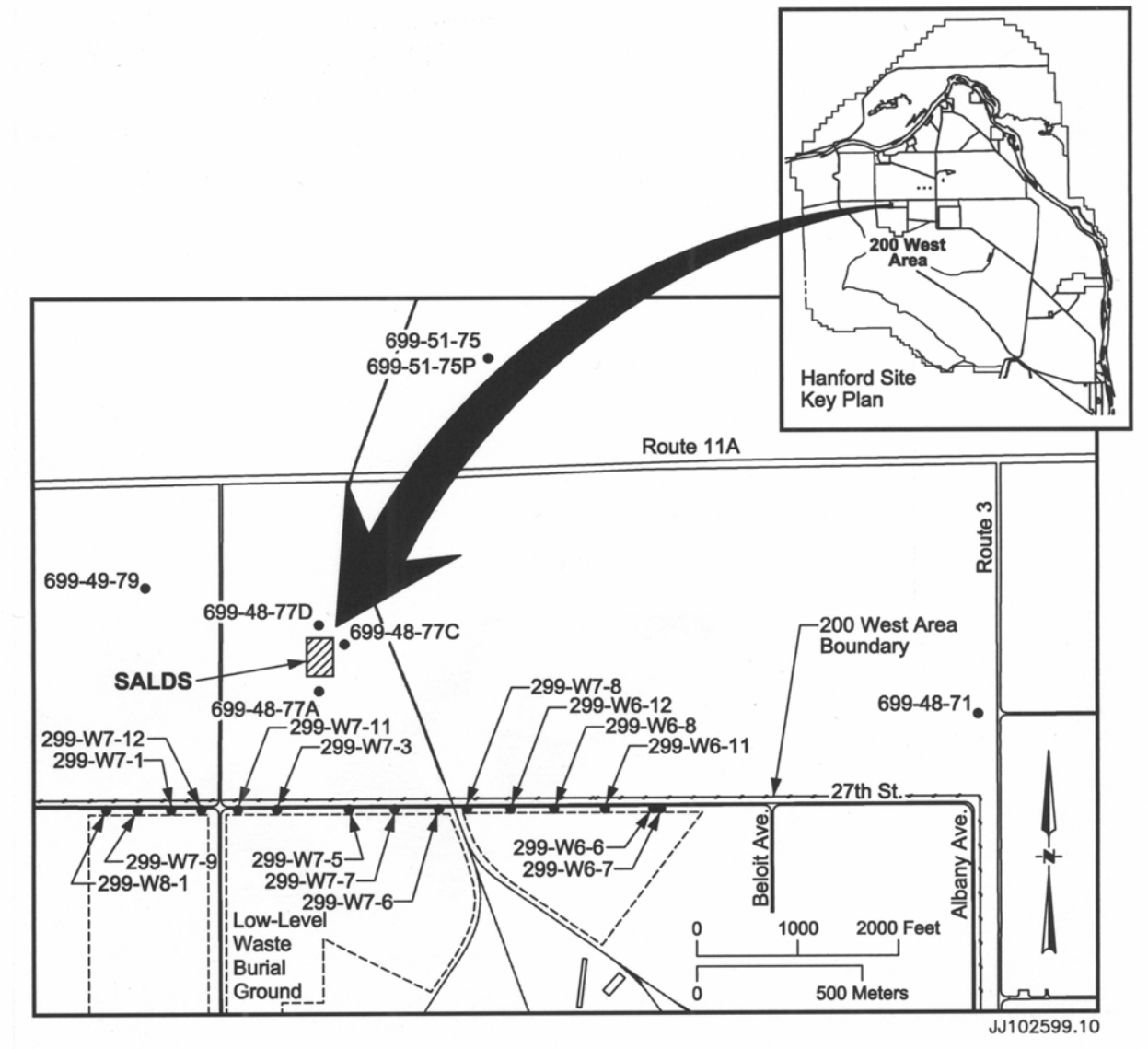

Figure 1. Location of the SALDS on the Hanford Site Showing all Wells That Have Been a Part of the SALDS Groundwater Monitoring and Tritium-Tracking Well Network. Due to declining regional water levels and subsequent drying of some wells, the number of wells in the tritium-tracking network has been reduced to 12 (see Barnett et al. 2003).

No attempt is made to provide an update of the entire Hanford Site, only those areas that are predicted to influence or be influenced by the SALDS. An updated conceptual model is also derived to provide a basis for numerical model refinement and to understand model behavior and the implications for any future groundwater monitoring for the SALDS.

1.2 Background

A Washington State Waste Discharge Permit (ST-4500) was granted for the SALDS in June 1995, and the facility began receiving effluent in December 1995. In January 1996, the *Groundwater Screening Evaluation/Monitoring Plan – 200 Area Effluent Treatment Facility (Project C-018H)* (Davis et al. 1996) was issued to: 1) summarize the hydrogeologic setting, 2) describe pre-operational groundwater monitoring results at the SALDS, 3) provide plans for continued groundwater monitoring for non-radiological constituents, and 4) establish a plan for monitoring and tracking of tritium entering groundwater from the facility. Also included in the 1996 document are plans for updating a numerical model for prediction of groundwater flow and tritium transport.

In 1997, a revised numerical groundwater model was developed to predict the pattern and rate of tritium migration in groundwater as it is discharged to the SALDS. The relevant predictions of this model and an evaluation of groundwater monitoring results through 1996 were presented in Barnett et al. (1997). A comparison of these predictions with actual conditions through early 2004 is presented in Section 4.1. The 1997 report also described results of previous groundwater numerical models for the SALDS.

Tritium originating from the SALDS was first detected in groundwater in July 1996 in well 699-48-77A, a well originally intended to serve as an upgradient background well, and which is most distant from the facility in the original SALDS network (see Section 3.2). Tritium appeared in wells closer to the facility at a later time. The probable reasons for this circumstance are related to hydro-geologic peculiarities beneath the facility, and are discussed in Section 3.0.

The current list of analytical parameters and constituents for groundwater monitoring at the SALDS proximal wells (699-48-77A, 699-48-77C, and 699-48-77D) was established by Davis et al. (1996), and is included in ST-4500. For a few years, well 299-W8-1 was used as an upgradient well in default of 699-48-77A. The same constituent list was applied to this well as in the other three SALDS proximal wells until it was realized that 299-W8-1 was not actually upgradient of the facility. All three proximal wells have been sampled quarterly since the sample program began. The only change to the original permit constituents list was effected in 1997, when it was discovered that natural soil chemistry was elevating sulfate and a few other parameters in groundwater, as the clean effluent infiltrated through the vadose zone (see Section 3.0). The enforcement limit for sulfate was raised from 30,000 to 250,000 μg/L to compensate for this condition.

Since the SALDS groundwater monitoring began in 1995, seven of the tritium-tracking wells to the south of the facility have become dry or unusable. This southern array of wells was selected not as upgradient monitoring points (as they have sometimes been mistakenly labeled), but to resolve the influence of the SALDS tritium from the tritium plume emanating from the northeast corner of the 200-West Area. As more of these wells become dry, the ability to differentiate between these two tritium sources may be impaired, but downgradient detection of SALDS tritium should be unaffected.

1.2.1 Permit Requirements

Permit ST-4500 requires an updated numerical groundwater model run at least once during a permit cycle (every 5 years) to predict tritium movement and distribution in the aquifer resulting from SALDS discharges. The permit also requires that the model be reapplied "within 6 months of detection of the tritium plume in a new monitoring well." This requirement indicates that the numerical model will be reapplied when the tritium plume associated with the SALDS is positively identified in a location not predicted by the most recent model run, or within a well not previously affected by an incursion of SALDS-derived tritium.

As of this writing, no conclusive evidence exists that the tritium plume from the SALDS has reached any wells beyond the three proximal wells. Well 299-W7-1 has produced very infrequent detections of tritium, and those have all been near the minimum detectable activities (MDAs). Results in FY 2003 (Barnett et al. 2003) in this well produced one non-detect and one barely above detection (334 pCi/L in March 2003). Scattered results barely above MDAs are observed in other wells near well 299-W7-1 (e.g., see Hartman et al. 2003), but there are no known plumes affecting the immediate area of this well.

Well 299-W7-5 has produced detectable tritium results sporadically since 1988. Some of the detections from this well may be false because of large counting errors, or they may be actual detections of the decaying plume originating from the 200-West Area. The results from this well in the February 2003 sampling event were above detection, but below the maximum results for FY 2002. Subsequent results through March 2004 have not produced detections. Because of its location and history, it is premature to conclude that tritium in this well is from SALDS or the existing plume in the 200-West Area.

2.0 SALDS Operational History and Future Projections

Figures 2 and 3 illustrate the pattern of discharge and tritium inventory for the SALDS effluent since operations began in 1995. From December 1995 through February of 2004, over 675 M liters (178 M gal) of water have been discharged to the SALDS. During the same time period approximately 340 Ci of tritium were disposed to the site. The pattern of discharge volume has been relatively constant when the entire period of SALDS operation is considered, with intra-annual discharges usually peaking in late year (corresponding to ETF campaigns to treat 242-A Evaporator process condensate), with a conspicuous exception during 1996-1997 when a hiatus in evaporator streams occurred.

Table A.1 (Appendix A) lists current and anticipated future sources of waste water to be treated by the ETF. Historically, the 242-A Evaporator process condensate has been, by far, the single most important source of tritium to the ETF and SALDS. In updated projections made in 2004, the dominant source of new effluents will originate from liquid effluents treated at the ETF from the Waste Treatment Plant and supplemental low-level treatment facilities between years 2009 and 2030. These effluents are expected to account for about 63 percent of the total effluent and about 95 percent of total tritium inventory discharged to the SALDS facility between year 2004 and 2030.

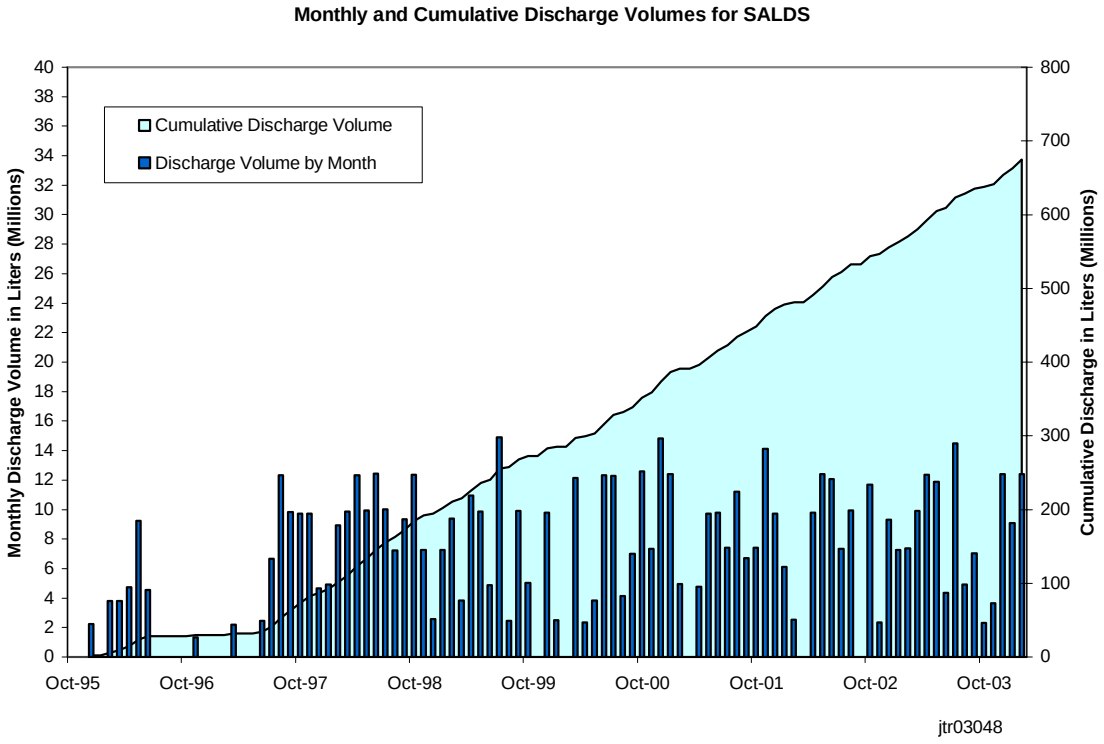

Figure 2. Monthly and Cumulative Volume Discharged to SALDS Facility – October 1995 through October 2003

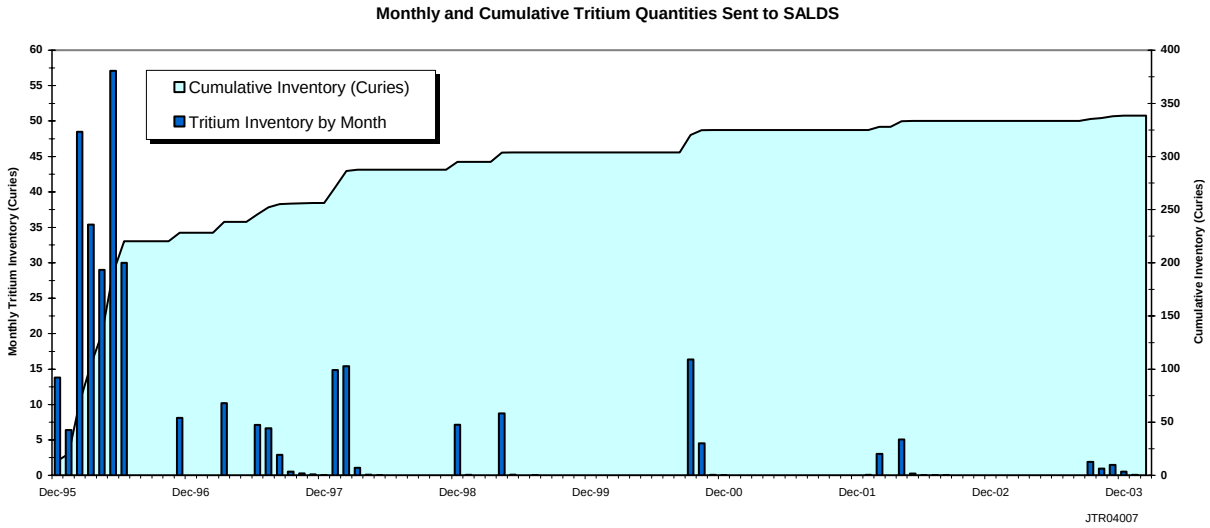

Figure 3. Monthly and Cumulative Tritum Inventory Discharged to SALDS Facility – October 1995 through October 2003

3.0 Hydrogeologic and Hydrogeochemical Setting of the SALDS

3.1 Stratigraphic Units

The general stratigraphy of the Hanford Site is illustrated in Figure 4. A generalized stratigraphic cross section from near Gable Butte, north of the SALDS, to south of the 200-West Area, along a north-south trend, is represented in Figure 5. The Elephant mountain member of the Columbia River basalt forms the base of the sedimentary sequence that host the uppermost aquifer on the Hanford Site. Approximately 150 m (500 ft) of continental sediments overlies basalt. From oldest to youngest these deposits are:

- Facies and members of the Miocene-to-Pliocene age, fluvial-lacustrine Ringold Formation
- Variably cemented (some thick caliche horizons) and pedogenically altered deposits of the Cold Creek Unit, which developed on the eroded and weathered surface of the Ringold Formation
- Largely unconsolidated, fine-grained silty to sand, gravel and occasional silt units, designated the Hanford formation derived from Pleistocene-age cataclysmic floods
- A relative thin veneer of Holocene dune sand

3.1.1 Columbia River Basalt Group

The surface of the Columbia River Basalt Group (CRBG) forms the bedrock base of the aquifer beneath the SALDS. There are a minimum of 50 basalt flows beneath the Hanford Site with a combined thickness of >3,000 m (10,000 ft) (DOE 1988). The Elephant Mountain Member of the Saddle Mountains Basalt, the youngest flow in the area, lies about 150 m (500 feet) below land surface. The Elephant Mountain Member it is about 25-27 m (80-90 ft) thick in the 200-West Area (Reidel and Fecht 1981) and the top of this unit dips gently southwest about 0.7 degrees.

3.1.2 Ringold Formation

The Ringold Formation is a fluvial-lacustrine deposit associated with the ancestral Columbia River drainage system, following the last eruption of basalt at the Hanford Site about 10.5 million years ago (Tallman et al. 1981; DOE 1988; Lindsey et al. 1994b; Lindsey 1996). Deformation of the Yakima folds, which began in the middle Miocene Epoch, concurrent with the Columbia River basalt volcanism, continued into Ringold time so the centers of down warped basins received more sediments than the margins.

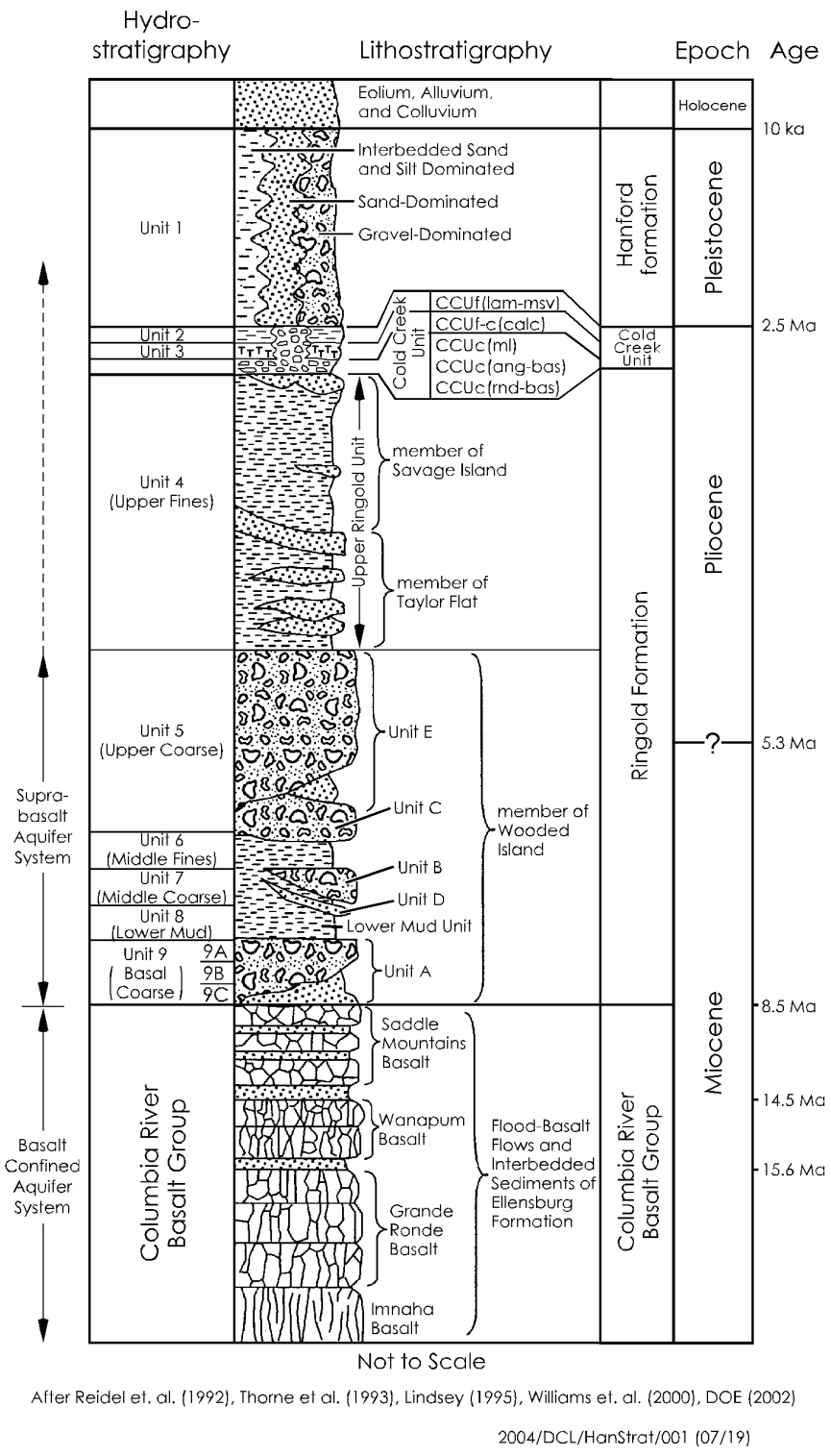

Figure 4. General Stratigraphy of the Hanford Site. Unit numbers referenced in the SALDS hydrostratigraphic conceptual model (see Section 4.3.2) are shown in the left hand column of the chart.

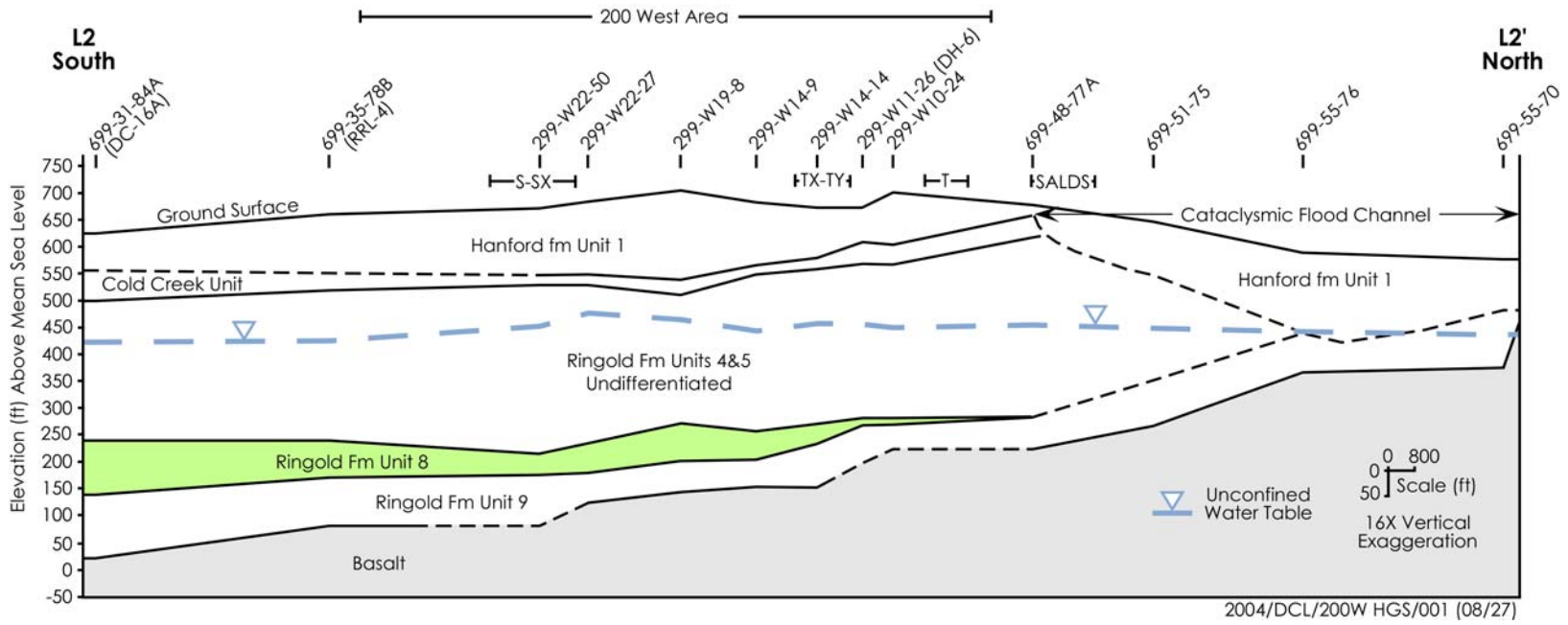

Figure 5. General Cross Section of Stratigraphy in the Vicinity of the SALDS. The blue dashed line is the approximate, average level of the water table in 2002. Dashed contacts between units indicate inferred locations (after Williams et al. 2002).

At the SALDS, the Ringold Formation accounts for ~84% (~119 m) of thickness of the suprabasalt strata beneath the SALDS. The top of the Ringold occurs approximately 19 m below land surface at this location. The dominant facies of the Ringold Formation beneath the SALDS are fluvial sand and gravel of the upper Ringold and units A and E, corresponding to units 5 and 9, respectively, of Thorne et al. (1994) (see Figure 4). These two units are elsewhere distinguished by the intervening Ringold lower mud unit. However, at the SALDS location this mud unit is absent, thus making the two similar A and E units difficult to differentiate. The Ringold Formation sediments are variably cemented at this location with calcium carbonate and probably other evaporite minerals (see Section 3.3.3). The structural trend of these strata appears to be concordant with that of the underlying basalt (i.e., dipping gently south).

3.1.3 Cold Creek Unit

The Cold Creek Unit (formerly Plio-Pleistocene Unit) lies uncomformably on the tilted and truncated Ringold Formation. Several different facies comprise the Cold Creek Unit at the Hanford Site, including (1) pedogenic calcrete (i.e., carbonate-cemented paleosol), (2) sidestream-alluvium, (3) coarse-grained mainstream-alluvium (Bjornstad 1984; DOE 1988; Lindsey et al. 1994b; Slate 2000; Wood et al. 2000; DOE 2002), and (4) a silt-rich alluvial and/or eolian facies (Lindsey et al. 1994b; Wood et al. 2000). Neither the mainstream alluvial facies of the Cold Creek Unit, also referred to as pre-Missoula gravels, nor the sidestream alluvial facies are present beneath the or SALDS. The calcrete facies of the Cold Creek Unit, also referred to as the “caliche layer,” and is locally a significant impediment to infiltration.

The thickness and degree of calcic-soil development within the Cold Creek Unit calcrete varies laterally. In some locations a single, thin (1 meter or less) well-cemented horizon is all that is present. Elsewhere, multiple carbonate-rich horizons, an indication many periods of soil development, occur locally. These horizons are separated by relatively non-calcareous, uncemented sand, silt or locally derived basaltic gravel.

The Cold Creek Unit is ~16 m thick beneath the SALDS. The top of the unit is encountered at only 2 m (6 ft) below the surface in well 699-48-77D, and, like the basalt surface, dips gently to the south. The Cold Creek Unit is typically silt, sand, and local basaltic gravel, with abundant carbonate cement and local caliche layers. Lindsey and Reidel (1992) describe this unit as occurring discontinuously throughout much of the 200-West Area. Lindsey et al. (1994a) state that it is continuous beneath the LLBG immediately south of the SALDS, but add that considerable variability exists in carbonate cementation and degree of caliche development at this location. The caliche of the Cold Creek Unit is a persistent feature in the 200-West Area, but varies considerably in thickness and degrees of development. From cored intervals of boreholes at the SALDS, Reidel and Thornton (1993) note a lack of “significant” caliche layers or calcrete zones in the Cold Creek Unit, with mostly thin (<0.5 cm) stringers of caliche present. Observations made by Swanson (1994) during the excavation of infiltration test holes near the SALDS also attest to the lateral variability in cementation and permeability of the Plio-Pleistocene unit at this site.

3.1.4 Hanford formation

In the vicinity of the SALDS, the Hanford formation is encountered at approximately 0.5 m below land surface, and is only 1.4 m thick near the northern edge of the facility, to 6.4 m thick near well

699-48-77A. However, as Figure 5 illustrates, the SALDS location is at the edge of a large, deep channel consisting of Hanford sand and gravel. Because of its permeable nature, and importance in transmitting groundwater, the major components of the Hanford formation are described in some detail here. The thin sequence of Hanford formation beneath the SALDS consists mostly of sandy gravel with only minor, discontinuous cementation. This sediment is very conducive to infiltration of effluent or meteoric water, particularly where vegetation is lacking.

The Hanford formation is the informal name given to all glacio-fluvial strata deposited from cataclysmic ice-age floods within the Pasco Basin (DOE 1988). Sources for floodwaters included Glacial Lake Missoula, Pluvial Lake Bonneville, and ice-margin lakes that formed around the margins of the Columbia Plateau (Baker et al. 1991). Cataclysmic floods were released during at least four major glacial events that occurred between about 1 Ma and 13 Ka (early to late Pleistocene time). The Hanford formation consists predominantly of unconsolidated sediments that cover a wide range in grain size from pebble- to boulder-gravel, fine- to coarse-grained sand, silty sand, and silt. The Hanford formation is further subdivided into a gravel-, sand-, and silt-dominated facies. Gravel-, sand-, and silt-dominated facies are also referred to as the coarse-grained, transitional, and rhythmite facies, respectively, of the Hanford formation (Baker et al. 1991). Facies of the Hanford formation are commonly described as laterally interfingering. The relative proportion of each facies at any given location is related to distance from main, high-energy flood flows at the time of deposition.

1) GRAVEL-DOMINATED FACIES. This facies generally consists of coarse-grained basaltic sand and granule to boulder gravel. These deposits display an open framework texture, massive bedding, plane to low-angle bedding, and large-scale planar cross bedding in outcrop. Gravel-dominated beds sometimes grade upward into sand- and silt-dominated facies. Gravel clasts are dominantly basalt with lesser amounts of Ringold Formation clasts, granite, quartzite, and gneiss. The very small pebble size fraction of these deposits typically consists almost entirely of basalt. The gravel-dominated facies was deposited by high-energy floodwaters in or immediately adjacent to the main cataclysmic flood channel ways. This type of channel exists immediately north and west of the SALDS (see Figure 5).

2) SAND-DOMINATED FACIES. This facies consists of fine- to coarse-grained sand and granule-sized gravel. The coarser sands typically have high basalt content and are commonly referred to as black, gray, or “salt-and-pepper” sands. Finer sands can be more quartzo-feldspathic. The facies may contain small pebbles and rip-up clasts, pebble-gravel interbeds, and often grade upward into thin (<1 m) zones of silt-dominated facies. This facies also commonly displays plane lamination and bedding and less commonly channel cut-and-fill sequences. The sand-dominated facies was deposited adjacent to main flood channels during the waning stages of flooding. The facies is transitional between the gravel-dominated facies and the silt-dominated facies.

3) SILT-DOMINATED FACIES. This facies consists of thin-bedded, plane-laminated and ripple cross-laminated silt and fine- to coarse-grained sand. Beds are typically a few inches to several tens of inches thick and commonly display normally graded-bedding. Sediments of this facies were deposited under slack water conditions and in back-flooded areas (DOE 1988; Baker et al. 1991).

3.1.5 Holocene Deposits

Holocene (i.e., <8 Ka) deposits emplaced since the last floods are limited to recent windblown silt and sand. Subaerial dune sand occurs sporadically at the surface and is generally less than 1-2 m thick in the vicinity of the SALDS.

3.2 Groundwater Hydrology

The uppermost aquifer beneath the SALDS occurs within the Ringold Formation sand and gravels (units A and E). The current (March 2004) depth to groundwater beneath the SALDS is approximately 69 m (226 ft), and the lower boundary of the aquifer is formed by the Elephant Mountain Member Basalt at ~134 m (~433 ft). Thus, the aquifer is approximately 65 m (~207 ft) thick at this location. The water table surface in the vicinity of the SALDS for March 2004 is shown in Figure 6.

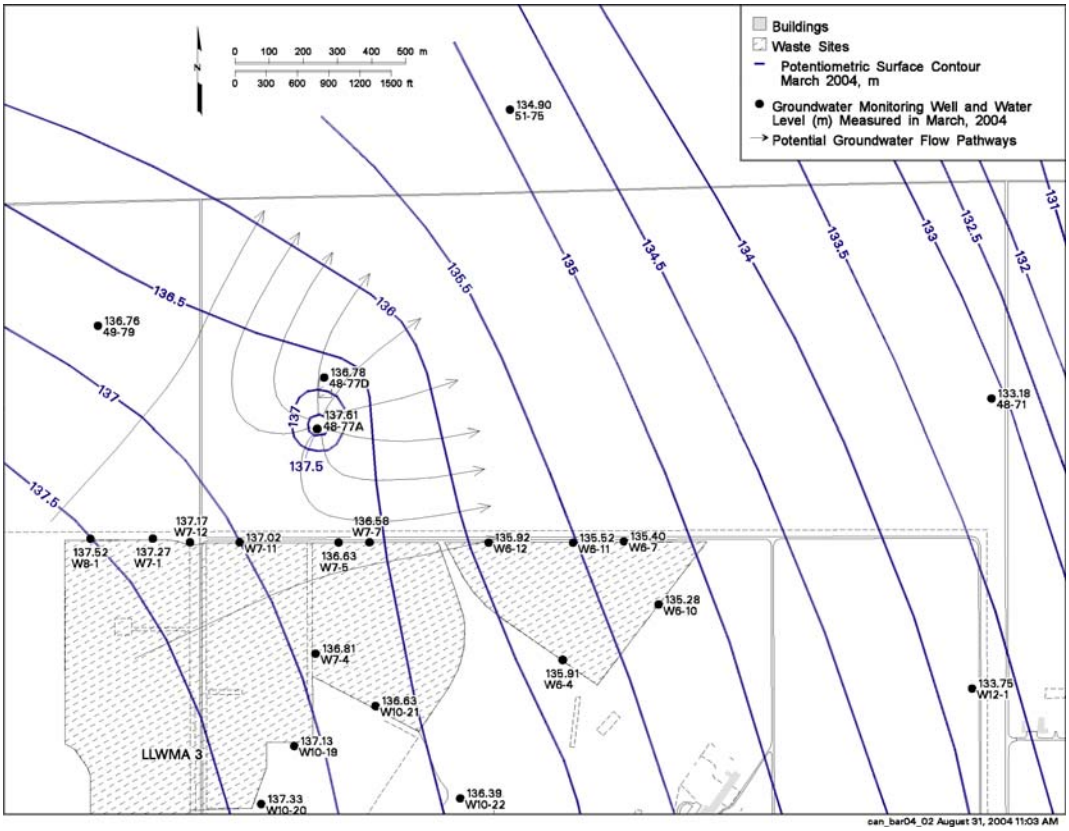

Figure 6. Water Table Map Near the SALDS for March 2004 Showing Interpreted Groundwater Flow Directions Around the SALDS

The saturated zone begins approximately 50 m below the upper contact of the Ringold Formation (within unit E). No identifiable confining layers have been recognized in this aquifer, but pumping tests suggest that it is partially and/or locally confined. Swanson (1994) identified the general locations of two of these layers within the aquifer. The aquifer is shown as divided roughly into three unequal layers

because of the semi-confining strata. The confinement may be the result of layers of cementation within the Ringold Formation. The horizontal component of hydraulic gradient in the general vicinity of the SALDS for March 2004 is approximately 0.002, but is probably significantly higher beneath the drain field during SALDS infiltration events.

The interpreted groundwater mound associated with the SALDS operation is shown near the facility based primarily on water levels measured in two of the SALDS proximal wells, 699-48-77A and 699-48-77D. The center of the mound is not necessarily located at well 699-48-77A; rather, this is an approximate location, with the actual center probably located somewhere between well 699-48-77A and the facility. Arrows denoting the interpreted flow paths (or the hydraulic potential for flow) of groundwater in the vicinity of the SALDS indicate that effluent from the SALDS could eventually affect wells to the south of the facility. Exactly how far south the effluent from SALDS could actually flow before turning east is not known. The interpretation of the hydraulic head distribution in Figure 6 indicates that wells 699-51-75, 699-51-75P, and 699-48-71 northeast and east of the SALDS are regionally downgradient of the facility, and are in appropriate horizontal locations for intercepting SALDS effluent. The interpreted flow direction near SALDS has acquired a slightly more easterly component in the past few years (compare Barnett et al. 2003 with Barnett 2000), perhaps as a result of the continuing regional decline in water levels combined with SALDS effects.

Vertically-separated well pairs to the southeast and northeast of the SALDS indicate that there is virtually no measurable vertical gradient within the uppermost aquifer in this area, away from the immediate vicinity of the SALDS. Hydrographs of wells 299-W6-7 and 299-W6-6 indicate a historical lack of significant vertical hydraulic potential in this area. Well 299-W6-6 is screened 52 m (172 ft) lower in the aquifer than well 299-W6-7. As expected, proximal SALDS wells (699-48-77A, 699-48-77C, and 699-48-77D) indicate a consistent downward-directed vertical gradient near the facility as a result of SALDS discharges (Figure 7). The higher head in well 699-48-77A suggests that infiltration of effluent to groundwater (mounding) from the SALDS is occurring closer to this well than well 699-48-77D. Both 699-48-77A and 699-48-77D are screened at the water table; 699-48-77C is screened ~20 m below the water table.

3.3 Groundwater Chemistry and Monitoring Results

The first list of groundwater analytes was derived as part of an evaluation of several potential SALDS locations (Harris and Delaney 1991). This list (see Barnett 2000) was applied to well 699-48-77A immediately after it was drilled in 1992 to gather “pre-facility baseline data.” The list was applied through June 1993, whereupon a revised constituent list was adopted (Reidel 1993) that was later

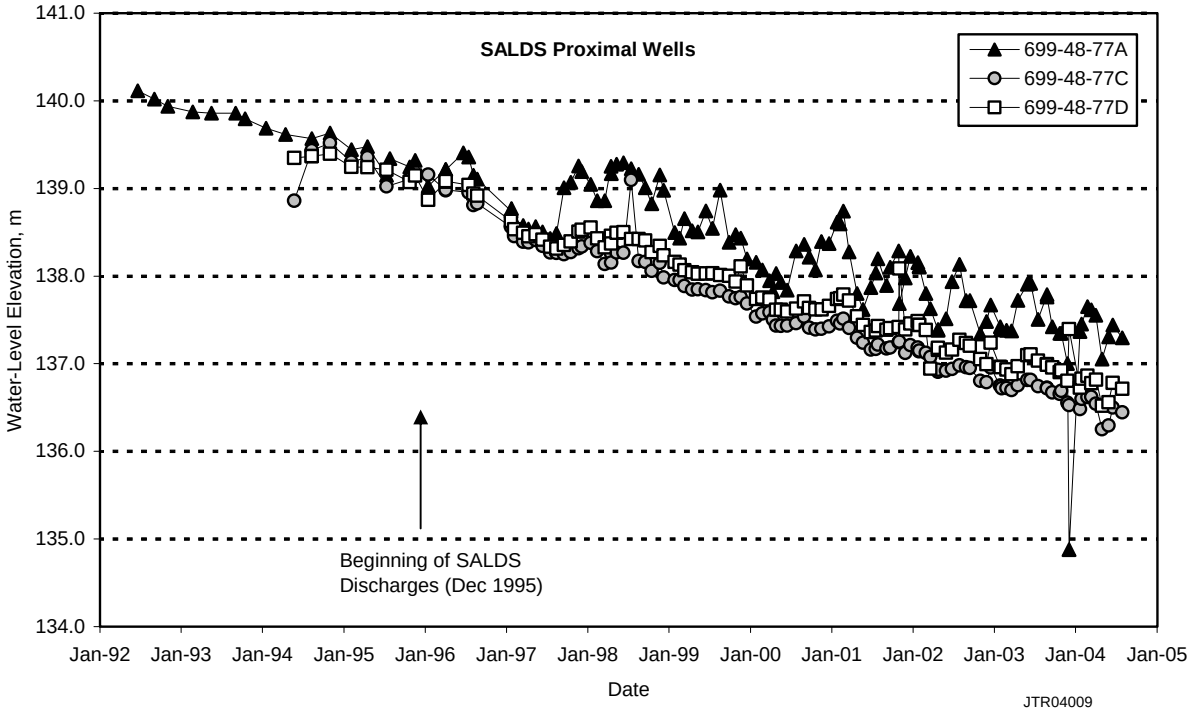

Figure 7. Hydrograph of SALDS Wells

applied to the other two SALDS proximal wells (699-48-77C and 699-48-77D) drilled in 1994. Both of these early constituent lists were aimed at defining pre-operational groundwater conditions at the SALDS, and preceded the current list found in ST-4500.

3.3.1 Tritium Tracking

Currently, groundwater is analyzed for tritium quarterly in the SALDS proximal wells (699-48-77A, 699-48-77C, and 699-48-77D) and annually to semiannually in 12 additional "tritium-tracking" wells in the vicinity of the facility. Peak tritium activities in groundwater occurred in late 1997 and early 1998 in wells 699-48-77A and 699-48-77D, respectively (Figure 8). Since the time of peak activities, the general trends are down for all three wells. However, note that the curve for well 699-48-77A in Figure 8 is irregular, with what appears roughly to be annual highs and lows of significant amplitude (more than two orders of magnitude) in tritium activity during the past ~4 years. This periodicity probably reflects annual ETF campaigns to treat 242-A Evaporator process condensate. Well 699-48-77D is nearest the SALDS, and showed tritium incursion about 18 months later than the more distant well 699-48-77A. The reason for this delay is related to the fact that the SALDS drain field fills from the south end of the facility farthest away from well 699-48-77D, and that the aforementioned geologic features beneath the SALDS divert infiltration southward. These two conditions shunt the subsurface flow of effluent away from well 699-48-77D before it reaches groundwater. Some hint of quasi-annual fluctuation is suggested by the curve for well 699-48-77D, but the amplitude is significantly less, compared with 699-48-77A.

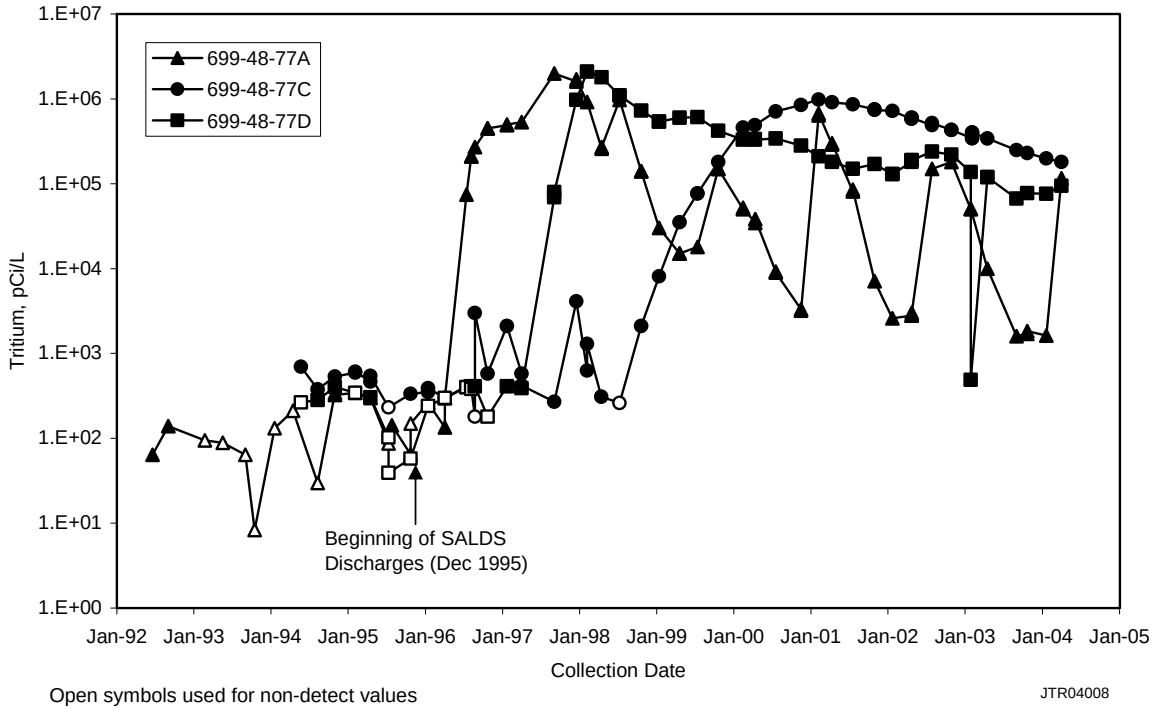

Figure 8. Tritium Activity Trends in SALDS Proximal Wells. Well 699-48-77C is completed ~20 meters deeper in the aquifer than wells 699-48-77A and 699-48-77D.

Well 699-48-77C is screened ~20 meters deeper in the aquifer than wells 699-48-77A and 699-48-77D, and did not detect a peak tritium activity until late 2000. Because of its deeper position in the aquifer, tritium incursions from the SALDS operation have been historically lower in activity. During times of high discharge, the hydraulic head beneath the SALDS is increased, and effluent is forced deeper into the aquifer. Figure 8 shows that historical, maximum tritium activities are slightly less in this well compared with 699-48-77A and 699-48-77D, and cyclical variations are absent or subdued. This difference is undoubtedly due to the dilution of the effluent in reaching groundwater at this depth. Wells generally southeast of the SALDS have produced elevated values for tritium as a result of historical disposal practices in the 200-West Area (see Figure 1). Tritium activities in these wells have generally decreased or remained unchanged over the past several years.

3.3.2 Additional Monitoring

Groundwater from the SALDS proximal wells (699-48-77A, 699-48-77C, and 699-48-77D) is analyzed for a list of 15 constituents (including tritium) required by the State Waste Discharge Permit ST-4500 Special Condition S1 (A). Permit limits are set for most of these constituents: acetone, benzene, cadmium (total), chloroform, copper (total), lead (total), mercury (total), pH, sulfate, tetrahydrofuran, and TDS. Gross alpha, gross beta, strontium-90, and tritium are not assigned enforcement limits, but are

monitored and reported. Additional parameters, such as alkalinity, dissolved oxygen, temperature, and turbidity are monitored for determination of general groundwater characteristics and verifying the quality of analytical results.

With detection of the first elevated tritium in late 1996, concentrations of anions, metals, and other parameters were also found to have increased in groundwater from well 699-48-77A. This is interpreted to be a result of the dilute (clean water) effluent from SALDS dissolving soluble mineral species (such as gypsum in the case of sulfate) in the vadose zone during infiltration (Thornton 1997; Barnett et al. 1997). More recently, wells 699 48-77C and 699-48-77D have shown similar, but more subtle, incursions of these constituents. Parameters in the SALDS wells that best reflect this phenomenon are sulfate and conductivity. Other species, such as calcium and sodium, show a more subdued response during the same time period. The initial rise in these constituents can be traced to the leaching of minerals in the vadose zone. Several other metals show similar trends of increase with subsequent decreases. The trends are most pronounced in wells 699-48-77A and 699-48-77D because these wells are screened at the water table. The ions and indicators (e.g., conductivity) have trended downward for the past few years in wells 699-48-77A and 699-48-77D, and appear now to be stabilizing below initial background (pre-1995) concentrations in these two wells. Well 699-48-77C is screened ~20 meters below the water table, so the effects of SALDS discharges in this well are significantly delayed and subdued with respect to the two shallow wells. The peak concentrations of the parameters occurred in this well in late 1999 to early 2000, approximately 3 years later than in wells 699-48-77A and 699-48-77D. Concentrations in all three wells now reflect the dilute effluent from the SALDS that have replaced the natural concentrations to a minor degree in well 699-48-77C and more so in wells 699-48-77A and 699-48-77D. The most recent results of groundwater are reported by Barnett et al. (2003).

3.3.3 Effects of Stratigraphy and Sediment Chemistry

Two of the SALDS monitoring wells were less affected by the effluent, and at a delayed time compared with well 699-48-77A. It was at first perplexing that the incursion of elevated ions in well 699-48-77D, directly adjacent to the SALDS, occurred at a later date than in well 77A, but *without* elevated tritium activities. Site characterization efforts revealed that the Cold Creek unit dips slightly to the south and forms a discontinuous, but locally impermeable barrier to downward infiltration. It is postulated that this feature intercepted and directed the small, tritium-free, initial test discharges (before December 1995) southward an indeterminate distance before infiltrating to the water table. The effluent then moved with the regional groundwater flow toward well 699-48-77D, but the discharges were of insufficient volume to reach well 699-48-77A. Shortly afterward, the first major discharges containing tritium followed roughly the same pathways to groundwater, but were voluminous enough to create a hydraulic reversal in gradient locally, and thus reached well 699-48-77A before the effects of the small test discharges could reach the next nearest well at the water table (699-48-77D) or the deep-completion well (699-48-77C).

During the initial characterization of the site, laboratory analysis and leaching tests were conducted on vadose-zone sediment samples from the SALDS (Reidel and Thornton 1993). Sediment chemistry, together with aqueous-speciation and mineral-saturation modeling results, was used to predict the

groundwater chemical changes at the SALDS as the result of water disposal activities. Insight into the transport of solutes from the vadose zone to the aquifer was obtained by examining the results of the tests. In particular, these data indicate that sulfate and other anions and cations are present in the vadose zone in sufficient quantities to account for the observed increases in constituent levels in the groundwater that occurred in 1996 and afterward.

Soil sulfate concentrations obtained from soil analyses and leach tests performed during the characterization study suggest that an average value of about 10.6 mg/kg sulfate is present in the vadose zone. The observed maximum groundwater concentration of 190 mg/L sulfate could be achieved if 0.3 pore volumes of vadose zone water were to dissolve all of the gypsum present in vadose zone soils. This sulfate level was maintained for roughly a year before declining. A maximum sulfate concentration of about 879 mg/L potentially could be achieved if water infiltrating the vadose zone were saturated with respect to gypsum and calcite. It would be necessary for all of the sulfate in the vadose zone to be dissolved in only about 0.07 pore volumes of water for saturation to be maintained with respect to gypsum, however, and this level could be maintained for only a month or two. It is thus inferred that maximum groundwater sulfate levels were constrained by the dissolution rate of gypsum (Barnett et al. 2003).

4.0 Conceptual and Numerical Model of Aquifer System

The following sections of this report provides background on previous groundwater modeling of the SALDS facility (Section 4.1), a summary of results from the most recent modeling (Section 4.2), and a discussion and description of the basis of the revised site-wide model used in this analysis (Section 4.3).

4.1 Background

Since the search for a disposal site began in the early 1990s, groundwater modeling has been used as a tool for site select and effluent fate predictions. Because of the effluent that will be discharged to the SALDS over its 30-year planned operation, tritium transport in the unconfined aquifer near the SALDS has been the focal point of some modeling efforts and an important subset of others. In this section, numerical models that have been used to evaluate the SALDS discharges with respect to tritium migration in the vadose zone and groundwater are discussed and compared in broad terms. As a result of shortcomings in earlier models, a more refined groundwater model was produced in 1997, incorporating more realistic assumptions. Results of previous modeling efforts for SALDS are described in greater detail in Barnett et al. (1997).

In 1993, as part of the evaluation of the SALDS, Lu et al. (1993) developed a conceptual model and a two-dimensional cross section numerical model to predict travel time of effluent and tritium activities in the unsaturated zone beneath the facility. The computer code VAM3D-CG was used for simulations of flow and transport in the SALDS vadose zone. Hydraulic properties of the sediments, for modeling parameters, were obtained from laboratory analyses of drilling samples from well 699-48-77A and from the literature (for the Hanford formation). In this model, tritium was predicted to reach groundwater beneath the SALDS within ~1 year after start up of the facility, and a hypothetical well 100 m down-gradient of the facility would first detect tritium after 9 years of operation. Near steady-state saturation and maximum tritium concentrations were established approximately 14 years from the start of tritium disposal. Significant concentrations did not spread beyond 100 m from the facility; after 19 years the maximum contour (1.4×10^7 pCi/L) propagated to approximately 75 m below and about 20 m laterally in both directions from the source.

Another vadose-zone model by Collard et al. (1996) predicted rates of infiltration of low-volume discharges in the 200-West Area to several generic discharge facilities. This model incorporated discontinuities in the Cold Creek Unit based on existing characterization data, but did not include contaminant transport. This model predicted significant lateral spreading of effluent (156 m from the source) when a continuous Cold Creek Unit was assumed, but spreading was greatly reduced when ~3-m-wide “windows” were introduced into the layer every ~30 m to simulate lateral discontinuities. Both the Lu et al. and Collard vadose zone models predicted that liquid effluent discharged to soils in the same general region of the 200-West Area would reach groundwater within 1 year of the start of discharges. Subsurface conditions at the SALDS are very similar to those modeled by Collard, except that the Cold Creek Unit is much nearer the surface at the SALDS.

Numerous groundwater, saturated-flow models have been applied to the SALDS or have incorporated the SALDS in the domains. The Hanford Groundwater Project uses site-wide modeling to predict future conditions of the unconfined aquifer as it is affected by cessation of Hanford Site operations (e.g., determining which monitoring wells will become dry because of declining water levels), to assess the potential for contaminants to migrate from the Hanford Site through the groundwater pathway and to address site-specific contaminant issues, such as SALDS. Developed by PNNL, the model is based on the Coupled Fluid, Energy, and Solute Transport (CFEST) code (Gupta et al. 1987). This code has become the key component of forward modeling of groundwater flow and transport in subsequent numerical models by PNNL.

In 1995, the Environmental Restoration Contractor, Bechtel Hanford, Inc. (BHI) developed and applied a groundwater flow and contaminant transport model of the unconfined aquifer, to provide a basis for evaluation and prioritizing environmental restoration activities and remediation options. This site-wide model included SALDS tritium releases. Connelly et al. (1992) evaluated hydrology and contaminant distributions for the 200-West Area Groundwater Aggregate Area Management Study. Geologic, hydrologic, and geochemical data are summarized by Connelly et al. (1992) and interpretations are made using several Dynamic Graphics Inc. (DGI) software packages. These data were used in subsequent modeling efforts to address fate and transport at SALDS. Golder Associates (1991) assessed the movement of treated effluent from the SALDS in the unconfined aquifer between the disposal site and the Columbia River to support the groundwater screening evaluation/monitoring plan for SALDS (Davis et al. 1996). The model was based on the Golder Associates proprietary two-dimensional codes, Aquifer Porous Media (AFPM) and Solute Transport (SOLTR). Maximum tritium concentrations in the unconfined aquifer predicted by the Golder model after 205 years were predicted to be greater than 2,000,000 pCi/L, but maximum concentrations predicted to reach the Columbia River were less than the 20,000 pCi/L Drinking Water Standard (DWS).

Dresel et al. (1995) report the results of applying the two-dimensional flow model of the unconfined aquifer based on CFEST to evaluate pathlines from the SALDS to the Columbia River. The model was applied under transient conditions from 1980 through 2040 and steady-state conditions were assumed after 2040. The pathlines from the SALDS under these assumed conditions were predicted to extend eastward to the Columbia River near the old Hanford Town site or slightly north of Gable Mountain. A one-dimensional analytical transport code was used to predict concentrations along several of the pathlines. The source of tritium was assumed to be a pulse lasting for 60 years (i.e., the facility was assumed to operate for 60 years). With these overly robust assumptions, and by restricting the contaminant transport along one-dimensional pathlines, tritium was predicted to eventually reach the Columbia River, but in concentrations far below DWS.

Chiaramonte et al. (1996) performed simulations of tritium transport for a 200-year period under transient flow conditions using VAM3DCG. These simulations included discharges from the SALDS, which was assumed to receive 50.3 L/min (72 m^3/day) for the first 10 years of operation and 410.3 L/min (590 m^3/day) from 10 to 20 years. Tritium concentrations input to SALDS were assumed to be 5.6 million pCi/L per year for 20 years. Under these assumed conditions, only a small amount of tritium is predicted to remain beneath the SALDS after 100 years. The peak concentration of 800,000 pCi/L was predicted to occur 20 years into the simulation. This model predicts that tritium from the SALDS will not

leave the central plateau at levels above the 20,000 pCi/L DWS. The tritium plume from SALDS is predicted to stay close to its source, then shrink as a result of decay. A summary of results of the original three-dimensional groundwater modeling of SALDS discharges, as presented in Barnett et al. (1997), is briefly described in the following discussion.

4.2 Overall Performance of the 1997 Numerical Model

In 1997, as a requirement of the SALDS permit, predictions of the impacts from water and tritium disposal to the SALDS were performed with the three-dimensional CFEST model using updated model input parameters (Barnett et al. 1997). Simulations were based on the three-dimensional conceptual model described in detail by Wurstner et al. (1995) and were derived in conjunction with the original Hanford site-wide composite analysis as described in Kincaid et al (1998).

Flow Modeling was performed with a regional-scale model and a localized refinement of the grid to better account for the position of the SALDS discharges in the regional-scale model. In vicinity of the SALDS, results of flow modeling showed a localized groundwater mound with a water level rise of about 2 m above pre-operational levels. The mound at the facility creates a radial pattern of flow around the SALDS during the period of operational discharges. After cessation of discharges, the mound dissipates near the SALDS in response to a decline in the regional water table. Groundwater flow direction changes first to northeasterly, then easterly toward the Columbia River. Results of transient flow conditions after the operation phase of the SALDS showed that the unconfined aquifer would reach steady state conditions by about year 2100.

Predicted flow conditions beneath the SALDS cause tritium to spread in a radial pattern in the vicinity of the facility. Tritium concentrations reached their maximum, thus far, between 1996 and 1999. Average concentration levels in the 1997 model reached a maximum value of about 3.4 million pCi/L. The average overall concentration in the node immediately below the facility was 1.1 million pCi/L at this time. Peak concentrations dropped below 2 million pCi/L between the years 2000 and 2005 and after this time, the predicted plume declined to lower levels in response to projected lower discharges to the facility through the year 2034. The actual maximum detected activity in groundwater at SALDS thus far was 2.1 million pCi/L in well 699-48-77A in February 1998. The maximum areal extent of the roughly circular SALDS plume occurs in 2045, and places the edge of the 500 pCi/L contour at ~1.5 km northeast of the facility.

At year 2035, the predicted plume as defined by the 500 pCi/L contour migrated outward about 1500 m downgradient of the facility toward observation well, 699-51-75. By the year 2100, predicted tritium concentration dropped below the 500 pCi/L level at all locations within the SALDS-generated plume.

The basis for revised modeling of updated past SALDS discharges and projected additional discharges through site closure with the current site-wide groundwater flow and transport model are described in the following section.

4.3 Basis for the Revised 2004 Model

More detailed flow simulation of the historical operational period presented here is based on the calibrated hydraulic properties and boundaries estimated in Cole et al. (2001), as represented in a more refined grid that provides higher resolution in source areas in the Central Plateau and between the Central Plateau and the Columbia River (Figure 9) than was used in Bryce et al. (2002). In general, the grid is on the order of 80 m on a side in 200-West Area and 250 m on a side from just west of 200-East Area to the downgradient areas to the Columbia River. This grid is being used to perform all contaminant transport analysis supporting a revised Composite Analysis.

Simulated flow conditions during the historical period of Hanford operations that provided the basis for the detailed flow calculations are described in Cole et al. (2001). These flow conditions incorporate the effect of large-volume discharges of wastewater to a variety of waste facilities since the inception of the Hanford Site in 1943. These operational discharges have raised the water table, created groundwater mounds, and have been the source of local and regional-scale contaminant plumes under waste management sites and facilities along the Columbia River and in the central part of the site. Since 1988, the mission of the Hanford Site has changed from weapons production to environmental restoration. As a result, wastewater discharges have declined significantly, which caused the water table to decrease significantly over the past decade. Simulation of future water table decline indicates that the aquifer would return to more natural levels within 150 to 300 years. These results are consistent with previous work on future water table declines described in Cole et al. (1997) and Kincaid et al. (1998).

The current approach relies on a three-dimensional representation of the aquifer system that was calibrated to Hanford Site-wide groundwater monitoring data collected during Hanford Operations from 1943 to the present as described in Cole et al. (2001). This three-dimensional, transient, inverse calibration, which was recommended by an external peer-review panel, is being performed using UCODE, a universal inverse modeling code developed jointly by the U.S. Geological Survey and the International Groundwater Modeling Center of the Colorado School of Mines. The work uses the existing consolidated SGM implemented with the Coupled Fluid Energy and Solute Transport code (CFEST), which is the forward model whose parameters are estimated by UCODE. The transient inverse calibration uses over 76,000 water level measurements taken in about 1,200 wells at Hanford since the mid 1940s.

4.3.1 Conceptual Model and Numerical Implementation

The conceptual model and numerical implementation of groundwater flow for the unconfined aquifer is the same conceptual model and numerical implementation summarized by Thorne (2004) for use in the Updated Composite Analysis due to be completed in FY 2005. This conceptual model and implementation focuses on the major hydrogeologic unit within the unconfined aquifer system that lies in the Pasco basin west and south of the Columbia River and east and north of the Yakima River. This implementation also is limited to evaluation of groundwater flow to the supra-basalt sediments without consideration of interaction between the unconfined aquifer and the uppermost basalt-confined aquifers. The nature of

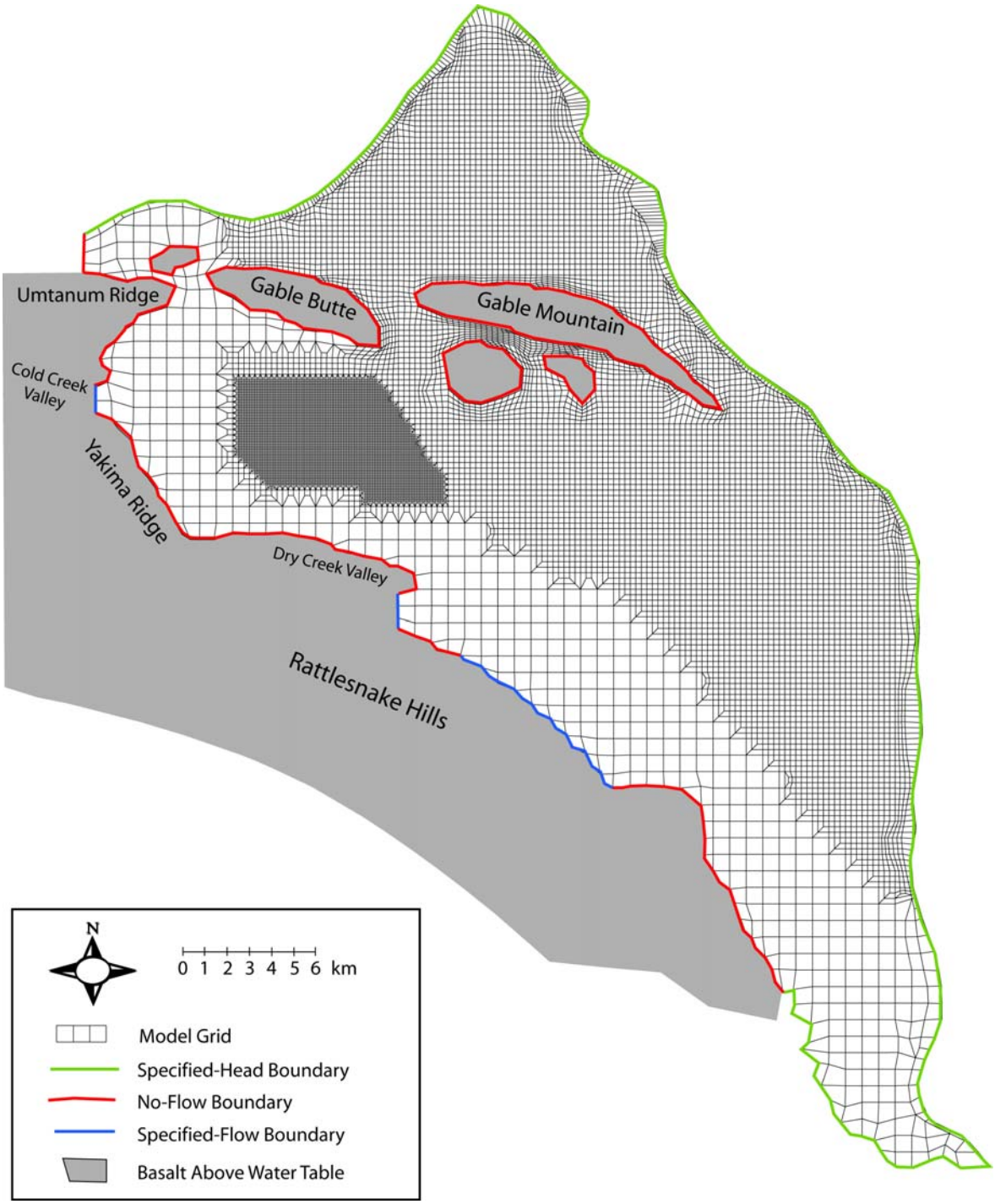

Figure 9. Finite Element Grid Used in Revised Flow System Simulations

interactions between the unconfined aquifer and uppermost basalt confined aquifers is in the process of being evaluated in the development and calibration of alternative conceptual models as part of a separate groundwater model development task (see Vermeul et al. 2001, 2003).

4.3.2 Major Hydrogeologic Units

For purposes of this analysis, sediments overlying the basalt bedrock have been grouped into nine major hydrogeologic units (Thorne 2004) that include the following units:

Unit 1 – Hanford formation and the underlying, texturally similar, coarse-grained multi-lithic facies of the Cold Creek Unit (pre-Missoula gravels).

Unit 2 – Fluvial/eolian facies of the Cold Creek Unit (formally called the Plio-Pliestocene Unit).

Unit 3 – Calcic paleosol sequence of the Cold Creek Units.

Unit 4 – Silt and clay facies of the Upper Ringold Unit.

Unit 5 – Lindsey's (1995) Ringold gravel units E and C, also includes sand facies of the Upper Ringold Unit where it directly overlies the other E and C gravel units.

Unit 6 – Fine-grained overbank and paleosol deposits that vertically separate Lindsey's (1995) unit B from overlying unit C in the eastern part of the Hanford Site.

Unit 7 – Lindsey's (1995) Ringold gravel units B and D.

Unit 8 – Lower Ringold mud unit (Lindsey 1995).

Unit 9 – Lindsey's (1995) Ringold unit A, a gravel and sand facies that is dominated by sand in the western part of the Pasco Basin.

Seven of these units are found below the water table and compose the modeled aquifer system. Units 2 and 3 are above the water table in this implementation of the model.

In subsequent model implementations (Vermeul et al. 2003), the coarse-grained multi-lithic facies of the Cold Creek Unit (pre-Missoula gravels) were included in model unit 3 and are found below the water table. This later implementation was still undergoing calibration refinement at the time of the SAC simulations. Information on the geologic setting and additional details on the grouping of sediment for the model units is provided in Cole et al. (2001a).

4.3.3 Estimates of Hydraulic Properties

To model groundwater flow, the distribution of hydraulic properties, including horizontal and vertical hydraulic conductivity, storativity, and specific yield, was needed for each hydrogeologic unit defined in the model. In the original model calibration procedure described in Wurstner et al. (1995), measured values of aquifer transmissivity (i.e., thickness of the aquifer times the hydraulic conductivity) were used in a two-dimensional model with an inverse model-calibration procedure to determine the transmissivity distribution. Hydraulic head conditions for 1979 were used in the inverse calibration because measured hydraulic heads were relatively stable at that time. Details concerning the updated calibration of the two-dimensional model are provided in Cole et al. (1997). The resulting transmissivity distribution for the unconfined aquifer system is shown in Figure 10.

Hydraulic conductivities were assigned to the three-dimensional model units so that the total aquifer transmissivity from inverse calibration was preserved at every location. The vertical distribution of hydraulic conductivity at each spatial location was determined, based on the transmissivity value and other information, including facies descriptions and hydraulic property values measured for similar facies. A complete description of the seven-step process used to vertically distribute the transmissivity among the model hydrogeologic units is described in Cole et al. (1997).

The current version of the site-wide model relies on a three-dimensional representation of the aquifer system that was calibrated to Hanford Site-wide groundwater monitoring data collected during Hanford operations from 1943 to the present. The calibration procedure and results for this model are described in Cole et al. (2001a). This recent work is part of a broader effort to develop and implement a stochastic uncertainty estimation methodology in future assessments and analyses using the site-wide groundwater model (Cole et al. 2001b). Resulting distribution of hydraulic conductivities for the major hydrogeologic units found at the water table from this recent calibration effort is provided in Figure 11.

The distribution of best-fit estimates for the hydraulic conductivity of the Hanford formation (primarily Unit 1) is found at the water table over most of the eastern and northern part of the Hanford Site. The best-fit estimates for the hydraulic conductivity of the Hanford formation (Unit 1) were found to be well within the reasonable range of previous estimates for this parameter. Previous work summarized in Thorne and Newcomer (1992) and Wurstner et al. (1995) indicate that the hydraulic conductivity of Unit 1 generally ranges from tens to several thousand m/d and is much higher than any of the other units that make up the unconfined aquifer system. Aquifer tests indicate that the minimum estimated hydraulic conductivity is about 1 m/d (Thorne et al. 1993), and the maximum estimated value is about 10,000 m/d (Thorne and Newcomer 1992; DOE 1988). However, the maximum hydraulic conductivity that can be estimated by an aquifer test is limited by the well efficiency and the flow rate that can be pumped with available equipment. Past calibration efforts by Wurstner et al. (1995) and Cole et al. (1997) have estimated that an upper limit of hydraulic conductivity for coarse-gravel flood deposits found in the central part of the Hanford Site is on the order of several tens of thousands of m/d. The scaled parameter estimates and confidence intervals for the parameters of interest in the best-fit inverse model are summarized in Table 1.

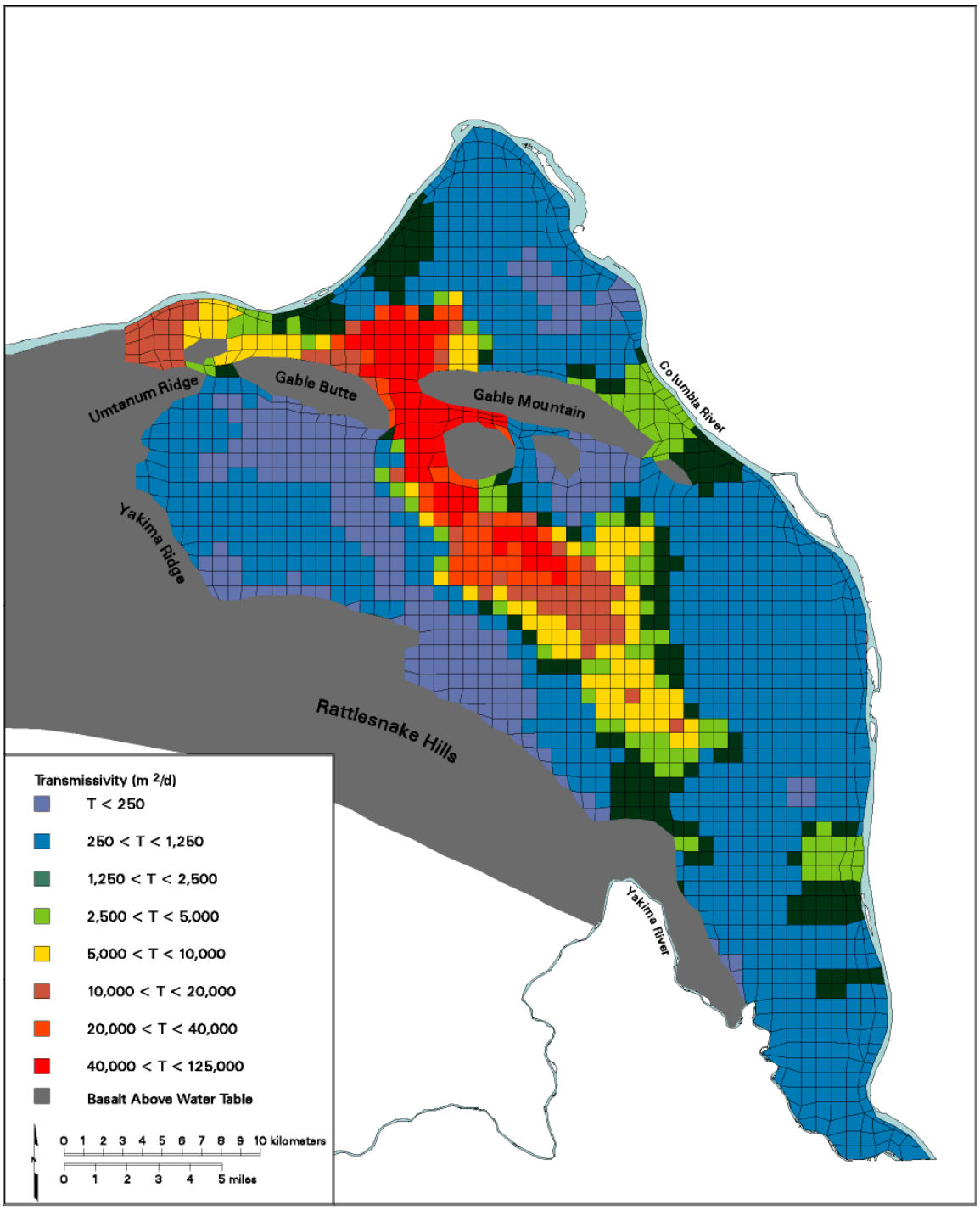

Figure 10. Transmissivity Distribution for the Unconfined Aquifer System Based on Two-Dimensional Inverse Model Calibration (after Wurstner et al. 1995)

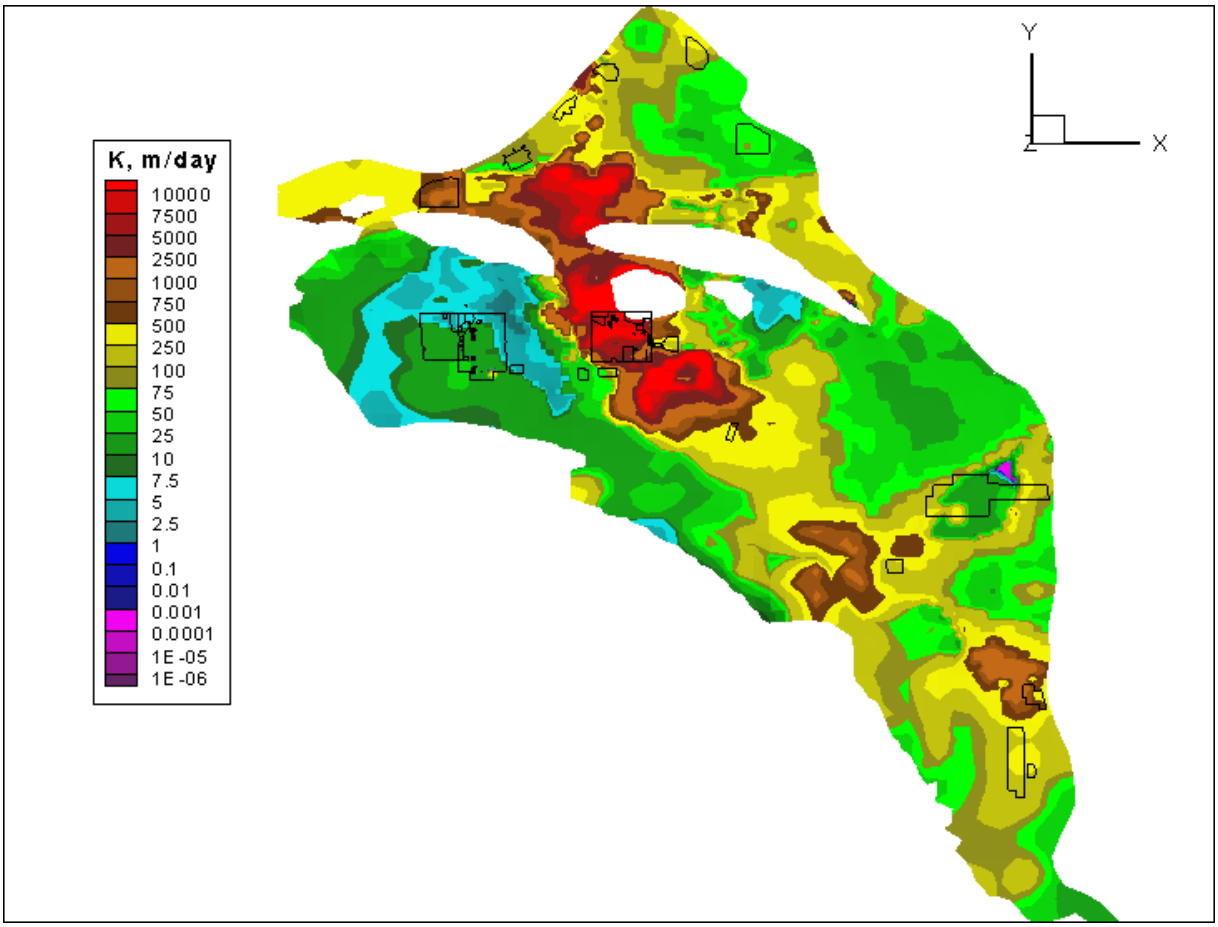

Figure 11. Hydraulic Conductivity Distribution at the Water Table Using a Refined Flow Model Based on the Transient Inverse Calibration Performed by Cole et al. (2001)

Table 1. Scaled Parameter Estimates and Confidence Intervals (best-fit inverse model)

Model Parameters	95% Confidence Interval	Best Fit Estimate	-95% Confidence Interval
Hanford (Unit 1) K	0.91	0.90	0.89
Ringold (Unit 5) K	2.27	2.25	2.23
Hanford (Unit 1) SY	0.29	0.28	0.27
Ringold (Unit 5) SY	2.15	2.12	2.08
Cold Creek Flux	2.12	2.09	2.05
Natural Recharge	1.78	1.71	1.65
Rattlesnake Hills Flux	4.48	4.37	4.27

The resulting distribution of the best-fit estimates for the hydraulic conductivity (see Figure 12) of the Ringold Formation (primarily Unit 5) which is found at the water table over most of the west and southwest part of the site were found to be well within the reasonable range of previous estimates for this

parameter documented in Cole et al. 2001b. The Ringold Formation consists of sand to muddy sandy gravel with varying degrees of consolidation or cementation. Unit 5 is the most widespread unit within the unconfined aquifer and is found below the water table across most of the model region. In 200-West Area, hydraulic conductivities of Unit 5 of the Ringold in the revised site-wide model range from about 1 to about 30 m/day. This range of estimated hydraulic conductivity is very consistent with hydraulic conductivity values determined largely from aquifer slug tests in 200-West Area which range of about 0.1 to about 80 m/d. The majority of values estimated from these hydraulic tests are found in the range between 1 and 30 m/day. An area of higher aquifer permeability is postulated above the Ringold Unit 5 sediments in a small area in the southeast part of 200-West Area when the water table was at its highest levels in the past.

4.3.4 Boundary Conditions

The past development of the site-wide model considered both natural and artificial recharge to the aquifer. Natural recharge to the unconfined aquifer system occurs from infiltration of (1) runoff from elevated regions along the western boundary of the Hanford Site; (2) spring discharges originating from the basalt-confined aquifer system, also along the western boundary; and (3) precipitation falling across the site. Some recharge also occurs along the Yakima River in the southern portion of the site. Natural recharge from runoff and irrigation in the Cold Creek and Dry Creek Valleys, upgradient of the site, also provides a source of groundwater inflow. Natural recharge from precipitation on the site is highly variable, both spatially and temporally, and depends on local climate, soil type, and vegetation.

The other source of recharge to the unconfined aquifer is artificial recharge from wastewater disposal. Over the past 60 years, the large volume of wastewater discharged to disposal facilities at the Hanford Site, estimated at 1.3 billion m3 has significantly affected groundwater flow and contaminant transport in the unconfined aquifer (see Figure 13). The majority of discharges have occurred in 200 East, 200 West, 100-K, and 100-N Area of the 100 Areas, and the 300 Area. The estimated cumulative discharges by each operational area and their relative percentage of the total estimated discharge for the period of interest is provided in Table 2. The volume of artificial recharge has decreased significantly during the past 10 years and continues to decrease. Wurstner et al. (1995) summarized the major discharge facilities incorporated in the three-dimensional model. Cole et al. (1997) summarized the major wastewater discharges from both past and future sources. Significant uncertainties associated with the artificial discharges relate to the spatial location and timing of their arrival at the water table as well as the quantity. These uncertainties were not addressed in the calibration performed by Cole et al. 2001a but will be evaluated in other evaluations of alternative conceptual model studies in the future. A summary of Hanford wastewater discharge from 1943 through 2001 used in simulation results used in this report are provided in Appendix C.

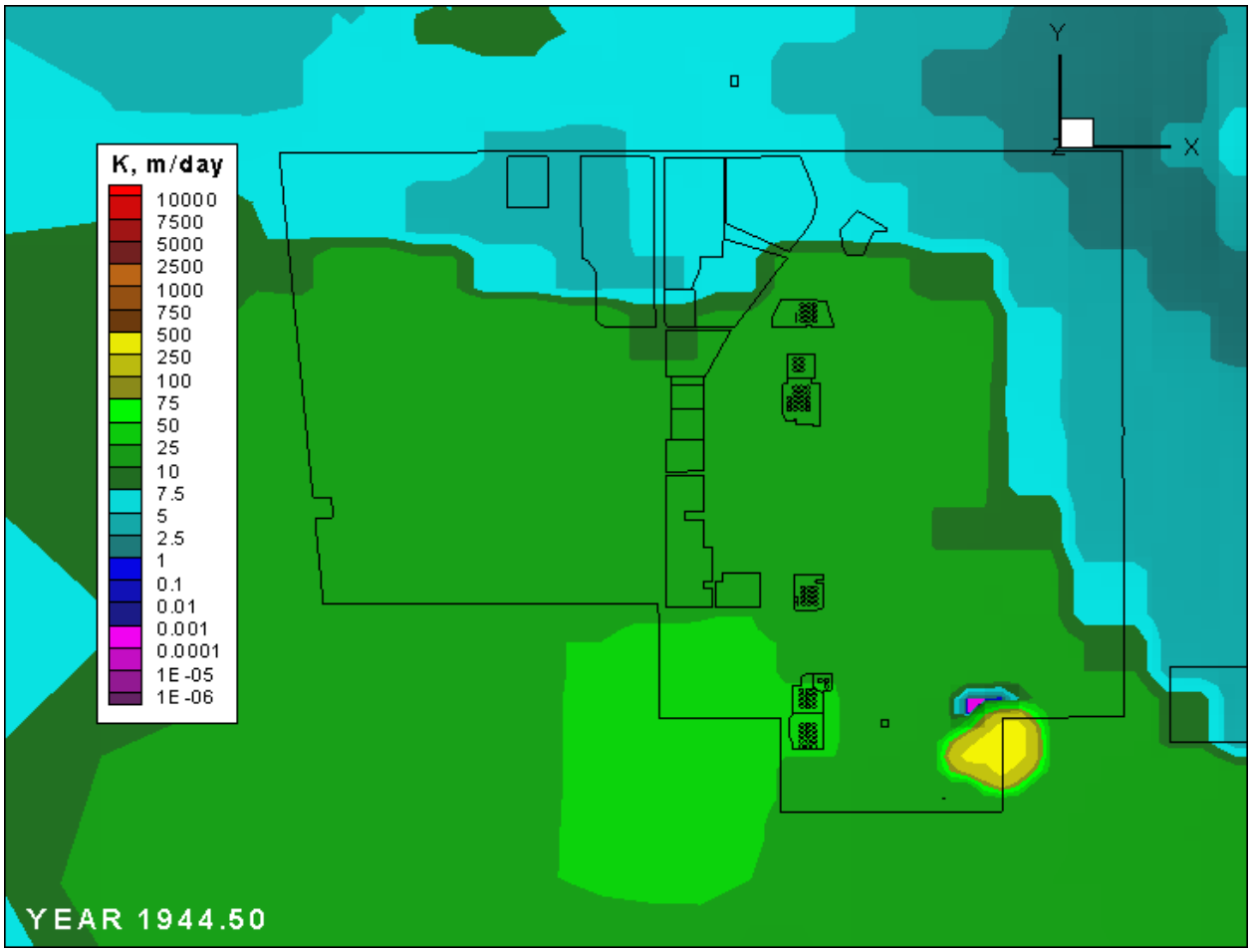

Figure 12. Hydraulic Conductivity Distribution at the Water Table in 200-West Area Using a Refined Flow Model Based on the Transient Inverse Calibration Performed by Cole et al. (2001)

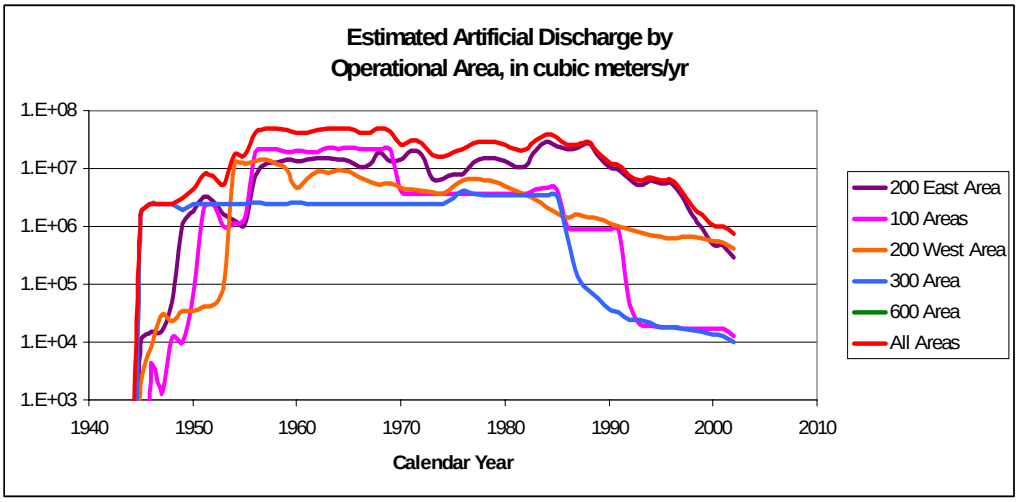

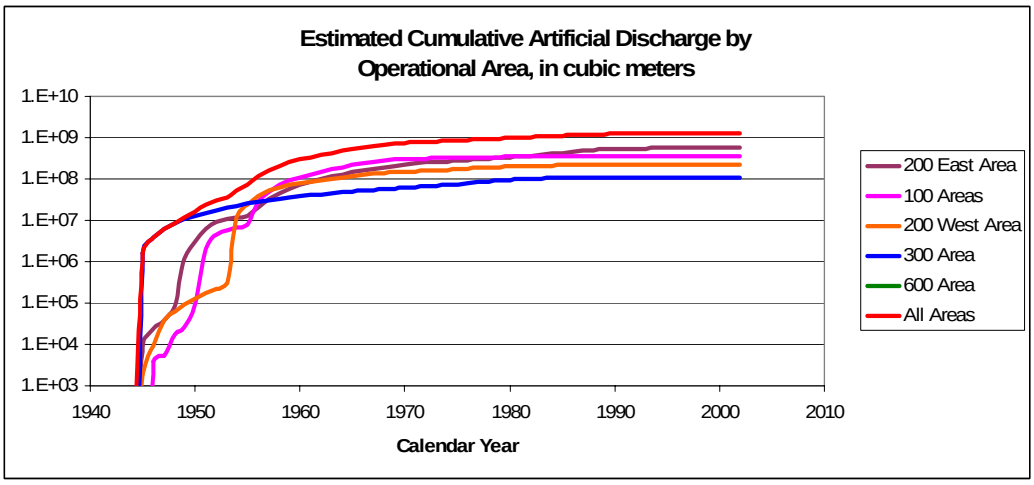

Figure 13. Estimated Annual and Cumulative Artificial Discharges to Unconfined Aquifer by Operating Areas from 1944-2002

Table 2. Cumulative Artificial Discharges to Unconfined Aquifer by Operational Areas from 1944-2002

Operational Area	Total (m^3)	Percent of Total
200-East Area	5.75E+08	44.8
100 Areas	3.70E+08	28.8
200-West Area	2.29E+08	17.8
300 Area	1.12E+08	8.7
600 Area	2.53E-07	Much less than 1 percent
All Areas	1.29E+09	

Peripheral boundaries defined for the three-dimensional model are shown in Figure 9, together with the three-dimensional flow-model grid. The flow system is bounded by the Columbia River on the north and east and by the Yakima River and basalt ridges on the south and west. The Columbia River represents a point of regional discharge for the unconfined aquifer system. The amount of groundwater discharging to the river is a function of local hydraulic gradient between the groundwater elevation adjacent to the river and the river-stage elevation. This hydraulic gradient is highly variable because the river stage is affected by releases from upstream dams.

Because of the regional-scale nature and long-time frame being considered in the current assessment, site-wide flow and transport modeling efforts did not attempt to consider the short-term and local-scale transient effects of the Columbia River system on the unconfined aquifer. However, the long-term effect of the Columbia River as a regional discharge area for the unconfined aquifer system was approximated in the three-dimensional model with a constant-head boundary applied at the uppermost nodes of the model at the approximate locations of the river's left bank and channel midpoint. Nodes representing the thickness of the aquifer below the nodes representing mid-point of the river channel were treated as no-flow boundaries. This boundary condition is used to approximate the location of the groundwater divide that exists beneath the Columbia River where groundwater from the Hanford Site and the other side of the river discharge into the Columbia. The long-term, average river-stage elevations for the Columbia River implemented in the site-wide model were based on results from previous work performed by Walters et al. (1994) for the Columbia River with a river simulation model. The Yakima River was also represented as a specified-head boundary at surface nodes approximating its location. Like the Columbia River, nodes representing the thickness of the aquifer below the Yakima River channel were treated as no-flow boundaries. Short-term fluctuations in the river levels do not influence modeling results.

At Cold Creek and Dry Creek Valleys, the unconfined aquifer system extends westward beyond the boundary of the model. To approximate the groundwater flux entering the modeled area from these valleys, both constant-head and constant-flux boundary conditions were defined. A constant-head boundary condition was specified for Cold Creek Valley for the steady-state model calibration runs. The fluxes resulting from the specified-head boundaries in the calibrated steady-state model were then used in the steady-state flow simulation of flow conditions after Hanford Site closure. The constant-flux

boundary was used because it better represents the response of the boundary to a declining water table than does a constant-head boundary. Discharges from Dry Creek Valley in the model area, resulting from infiltration of precipitation and spring discharges, are approximated using the same methods.

The basalt underlying the unconfined aquifer sediments represents a lower boundary to the unconfined aquifer system. The potential for interflow (recharge and discharge) between the basalt-confined aquifer system and the unconfined aquifer system is largely unquantified but is postulated to be small relative to the other flow components estimated for the unconfined aquifer system. Therefore, interflow with underlying basalt units was not included in the current three-dimensional model. The basalt was defined in the model as an essentially impermeable unit underlying the sediments.

The estimated fluxes developed from a constant head boundary during previous calibration efforts provide the basis for the initial estimate used in this inverse modeling. While the various boundary fluxes at the Cold Creek and Dry Creek Valleys and at the base of Rattlesnake Hills cannot be independently verified, the estimated fluxes were found to be well within the reasonable range, given the uncertainty that could be expected in hydraulic properties of the principal hydrogeologic units found close to these units. The best-fit flux at Cold Creek Valley was a little over a factor of 2 higher than the initial estimates. The best-fit flux estimated for Rattlesnake Hills was about a factor 4 higher than the initial estimate. Given the uncertainty in the overall hydraulic properties of the Ringold Formation found in the vicinity of Cold Creek Valley and the hydraulic properties of the Hanford and Ringold Formations found along the base of Rattlesnake Hills, the increase in the overall estimate is not considered unreasonable.

The range in confidence limits for the best-fit flux from Dry Creek Valley was very large, suggesting that either this flux is not a very sensitive parameter in the model or that insufficient information is available (or both) in the observational database to effectively estimate this flux using the inverse method.

The best-fit estimates for the natural recharge were about 71 percent greater than the estimates previously made by Fayer and Walters (1995). This increase in the overall estimate of recharge is not considered unreasonable for most areas of the site where recharge rates are on the order of 5 to 20 mm/yr. However, for some areas of the site where coarse soils exist and previous estimated recharge rates approach 50 to 60 mm/yr, this 71-percent increase in the overall recharge rate results in rates of 80 to 90 mm/yr, which are not considered reasonable. The best-fit estimate of recharge for this conceptual model may be higher to compensate for a variety of factors, including

- underestimating previous estimates of regional natural recharge
- underestimating artificial discharges at waste-water facilities in the operational areas due to
    - reporting errors
    - inadvertent losses of water within the Hanford Site infrastructure between points of withdrawal from the Columbia River to points of discharges within the operational areas

- not considering the interaction of the uppermost basalt confined aquifer in the current model leading to underestimates of flow into the unconfined aquifer system in areas along the Columbia River where the regional basalt aquifer is likely discharging upward into the unconfined system.

Updates to the baseline inverse model used in the original analysis, which have been included as part of this revised detailed flow analysis, are discussed below.

4.3.5 Changes in Approximating Artificial Discharges to Water Table

Recent approaches used to incorporate artificial recharge from wastewater disposal into the unconfined aquifer (Vermeul et al. 2003) was improved from methods used in the earliest inverse calibration described in Cole et al. (2001) and (Vermeul et al. 2001). Cole et al. (1997) summarized the major wastewater discharges from both past and future sources. Significant uncertainties are associated with the artificial discharges related to the spatial location and timing of their arrival at the water table. As discussed below, recent inverse modeling efforts have implemented a new application of artificial discharges to account for the lag time associated with movement of the initial wetting front through the vadose zone. Investigation and verification of the spatial locations of the various discharge locations, and their change over time, is ongoing.

Previous versions of the Sitewide Groundwater Model (SGM) have been calibrated and used with records of artificial liquid discharges specified as inputs to the saturated flow system without regard to the vadose zone. In effect, the vadose zone was ignored and disposals of liquid to ground were considered to instantly reach the unconfined aquifer at the time of disposal. Consideration of vadose zone effects coupled with the SGM has been problematic until recently.

Recent inverse modeling data input development used in Vermeul et al. (2003) has relied on vadose zone modeling capabilities based on the Subsurface Transport Over Multiple Phases (STOMP) code (White and Oostrom 1996) embodied in the recently developed System Assessment Capability (SAC), which is a tool developed to provide the first-ever total systems modeling of all waste disposal locations at the Hanford Site. SAC accounts for inventory distribution, release, environmental transport, and impacts to human, ecological, economic, and cultural resources. The software framework of the SAC necessarily included a coupling of many vadose zone site-specific models to the SGM. Because the SAC already includes a vadose zone model for all the Hanford waste disposal locations with full coupling to the SGM, it was recognized that, with relatively minor adaptations to the SAC framework and data, it could be used to account for the vadose zone's effects on liquid disposal arrival at the unconfined aquifer.

In SAC, vadose zone sites are modeled using the STOMP simulator. A separate STOMP model is used for each individual waste disposal site, as identified in the Waste Information Data System (WIDS).[(a)] Releases at all of these sites (hundreds) are accumulated in time and space by the VZDROP (Vadose Zone Data Restructure for Other Programs) code and used to prepare a single input file for CFEST.

(a) WIDS is the computerized database operated by Fluor Hanford to track all Hanford Site solid waste management units, as required by the Tri-Party Agreement.

The focus of the SAC is on constituent mass moving from the vadose zone to groundwater and beyond. To support improved treatment of fluid movement from the vadose zone to groundwater, some improvements were added to the SAC modification set of the STOMP code and to the VZDROP code. STOMP was modified to produce a record of fluid discharge to groundwater from the vadose zone in excess of the natural recharge rate declared as an upper boundary flux (that is, a Neumann-type boundary condition). Because artificial recharge is represented in SAC STOMP modeling as a nodal source, while natural recharge is represented as a boundary flux, we considered the difference between the lower and the upper boundary fluxes to represent the arrival of artificial recharge at the water table. The natural recharge rate in SAC simulations is not constant; it changes in time to represent changes to the surface condition. Hence, the difference between fluxes at the upper and lower boundaries is measured relative to the current time to preclude misclassifying variations in natural recharge as the artificial recharge signal. VZDROP was modified to have a runtime option that redirected its focus from the standard handling of constituent mass to handling liquid fluxes instead. Using this new option, VZDROP collects the STOMP-recorded values of liquid flux to the water table in excess of natural recharge at the vadose zone model's upper boundary for all sites and uses it to modify a CFEST L3I file's nodal fluid sources. The final product is a CFEST input set that represents artificial recharge sources to the unconfined aquifer from a vadose zone model rather than directly from the discharge record.

One consideration in applying the SAC database and software was that "clean" water sources were not included in the SAC site list. The SAC site list includes all sites that potentially received certain radioactive or chemical wastes. However, other sources of artificial discharge existed and still exist on the Hanford Site, such as septic disposal systems. These additional water source locations were identified and added to the SAC site list for the special fluid application of SAC to produce the CFEST input file with vadose zone fluid effects.

Recent corrections to specification of infiltration rates for input to the STOMP model in the SAC framework were incorporated in this special fluid application run of SAC. Additionally, a correction was introduced for the B-Pond complex. In the SAC database, all discharges to the B-Pond complex are represented as discharging at B-Pond itself (WIDS Site ID 216-B-3). Conditions during 1983-1995 involved considerable discharge to ditches 216-B-3A, 216-B-3B, and 216-B-3C as well. To account for this, the release predicted in the SAC simulation for site 216-B-3 was divided into four equal releases and each of these was reassigned to 216-B-3, 216-B-3A, 216-B-3B, and 216-B-3C before using the VZDROP code to distribute STOMP fluid releases at the water table.

Other improvements implemented into the refined model used in this analysis relates to the methods used to distribute larger water sources areally at the upper boundary of the model. In previous inverse modeling, the introduction of waste water discharges from all sources was emplaced in the SGM as a nodal source at the node that most closely approximated the centroid of the facility footprint. This approximation was sufficient in earlier modeling efforts where grid spacing used in flow modeling was on the order of 750 m on a side and the finest transport model grid spacing was on the order of 375 m on a side. However, with the grid refinement used in this analysis, which is on the order of 80 m on a side in most of 200-West Area and about 250 m on a side from 200-East Area to discharge points along the Columbia, the earlier approximation of applying facility discharges to a single node, particularly for larger facilities such as ponds and long ditches, needed improvement.

The revised methodology takes into consideration the approximate area of individual facility footprints in the distribution of water to surface nodes within the SGM. For larger facilities, the algorithm distributes water sources as nodal sources to all nodes found within constructed polygonal areas that approximate each facility footprint in proportion to the polygon area intercepted by the effective area of each node considered. This approach was used to affect the redistribution of water sources from about 29 facilities with significant artificial discharge considered in this historical analysis. The distributed sources are those specifically listed in Table 3.

4.3.6 Changes in Configuration of Basalt Cropping Out Above the Water Table

Minor changes were made to model design features used to represent more recent reinterpretations of subcrops of basalt bedrock that are postulated to be above the water table within the modeled area. A grid modification were made in an area where a gap along the subsurface basalt ridge extending southeast of the land surface expression of Gable Mountain, north and northwest of the Hanford Town Site was postulated. In this area, responses of long-term hydrographs from wells on either side of these postulated gaps in the basalt subcrops show hydrograph responses that are very different than those of local stresses to the aquifer in the Central Plateau and surrounding areas. In the first case along the river near the Hanford Town Site, hydrographs on the river side of the basalt ridge extension show a much more pronounced response to large fluctuations in the stage of the Columbia River than those on the opposite side of the basalt subcrop, which suggests that basalt bedrock does crop out above the water table in this area for the majority of the time of interest. In this case, a number of finite elements were removed for the previous grid thus eliminating the possibility of flow and transport through this area.

Table 3. Distributed Sources

Operating Area	WIDS Facility Name
100-BC	116_C_1
100-D	116_DR_1_2
100-K	216_K_2
100 N	116_N_1 116_N_3
200 East	216_A_10 216_A_12_13_15_5 216_A_30 216_A_6 216_B_3A 216_B_3C 216_B_3 216_B_63
200 West	216_S_11 216_S_16P 216_S_17 216_S_19 216_S_25 216_S_5 216_S_6 216_T_4A 216_U_10 216_U_14 216_Z_20
300	316_1

5.0 Results of the 2004 Groundwater Model Simulations

Model simulations were performed using the revised site-wide groundwater model for the interval between 1944 through 2100. Artificial recharge at all active Hanford discharge sites is included in the model. However, contaminant release is limited to the tritium source at the SALDS facility (see Appendix A). Barnett et al. (1997) used projected fluid volume and tritium activities for annual time steps. The current model has updated the fluid volume and tritium activity for monthly time steps starting in July 1997 and ending in June 2004. Values reported by Barnett et al. (1997) for the remainder of the discharge interval of 2005 through 2034 are used where measured data are absent. One year time steps are used prior to 1996 and after 2004. After 2030, release from the SALDS facility is assumed to end and no additional sources of tritium are assumed to enter into the aquifer. Tritium concentration declines in response to a combination of transport, dispersion and radioactive decay. The volume and tritium activity values used in the model are listed in Table 4. The flux is calculated by dividing the volume by the relevant time interval. The concentration is the activity divided by the volume and is corrected to the appropriate units of pCi/L.

A comparison of the projected and updated fluid flux and tritium concentration from 1996 through June 2004 are shown in Figure 14. The figure shows a high initial flux for the projected case, followed by declining flux in later years. The actual behavior shows that flux is highly variable through the year, but generally higher than predicted. The plot also shows that updated flux does not decline as much as for the projected case. Figure 14 also shows that the projected tritium concentration tends to be higher than the updated cases for most of the interval. The net result is that actual concentration is lower than projected and actual flux is higher than was projected.

Cumulative volume released and cumulative tritium activity for the period from 1996 through 2100 is shown in Figure 15. The volume and activity for 1996 through the first half of 2004 reflect the unique values of the projected and updated scenarios. In updated projections made in 2004 (Appendix A), the dominant source of new effluents will originate from liquid effluents treated at the ETF from the Waste Treatment Plant and supplemental low-level treatment facilities between years 2009 and 2030. These effluents are expected to account for about 63 percent of the total effluent and about 2,550 Ci or 95 percent of total tritium inventory discharged to the SALDS facility between year 2004 and 2030.

Following the convention established in the system assessment capability (Bryce et al. 2002), effluents were introduced in the model at two of the nearest node location shown in Figure 16. About 82.7% of the total volume is released at the north model node and 17.3% is released at the south model node. The north node is in close proximity with the north well, 699-48-77D adjacent to the SALDS. The south node is near the south edge SALDS boundary and north of the well 699-48-77A location. Selected model results are provided at these two nodal locations and two other nodes immediately upgradient and downgradient of the SALDS ("SALDS Southwest" and "SALDS Northeast"—see Figure 16) to provide detailed local-scale model results in the immediate vicinity of the SALDS.

Table 4. SALDS Release Fluid Volume and Tritium Activity

Date	Volume (Gal.)	Volume (m^3)	Tritium (Ci)	Date	Volume (Gal.)	Volume (m^3)	Tritium (Ci)
1-Jan-1996	7.60E+06	2.88E+04	222.1400	1-Apr-1999	2.62E+06	9.91E+03	8.7399
1-Jan-1997	1.14E+07	4.29E+04	204.3000	1-May-1999	2.61E+06	9.87E+03	0.1116
1-Jul-1997	1.76E+06	6.65E+03	6.6595	1-Jun-1999	1.28E+06	4.86E+03	0.0133
1-Aug-1997	3.25E+06	1.23E+04	2.8965	1-Jul-1999	3.94E+06	1.49E+04	0.0219
1-Sep-1997	2.60E+06	9.83E+03	0.5445	1-Aug-1999	6.54E+05	2.47E+03	0.0006
1-Oct-1997	2.62E+06	9.90E+03	0.2760	1-Sep-1999	2.62E+06	9.91E+03	0.0079
1-Nov-1997	2.56E+06	9.69E+03	0.1577	1-Oct-1999	1.33E+06	5.01E+03	0.0038
1-Dec-1997	6.00E+05	2.27E+03	0.0295	1-Nov-1999	0.00E+00	0.00E+00	0.0000
1-Jan-1998	1.30E+06	4.92E+03	14.8839	1-Dec-1999	2.58E+06	9.77E+03	0.0066
1-Feb-1998	2.37E+06	8.94E+03	15.4015	1-Jan-2000	6.62E+05	2.50E+03	0.0017
1-Mar-1998	2.60E+06	9.84E+03	1.0555	1-Feb-2000	0.00E+00	0.00E+00	0.0000
1-Apr-1998	3.25E+06	1.23E+04	0.0909	1-Mar-2000	3.21E+06	1.21E+04	0.0084
1-May-1998	2.63E+06	9.95E+03	0.0256	1-Apr-2000	6.15E+05	2.33E+03	0.0005
1-Jun-1998	3.29E+06	1.24E+04	0.0157	1-May-2000	1.01E+06	3.82E+03	0.0028
1-Jul-1998	2.64E+06	1.00E+04	0.0152	1-Jun-2000	3.26E+06	1.23E+04	0.0074
1-Aug-1998	1.91E+06	7.21E+03	0.0116	1-Jul-2000	3.25E+06	1.23E+04	0.0082
1-Sep-1998	2.47E+06	9.33E+03	0.0119	1-Aug-2000	1.09E+06	4.12E+03	0.0026
1-Oct-1998	3.26E+06	1.23E+04	0.0107	1-Sep-2000	1.85E+06	6.98E+03	16.3565
1-Nov-1998	1.92E+06	7.26E+03	0.0058	1-Oct-2000	3.33E+06	1.26E+04	4.5275
1-Dec-1998	1.30E+06	4.93E+03	7.1373	1-Nov-2000	1.94E+06	7.32E+03	0.0717
1-Jan-1999	1.92E+06	7.25E+03	0.0578	1-Dec-2000	3.92E+06	1.48E+04	0.0198
1-Feb-1999	2.47E+06	9.35E+03	0.0141	1-Jan-2001	3.28E+06	1.24E+04	0.0083
1-Mar-1999	1.01E+06	3.81E+03	0.0098	1-Feb-2001	1.31E+06	4.94E+03	0.0029

Table 4. (contd)

Date	Volume (Gal.)	Volume (m^3)	Tritium (Ci)	Date	Volume (Gal.)	Volume (m^3)	Tritium (Ci)
1-Mar-2001	0.00E+00	0.00E+00	0.0000	1-Feb-2003	1.95E+06	7.36E+03	0.0035
1-Apr-2001	1.26E+06	4.77E+03	0.0031	1-Mar-2003	2.62E+06	9.89E+03	0.0076
1-May-2001	2.57E+06	9.70E+03	0.0055	1-Apr-2003	3.27E+06	1.24E+04	0.0091
1-Jun-2001	2.59E+06	9.79E+03	0.0056	1-May-2003	3.14E+06	1.19E+04	0.0085
1-Jul-2001	1.95E+06	7.39E+03	0.0040	1-Jun-2003	1.16E+06	4.37E+03	0.0033
1-Aug-2001	2.96E+06	1.12E+04	0.0065	1-Jul-2003	3.83E+06	1.45E+04	0.0102
1-Sep-2001	1.77E+06	6.68E+03	0.0044	1-Aug-2003	1.16E+06	4.37E+03	0.0033
1-Oct-2001	1.96E+06	7.42E+03	0.0043	1-Sep-2003	1.86E+06	7.04E+03	1.9010
1-Nov-2001	3.71E+06	1.40E+04	0.0102	1-Oct-2003	6.08E+05	2.30E+03	0.9439
1-Dec-2001	2.57E+06	9.72E+03	0.0071	1-Nov-2003	9.63E+05	3.64E+03	1.4729
1-Jan-2002	1.61E+06	6.09E+03	0.0612	1-Dec-2003	3.27E+06	1.24E+04	0.5478
1-Feb-2002	6.70E+05	2.53E+03	3.0415	1-Jan-2004	2.40E+06	9.06E+03	0.0754
1-Mar-2002	0.00E+00	0.00E+00	0.0000	1-Feb-2004	3.28E+06	1.24E+04	0.0124
1-Apr-2002	2.59E+06	9.77E+03	5.0626	1-Mar-2004	1.33E+06	5.02E+03	0.0037
1-May-2002	3.27E+06	1.24E+04	0.2590	1-Apr-2004	3.06E+06	1.16E+04	0.0080
1-Jun-2002	3.19E+06	1.21E+04	0.0431	1-May-2004	2.62E+06	9.91E+03	0.0210
1-Jul-2002	1.94E+06	7.33E+03	0.0197	1-Jun-2004	1.94E+06	7.34E+03	11.6000
1-Aug-2002	2.63E+06	9.94E+03	0.0340	1-Dec-2004	6.23E+06	2.36E+04	0.7365
1-Sep-2002	0.00E+00	0.00E+00	0.0000	2005	1.51E+07	5.72E+04	54.1365
1-Oct-2002	3.09E+06	1.17E+04	0.0112	2006	7.95E+06	3.01E+04	49.5104
1-Nov-2002	6.23E+05	2.35E+03	0.0015	2007	8.45E+06	3.20E+04	22.4252
1-Dec-2002	2.46E+06	9.32E+03	0.0052	2005	1.51E+07	5.72E+04	54.1365

Table 4. (contd)

Date	Volume (Gal.)	Volume (m^3)	Tritium (Ci)	Date	Volume (Gal.)	Volume (m^3)	Tritium (Ci)
1-Jan-2003	1.92E+06	7.27E+03	0.0047	2008	8.53E+06	3.23E+04	16.5668
2009	5.02E+06	1.90E+04	8.2743	2020	9.91E+06	3.76E+04	171.4037
2010	1.24E+07	4.71E+04	156.2573	2021	9.36E+06	3.55E+04	158.5985
2011	1.18E+07	4.48E+04	155.9605	2022	8.43E+06	3.19E+04	141.7443
2012	1.15E+07	4.34E+04	182.2142	2023	9.88E+06	3.74E+04	170.6997
2013	9.51E+06	3.60E+04	143.4677	2024	9.91E+06	3.76E+04	171.4054
2014	1.05E+07	3.99E+04	163.6831	2025	9.95E+06	3.77E+04	172.0529
2015	1.11E+07	4.20E+04	174.9067	2026	8.85E+06	3.35E+04	150.1987
2016	1.11E+07	4.20E+04	174.8651	2027	8.29E+06	3.14E+04	139.0374
2017	8.75E+06	3.32E+04	128.2455	2028	9.99E+06	3.78E+04	172.8173
2018	9.88E+06	3.74E+04	150.7252	2029	1.04E+07	3.95E+04	181.4703
2019	1.07E+07	4.06E+04	187.3246	2030	9.96E+06	3.77E+04	172.3578

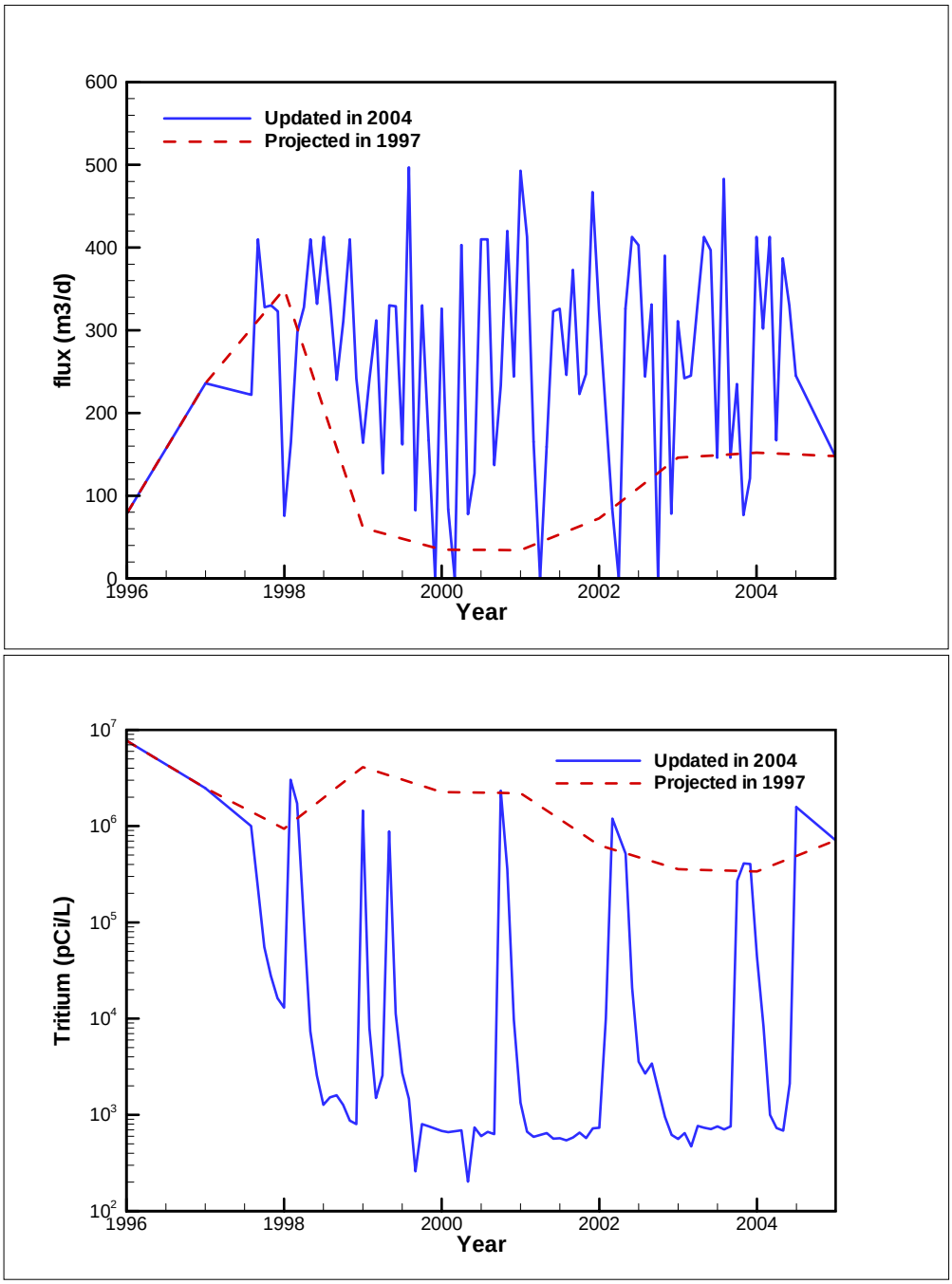

Figure 14. Efflent Volumes and Tritium Concentration Levels Discharges at SALDS 1996-2004

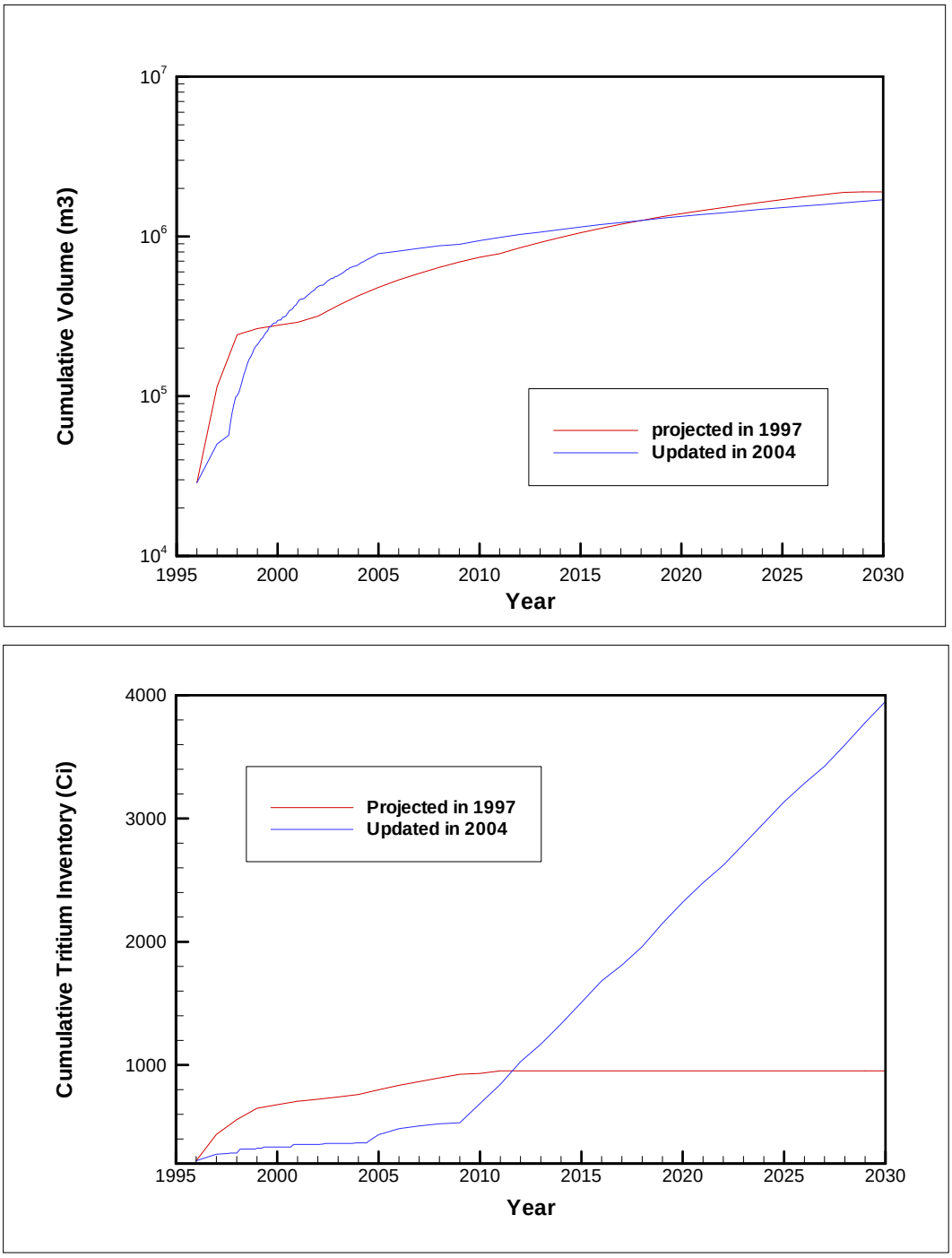

Figure 15. Cumulative Fluid Volume and Tritum Inventory at SALDS 1996-2030

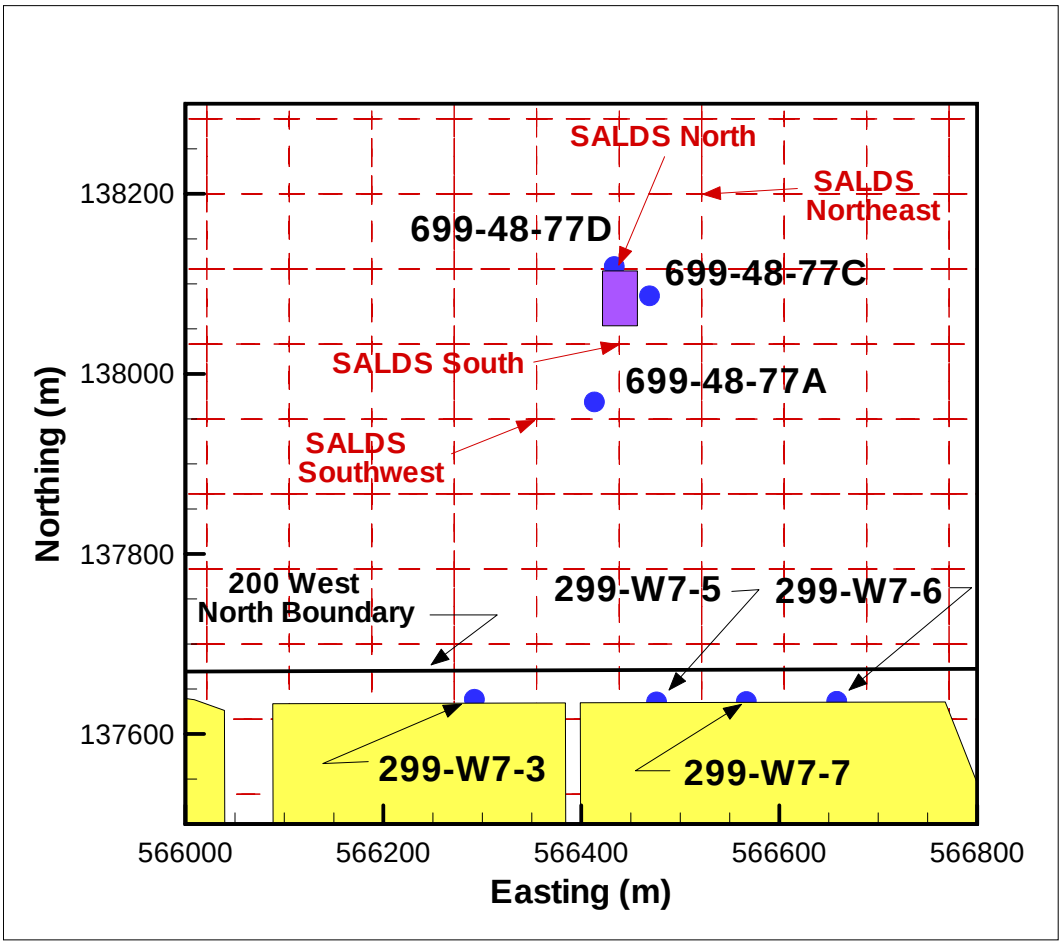

Figure 16. SALDS Facility, Monitoring Wells and Model Nodes

A comparison of the time-series of plots in Appendix B is in general agreement with time planes produced by Barnett et al. (1997). Both cases show a similar degree of decline in water level in each time plane, however, the general water table levels for the updated scenario is consistently about 1 meter lower over the results reported by Barnett et al. (1997). This difference appears to be related to the estimation of regional flow field rather than specifically to the fluxes from the SALDS facility.

Water table levels estimated in this assessment (Figure 17) also indicate that careful monitoring of the level of saturation in some of the current monitoring wells will be necessary as the water table continues to decline to more natural conditions. Wells that may be particularly vulnerable to going dry include one of the tritium tracking wells along the northern boundary of 200-West Area, 299-W7-9. Another well that could be vulnerable is one of the proximal observation wells 699-48-77A. This well will continue to functional through the end of facility operations but could be vulnerable if effluent discharges are less than volumes in current projects. Both wells in question are located south of the SALDS.

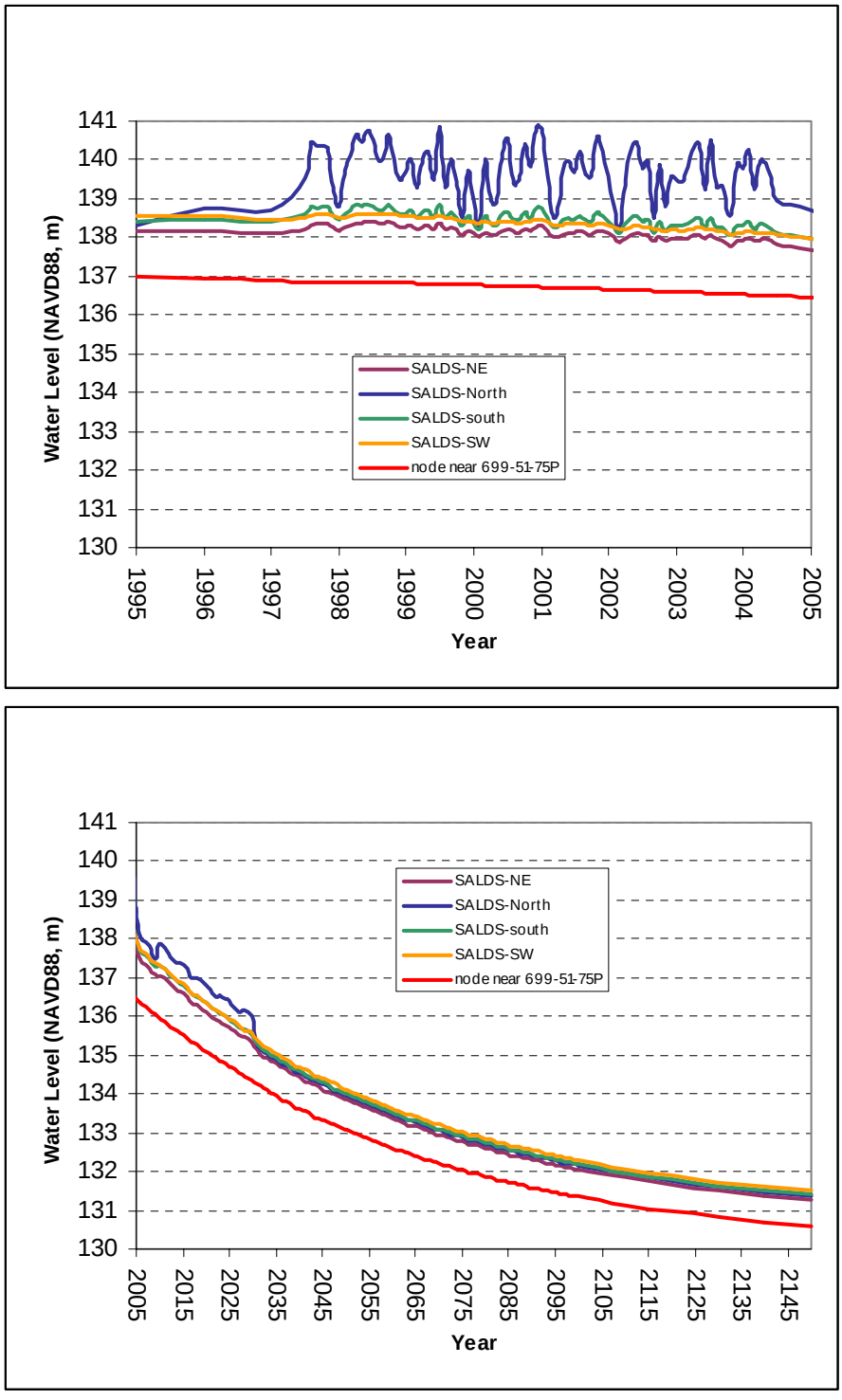

Figure 17. Actual and Predicted Water Table Elevations at Nodes North and South of the SALDS Facility

5.1 Predicted Distribution of Tritium from SALDS Discharges

Plot of results related to the transport part of the analysis presented in a series of tritium concentration plots in Appendix C show a general consistency of modeled results of the water table prediction made in previous modeling by Barnett et al (1997) for the period between 1996 and 2004. Results show the development of a localized tritium plume in the immediate vicinity of the SALDS facility.

Observed tritium concentration in Figure 8 shows that the maximum concentration achieved is about 3 million pCi/L in 1997 and is at a high of about 300,000 pCi/L in 2004. The highest concentration is first observed in the south well, 699-48-77C and over time, it shifts to the north well, 699-48-77D, and is highest in the east well, 699-48-77A by 2004. The tritium concentration for the model is shown in Figure 18. Concentration levels are generally highest at the north node during each of the annual cycles of discharges to the aquifer, but then tends to increase in the south well after each cycle. Highest concentrations in 1996 and 2004 are approximately in the same range as seen in Figure 8.

The areal tritium distribution at the north 200-West Area boundary and north of the SALDS facility, shown for a time-series of plots in Appendix C, shows a general consistency in terms of direction of transport with a similar series of plots are reported by Barnett et al. (1997). Concentrations in the updated simulation results show the same general trend of increase and subsequent decrease of tritium in the corresponding time frames. However, during the period of historical observations, the maximum concentration for the updated model are lower than that reported by Barnett et al. (1997) and the extent of the plume is smaller for the updated model. During the past operational period, the simulated plume as defined by the 500 pCi/L contour south of the SALDS does not quite reach the line of tritium tracking wells along the northern border of 200-West Area as it did in previous modeling. The updated model results are consistent with the 1997 model when the actual, historical effluent volumes and the lower activity levels in the waste streams are taken into account.

A significant difference between the updated modeling results and those predicted in 1997 can also be seen in the future period extending beyond year 2004. During the future period of simulation, concentrations level at the facility increase to about between 800,000 and 900,000 pCi/L in 2006 before declining to about 300,000 pCi/L in year 2008 in response to projected discharges in the next 4 years. After 2008, simulations show a significant increase in predicted tritium concentration levels. The primary cause of this difference reflects the significant change in effluent discharges and tritium inventory estimates associated effluents originating from the Waste Treatment Plant and supplemental low-level treatment facilities. Because of this inventory increase, concentration levels starting in the year 2009 will steadily increase from about 300,000 pCi/L in year 2008 to over 3 million pCi/L by the end of operation in the year 2030.

During the future period, the outermost edge of the plume as defined by the 500 pCi/L also moves downgradient of the SALDS in a northeasterly direction toward well 699-51-75p. Model predictions indicate that the plume has the potential of reaching the downgradient observation well 699-51-75P in concentrations exceeding 500 pCi/L in the next 5 to 10 yrs (See Appendix C).

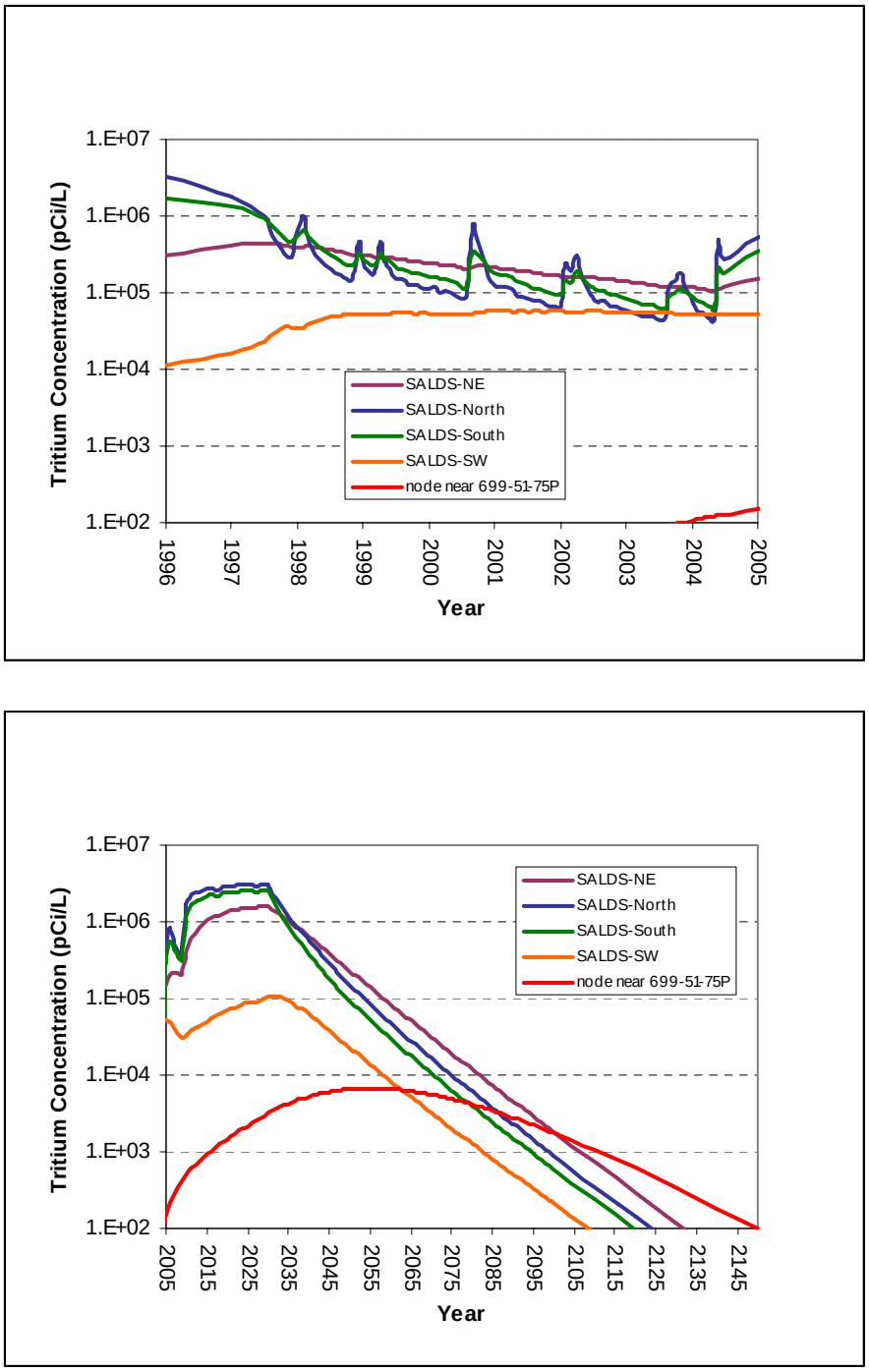

Figure 18. Actual and Predicted Tritium Concentration Levels at Model Nodes Closest (north and south) of the SALDS Facility

After 2004, the simulated plume as defined by the 500 pCi/L contour south of the SALDS does reach the line of tritium tracking wells along the northern border of 200-West Area in the period between 2020 and 2030. Concentration levels between 500 and 2,000 pCi/L are projected to be observed in some of these wells in this time frame. Owing to the processes of downgradient transport and decay, concentrations in impacted wells in this area would be expected to drop below 500 pCi/L in the 2080 to 2090 time frame.

The overall plume as defined by the 500 pCi/L reaches a maximum downgradient distance of about 2,000 m northeast of the SALDS facility by the year 2090 before plume dispersion and radioactive decay result in an overall decline of the tritium plume concentration levels. With updated increase in future tritium inventories in the current projection, modeled results suggest that tritium concentration levels would not decline below 500 pCi/L until between the years 2130 and 2140. Previous modeling had suggested that tritium concentration levels would drop below 500 pCi/L between years 2080 and 2090.

In addition to the plan view of the tritium plume, a SW to NE trending vertical transect through the SALDS facility for the same time planes was provided in Appendix C. The transect was made through the upgradient well, 699-48-77A to downgradient well 699-51-75P. The transect was selected to roughly correspond to groundwater flow direction. Figure 19 shows the transect in the plan view. Each profile shows the distribution of major hydrogeologic units. The concentration contours, well locations, and ground surface. Ground surface at the SALDS facility is approximately 205 m (NAVD88) and is about 196 m (NAVD88) at distal well 699-51-75P. As with the plan view plume, the highest concentrations occur in the first few years. The 1997 and 2000 time planes show concentrations consistent with the plan view plots ranging from 1.6 million to 300,000 pCi/L at the facility. The cross-sections show that the tritium plume penetrates the full vertical extent of the aquifer beneath the facility. The concentration profiles to the south remain fairly stationary during this period. Profiles through 2030 show the plume continuing to move northeast at lower concentrations at the later times. By 2075, the overall plume as defined by the 500 pCi/L level recedes and the south extent of the plume boundary also migrates away from those wells in the main direction of groundwater flow to the northeast. Between 2125 and 2135, the plume above the 500 pCi/L level recedes southwest of well 699-51-75P. By 2140 the plume is no longer detectable above 500 pCi/L.

In all instances, the 500 pCi/L tritium contour reaches a maximum distance of about 2,000 m from the SALDS facility before it disperses and decays. Consequently, the plume is not expected to migrate any significant distance out of the vicinity of the 200-West Area. The plume decays entirely before reaching the gap between Gable Butte and Gable Mountain (Figure 9).

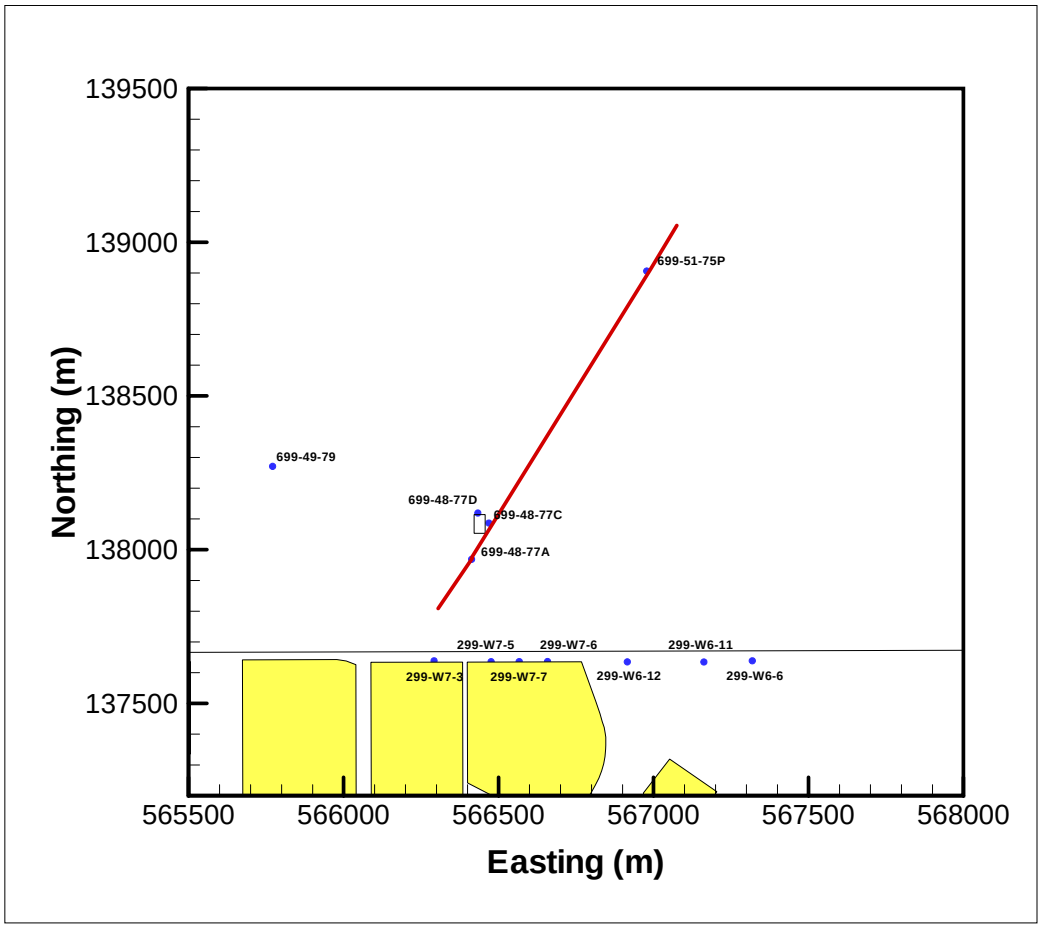

Figure 19. Location of Cross-Section of the Vertical Profiles in Appendix C

6.0 Conclusions and Recommendations

The model results presented in this report incorporates the reported data through June 2004 and then uses projected discharge and tritium inventory values through 2034 that have been updated with more current information. Simulation results show that the tritium concentrations are, in general, consistent with tritium concentration levels that have been observed in nearby observation wells closest to the SALDS facility. During the period of operations from 1995 through June of 2004, predicted tritium concentration levels in the vicinity of the SALDS facility reached an early high of about 1.6 million pCi/L in 1996. After that time, predicted concentration levels at the water table were variable ranging from 1.6 million to several hundred thousand pCi/L in June 2004 and on a downward trend. These simulated results generally reflect the changes in simulated monthly effluent discharges and tritium inventories discharged to the aquifer in the model analysis. Simulated results show the areal extent of the plume as defined by the 500 pCi/L contour is generally contained within an area currently monitored by the tritium tracking well network. These results are also generally consistent with tritium concentration levels and trends that have been observed in well 699-48-77A, the well south of the SALDS facility that is the first well impacted by SALDS operations.

After June 2004, discharges and tritium inventories projected for SALDS do not change significantly from past projections until the increase in tritium inventory is realized from effluents originating from the Waste treatment Plant and supplemental low-level treatment facilities after year 2009. Estimated tritium concentration levels beyond the year 2009 were projected to be much larger and to remain longer in the aquifer than was estimated in previous modeling efforts owing to this larger inventory projection. Because of this inventory increase, concentration levels starting in the year 2009 will steadily increase from about 300,000 pCi/L in 2008 to about 3 million pCi/L at the end of operation in 2030. With updated increase in future tritium inventories in the current projection, modeled results suggest that tritium concentration levels would not drop below 500 pCi/L until the year 2140. Previous modeling had suggested that tritium concentration levels would drop below 500 pCi/L by the year 2090.

Modeling results suggest that the current network, which consists of 3 proximal monitoring wells and 16 tritium tracking well, will continue to provide adequate coverage for tracking the impacts from tritium in effluent from the SALDS facility. Current predictions suggest that concentration levels of 500 pCi/L may potentially arrive at well 699-51-75P within the next 5 to 10 years. Once discharges cease on 2030, simulation results also suggest that the plume will not likely grow much beyond the area of this observation well as a result of radioactive decay.

Groundwater level monitoring and tritium sampling should continue at the current level of effort. Current monitoring and predictions of future plume migration with past and projected estimates of effluent volumes and tritium inventory suggest that adding additional monitoring wells at this time will not necessarily improve the effectiveness of the existing monitoring network to monitor the effect of current and projected effluents at the SALDS facility.

Estimated water table projections also suggest that some of the current monitoring wells may go dry, as the water table continues to decline to more natural conditions. Wells that may be particularly vulnerable include the tritium tracking wells along the northern boundary of 200-West Area. Another well that could be vulnerable is the proximal observation well, 699-48-77A. This well will continue to function through the end of facility operations, but could be vulnerable if effluent discharges are less than volumes in current projects. Both wells in question are located south of the SALDS.

7.0 References

Baker VR, BN Bjornstad, AJ Busacca, KR Fecht, EP Kiver, UL Moody, JG Rigby, DF Stradling, and AM Tallman. 1991. Quaternary Geology of the Columbia Plateau, *in* Morrison, R.B., ed., *Quaternary Nonglacial Geology; Conterminous U.S.* Boulder, Colorado, Geological Society of America, The Geology of North America, v. K-2.

Barnett DB, JT Rieger, and EC Thornton. 2003. *Results of Tritium Tracking and Groundwater Monitoring at the Hanford Site 200 Area State-Approved Land Disposal Site—Fiscal Year 2003*. PNNL-14449, Pacific Northwest National Laboratory, Richland, Washington.

Barnett DB. 2000. *Groundwater Monitoring and Tritium-Tracking Plan for the 200 Area State-Approved Land Disposal Site*. PNNL-13121, Pacific Northwest National Laboratory, Richland, Washington.

Barnett DB, MP Bergeron, CR Cole, MD Freshley, and SK Wurstner. 1997. *Tritium Monitoring in Groundwater and Evaluation of Model Predictions for the Hanford Site 200 Area Effluent Treatment Facility*. PNNL-11665, Pacific Northwest National Laboratory, Richland, Washington.

Bjornstad BN. 1984. *Suprabasalt Stratigraphy Within and Adjacent to the Reference Repository Location*. SD-BWI-DP-039, Rockwell Hanford Operations, Richland, Washington.

Bryce RW, CT Kincaid, PW Eslinger, and LF Morasch. 2002. *An Initial Assessment of Hanford Impact Performed with the System Assessment Capability*. PNNL-14027, Pacific Northwest National Laboratory, Richland, Washington.

Cole CR, SK Wurstner, MP Bergeron, MD Williams, and PD Thorne. 1997. *Three-Dimensional Analysis of Future Groundwater Flow Conditions and Contaminant Plume Transport in the Hanford Site Unconfined Aquifer System: FY 1996 and 1997 Status Report*. PNNL-11801, Pacific Northwest National Laboratory, Richland, Washington.

Cole CR, MP Bergeron, SK Wurstner, PD Thorne, S Orr, and MI McKinley. 2001. *Hanford Site-Wide Groundwater Model Calibration Using Inverse Methodology*. PNNL-13447, Pacific Northwest National Laboratory, Richland, Washington.

Collard LB, JD Davis, and DB Barnett. 1996. *Potential Effects of Low-Volume Effluent Discharges on Past-Practice Vadose-Zone Contamination*. WHC-SD-LEF-ER-001, Rev. 0, Westinghouse Hanford Company, Richland, Washington.

Connelly MP, BH Ford, and JV Borghese. 1992a. *Hydrogeologic Model for the 200 West Groundwater Aggregate Area*. WHC-SD-EN-TI-014, Westinghouse Hanford Company, Richland, Washington.

Davis JD, DB Barnett, CJ Chou, and PB Freeman. 1996. *Ground-Water Screening Evaluation/ Monitoring Plan—200 Area Effluent Treatment Facility (Project C-018H).* WHC-SD-C018H-PLN-004, Rev. 1, Westinghouse Hanford Company, Richland, Washington.

DOE. 1988. *Consultation Draft, Site Characterization Plan, Reference Repository Location, Hanford Site, Washington*. DOE-RW-0164, U.S. Department of Energy, Office of Civilian Radioactive Waste Management, vol. 1.

DOE-RL. 2002. *Standardized Stratigraphic Nomenclature for Post-Ringold-Formation Sediments Within the Central Pasco Basin.* DOE/RL-2002-39, Rev. 0, U.S. Department of Energy, Richland Operations Office. Richland, Washington, pp. 3-1 to 3.9.

Dresel PE, PD Thorne, SP Luttrell, BM Gillespie, WD Webber, JK Merz, JT Rieger, MA Chamness, SK Wurstner, and BE Opitz. 1995. *Hanford Site Ground-Water Monitoring for 1994*. PNL-10698, Pacific Northwest Laboratory, Richland, Washington.

Ecology. 2000. State Waste Discharge Permit Number ST 4500. Washington State Department of Ecology, Kennewick, Washington.

Fayer MJ and TB Walters. 1995. *Estimated Recharge Rates at the Hanford Site.* PNL-10285, Pacific Northwest Laboratory, Richland, Washington.

Fecht KR, SP Reidel, and AM Tallman. 1987. "Paleodraingae of the Columbia River System on the Columbia Plateau of Washington State - A Summary," in Schuster, J.E., ed., *Selected Papers on the Geology of Washington,* Washington Division of Geology and Earth Resources, Bulletin 77, p. 219-248.

Golder Associates, Inc. 1994. *Migration of Nondecaying and Nonretarding Constituents from the State Approved Land Disposal Site, Hanford Site, Washington*. Prepared for Westinghouse Hanford Company through WHC Contract No. MLW-SVV-073750, Westinghouse Hanford Company, Richland, Washington.

Gupta SK, CR Cole, CT Kincaid, and AM Monti. 1987. *Coupled Fluid, Energy, and Solute Transport (CFEST) Model: Formulation and User's Manual*. BMI/ONWI-660, Battelle Memorial Institute, Office of Nuclear Waste Isolation, Columbus, Ohio.

Harris SF and CD Delaney. 1991. *Groundwater Quality Characterization at Three Candidate Sites for the C-018H Soil Column Disposal Facility*. WHC-SD-EN-ES-013, Rev. 0, Westinghouse Hanford Company, Richland, Washington.

Hartman MJ, LF Morasch, and WD Webber. 2003. *Summary of Hanford Site Groundwater Monitoring for Fiscal Year 2002*. PNNL-14187-SUM, Pacific Northwest National Laboratory, Richland, Washington.

Kincaid CT, MP Bergeron, CR Cole, MD Freshley, NL Hassig, VG Johnson, DI Kaplan, RJ Serne, GP Streile, DL Strenge, PD Thorne, LW Vail, GA Whyatt, and SK Wurstner. 1998. *Composite Analysis for Low-Level Waste Disposal in the 200-Area Plateau of the Hanford Site*. PNNL-11800, Pacific Northwest National Laboratory, Richland, Washington.

Lindsey KA. 1991. *Revised Stratigraphy for the Ringold Formation, Hanford Site, South-Central Washington*. WHC-SD-EN-EE-004, Westinghouse Hanford Company, Richland, Washington.

Lindsey KA, MP Connelly, and BN Bjornstad. 1991. *Geologic Setting of the 200-West Area: An Update*. WHC-SD-EN-TI-008, Westinghouse Hanford Company, Richland, Washington.

Lindsey KA and SP Reidel. 1992. *Suprabasalt Geology of Soil Column Disposal Candidate Site Number 1: A Preliminary Evaluation of the Site Geology and Recommendations for Number of Boreholes*. WHC-MR-0291, Westinghouse Hanford Company, Richland, Washington.

Lindsey KA, JL Slate, GK Jaeger, KJ Swett, and RB Mercer. 1994a. *Geologic Setting of the Low-Level Burial Grounds*. WHC-SD-EN-TI-290, Westinghouse Hanford Company, Richland, Washington.

Lindsey KA, SP Reidel, KR Fecht, JL Slate, AG Law, and AM Tallman. 1994b. *Geologic Setting of the Hanford Site, South-Central Washington*, in Swanson, D.A., and R.A. Haugerud, *eds*., Geologic Field Trips of the Pacific Northwest: 1994 Geological Society of America Annual Meeting, Geological Society of America, Boulder, Colorado, pp. 1C-1 to 1C-16.

Lindsey KA. 1996. The Miocene to Pliocene Ringold Formation and Associated Deposits of the Ancestral Columbia River System, South-Central Washington and North-Central Oregon, Open-File Report 96-8, Washington Division of Geology and Earth Resources, Washington State Department of Natural Resources, Olympia, Washington.

Lindsey KA. 1995. *Miocene- to Pliocene-Aged Suprabasalt Sediments of the Hanford Site, South-Central Washington*. BHI-00184, Rev. 00, Bechtel Hanford Inc., Richland, Washington.

Lu AH, R Khaleel, and DL Harris. 1993. *Vadose Zone Flow and Transport Modeling: C-018H Soil Column Disposal Siting Evaluation*. Appendix D of WHC-SD-C018H-RPT-001, Rev. 0, Westinghouse Hanford Company, Richland, Washington.

McKee EH, DA Swanson, and TL Wright. 1977. *Duration and Volume of Columbia River Basalt Volcanism: Washington, Oregon, Idaho*, Geological Society of America Abstracts with Programs, v. 9, no. 4, pp, 463-464.

Reidel SP and KR Fecht. 1981. *Wanapum and Saddle Mountains Basalts of the Cold Creek Syncline Area*, in CW Myers and SM Price, *eds*., Subsurface Geology of the Cold Creek Syncline, RHO-BWI-ST-14, Rockwell Hanford Operations, Richland, Washington.

Reidel SP and EC Thornton. 1993. *Characterization Report, C-018H Disposal Siting Evaluation*. WHC-SD-C018H-RPT-001, Rev. 0, Westinghouse Hanford Company, Richland, Washington.

Slate JL. 2000. *Nature and Variability of the Plio-Pleistocene Unit in the 200-West Area of the Hanford Site*. BHI-01203, Bechtel Hanford Company, Richland, Washington.

Swanson. 1994. *1994 Characterization Report for the Proposed State-Approved Land Disposal Site*. WHC-SD-C018H-RPT-003, Rev. 0, Westinghouse Hanford Company, Richland, Washington.

Tallman AM, JT Lillie, and KR Fecht. 1981. *Suprabasalt Sediment of the Cold Creek Syncline Area,* in Myers, CW and SM Price, *eds*., Subsurface Geology of the Cold Creek Syncline, RHO-BWI-ST-14, Rockwell Hanford Operations, Richland, Washington.

Thorne PD and DR Newcomer. 1992. *Summary and Evaluation of Available Hydraulic Property Data for the Hanford Site Unconfined Aquifer System.* PNL-8337, Pacific Northwest Laboratory, Richland, Washington.

Thorne PD, MA Chamness, VR Vermeul, QC MacDonald, and SE Schubert. 1994. *Three-Dimensional Conceptual Model for the Hanford Site Unconfined Aquifer System, FY 1994 Status Report.* PNL-10195, Pacific Northwest Laboratory, Richland, Washington.

Vermeul VR, CR Cole, MP Bergeron, PD Thorne, and SK Wurstner. 2001. *Transient Inverse Calibration of Site-Wide Groundwater Model to Hanford Operational Impacts from 1943 to 1996--Alternative Conceptual Model Considering Interaction with Uppermost Basalt Confined Aquifer*. PNNL-13623, Pacific Northwest National Laboratory, Richland, Washington.

Vermeul VR, MP Bergeron, CR Cole, CJ Murray, WE Nichols, TD Scheibe, PD Thorne, SR Waichler, and Y Xie. 2003. *Transient Inverse Calibration of the Site-Wide Groundwater Flow Model (ACM-2): FY03 Progress Report.* PNNL-14398, Pacific Northwest National Laboratory, Richland, Washington.

Walters WH, MC Richmond, and BG Gilmore. 1994. *Reconstruction of Radionuclide Concentrations in the Columbia River from Hanford, Washington to Portland Oregon, January 1950–January 1971*. PNWD-2225 HEDR, Battelle Pacific Northwest Laboratories, Richland, Washington.

White MD and M Oostrom. 1996. *STOMP Subsurface Transport Over Multiple Phases: Theory Guide*. PNNL-11217, Pacific Northwest National Laboratory, Richland, Washington.

Williams BA, BN Bjornstad, R Schalla, and WD Webber. 2002. *Revised Hydrogeology for the Suprabasalt Aquifer System, 200-West Area and Vicinity, Hanford Site, Washington*. PNNL-13858, Pacific Northwest National Laboratory, Richland, Washington.

Wood MI, R Schalla, BN Bjornstad, and SM Narbutovskih. 2000. *Subsurface Conditions Description of the B-BX-BY Waste Management Area.* HNF-5507, Rev. 0, CH2M HILL Hanford Group, Inc, Richland, Washington.

Wurstner SK, PD Thorne, MA Chamness, MD Freshley, and MD Williams. 1995. *Development of a Three-Dimensional Groundwater Model of the Hanford Site Unconfined Aquifer System: FY 1995 Status Report*. PNL-10886, Pacific Northwest Laboratory, Richland, Washington.

Appendix A

Summary of Projected Liquid Effluent and Tritium Discharges to SALDS Facility

Table A.1. Projected ETF Stream Sources

Fiscal Year	200-UP-1 Groundwater		ERDF Leachate		GW Well Sampling Purgewater		Mixed Waste Trench Leachate		SNF Operation KE/KW Basin & CVDF Water		SNF KE/KW Basin Water Removal		LERF Basin 44 Inventory		FFTF Sodium Cleanout Waste	
	CERCLA		CERCLA		CERCLA		RCRA		CERCLA		CERCLA		CERCLA		CERCLA	
	Volume (gal)	Tritium (pCi/L)	Volume (gal)	Tritium (pCi/L)	Volume (gal)	Tritium (pCi/L)	Volume (gal)	Tritium (pCi/L)	Volume (gal)	Tritium (pCi/L)	Volume (gal)	Tritium (pCi/L)	Volume (gal)	Tritium (pCi/L)	Volume (gal)	Tritium (pCi/L)
2004	25,000,000	640	1,000,000	460			300,000	0	150,000	1.96E+06	248,000	1.96E+06	2,000,000	4.50E+06		
2005	12,500,000	640	1,000,000	460	325,000	640	300,000	0			1,160,000	1.96E+06	2,000,000	4.50E+06		
2006	25,000,000	640	1,000,000	460	325,000	640	300,000	0			1,192,000	1.96E+06	1,000,000	4.50E+06		
2007	25,000,000	640	1,000,000	460	225,000	640	300,000	0								
2008	25,000,000	640	1,000,000	460	225,000	640	300,000	0							1,500,000	0
2009	25,000,000	640	1,000,000	460	225,000	640	300,000	0								
2010			1,000,000	460	225,000	640	300,000	0								
2011			1,000,000	460	225,000	640	100,000	0								
2012			1,000,000	460	225,000	640										
2013			1,000,000	460	225,000	640										
2014			1,000,000	460	225,000	640										
2015			1,000,000	460	225,000	640										
2016			1,000,000	460	225,000	640										
2017			1,000,000	460	225,000	640										
2018			1,000,000	460	225,000	640										
2019					225,000	640										
2020					225,000	640										
2021					225,000	640										
2022					225,000	640										
2023					225,000	640										
2024					225,000	640										
2025					225,000	640										
2026					225,000	640										
2027					225,000	640										
2028					225,000	640										
2029					225,000	640										
2030					225,000	640										
TOTAL	137,500,000		15,000,000		6,050,000		2,200,000		150,000		2,600,000		5,000,000		1,500,000	

Fiscal Year	WESF Basin Water		Other Liquid Effluents		242-A Evaporator Process Condensate		IDF Trench Leachate		CHG Supplemental Treatment: BulkVit		CHG Supplemental Treatment: CH-TRUM		Waste Treatment Plant		TOTAL ALL SOURCES	
	CERCLA		CERCLA		RCRA		RCRA		RCRA		RCRA		RCRA			
	Volume (gal)	Tritium (pCi/L)	Volume (gal)	Tritium (pCi/L)	Volume (gal)	Tritium (pCi/L)	Volume (gal)	Tritium (pCi/L)	Volume (gal)	Tritium (pCi/L)	Volume (gal)	Tritium (pCi/L)	Volume (gal)	Tritium (pCi/L)	Volume (gal)	Tritium (Ci)
2004			100,000	5.00E+04	4,000,000	1.09E+06									32,798,000	14.2
2005			100,000	5.00E+04	4,000,000	1.09E+06			484,700	1.09E+06	2,940,000	1.09E+06			24,809,700	19.4
2006			100,000	5.00E+04	4,000,000	1.09E+06			1,131,000	1.09E+06	2,010,000	1.09E+06			36,058,000	14.6
2007			100,000	5.00E+04	4,000,000	1.09E+06	500,000	460	1,131,000	1.09E+06					32,256,000	5.61
2008			100,000	5.00E+04	4,000,000	1.09E+06	1,000,000	460							33,125,000	4.38
2009			100,000	5.00E+04	4,000,000	1.09E+06	1,000,000	460					6,250,000	5.26E+06	37,875,000	37.3
2010			100,000	5.00E+04	4,000,000	1.09E+06	1,000,000	460					5,770,000	5.26E+06	12,395,000	34.7
2011			100,000	5.00E+04	4,000,000	1.09E+06	1,000,000	460					6,900,000	5.26E+06	13,325,000	40.7
2012			100,000	5.00E+04			1,000,000	460					6,860,000	5.26E+06	9,185,000	36.1
2013			100,000	5.00E+04			1,000,000	460					6,660,000	5.26E+06	8,985,000	35.1
2014			100,000	5.00E+04			1,000,000	460					7,040,000	5.26E+06	9,365,000	37.1
2015			100,000	5.00E+04			1,000,000	460					6,850,000	5.26E+06	9,175,000	36.1
2016			100,000	5.00E+04			1,000,000	460					6,740,000	5.26E+06	9,065,000	35.5
2017			100,000	5.00E+04			1,000,000	460					6,800,000	5.26E+06	9,125,000	35.8
2018			100,000	5.00E+04			1,000,000	460					6,800,000	5.26E+06	9,125,000	35.8
2019			100,000	5.00E+04			1,000,000	460					6,800,000	5.26E+06	8,125,000	35.8
2020			100,000	5.00E+04			1,000,000	460					6,800,000	5.26E+06	8,125,000	35.8
2021	90,000	0	100,000	5.00E+04			1,000,000	460					6,800,000	5.26E+06	8,215,000	35.8
2022			100,000	5.00E+04			1,000,000	460					6,800,000	5.26E+06	8,125,000	35.8
2023			100,000	5.00E+04			1,000,000	460					6,800,000	5.26E+06	8,125,000	35.8
2024			100,000	5.00E+04			1,000,000	460					6,800,000	5.26E+06	8,125,000	35.8
2025			100,000	5.00E+04			1,000,000	460					6,800,000	5.26E+06	8,125,000	35.8
2026			100,000	5.00E+04			1,000,000	460					6,800,000	5.26E+06	8,125,000	35.8
2027			100,000	5.00E+04			1,000,000	460					6,800,000	5.26E+06	8,125,000	35.8
2028			100,000	5.00E+04			1,000,000	460						5.26E+06	1,325,000	5.60E-03
2029			100,000	5.00E+04			1,000,000	460							1,325,000	5.60E-03
2030			100,000	5.00E+04			1,000,000	460							1,325,000	5.60E-03
TOTAL	90,000		2,700,000		32,000,000		23,500,000		2,746,700		4,950,000		127,870,000		363,856,700	745

Volume and time data is from Steve Lowe's spreadsheet, "LERF - ETF Waste Receipts".

Tritium results were collected by Mark Bowman from various sources, as noted. When possible, actual sample results were used.

Appendix B

Maps of Simulated Water-Level Elevations for Selected Time Planes between 1997 and 2140 in Vicinity of the SALDS Facility

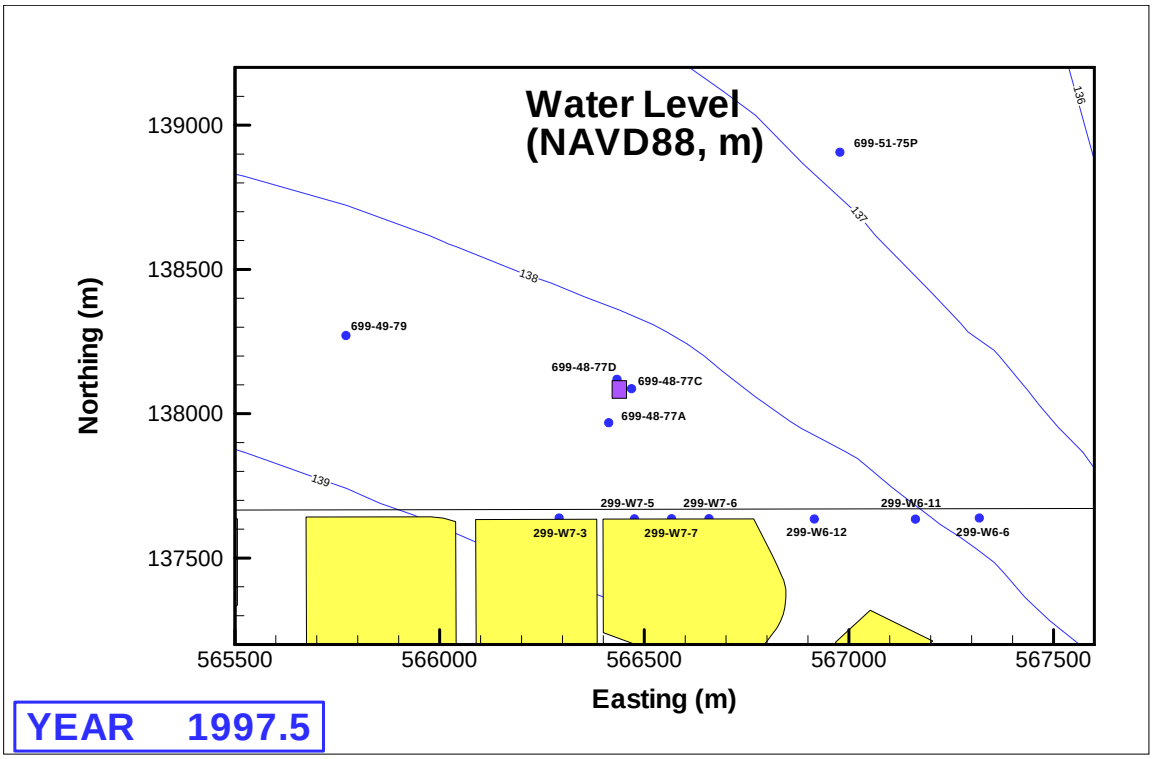
Water Level
(NAVD88, m)
699-51-75P
699-49-79
699-48-77D
699-48-77C
699-48-77A
299-W7-5
299-W7-6
299-W6-11
299-W7-3
299-W7-7
299-W6-12
299-W6-6
136
137
138
139
139000
138500
138000
137500
565500
566000
566500
567000
567500
Northing (m)
Easting (m)
YEAR 1997.5

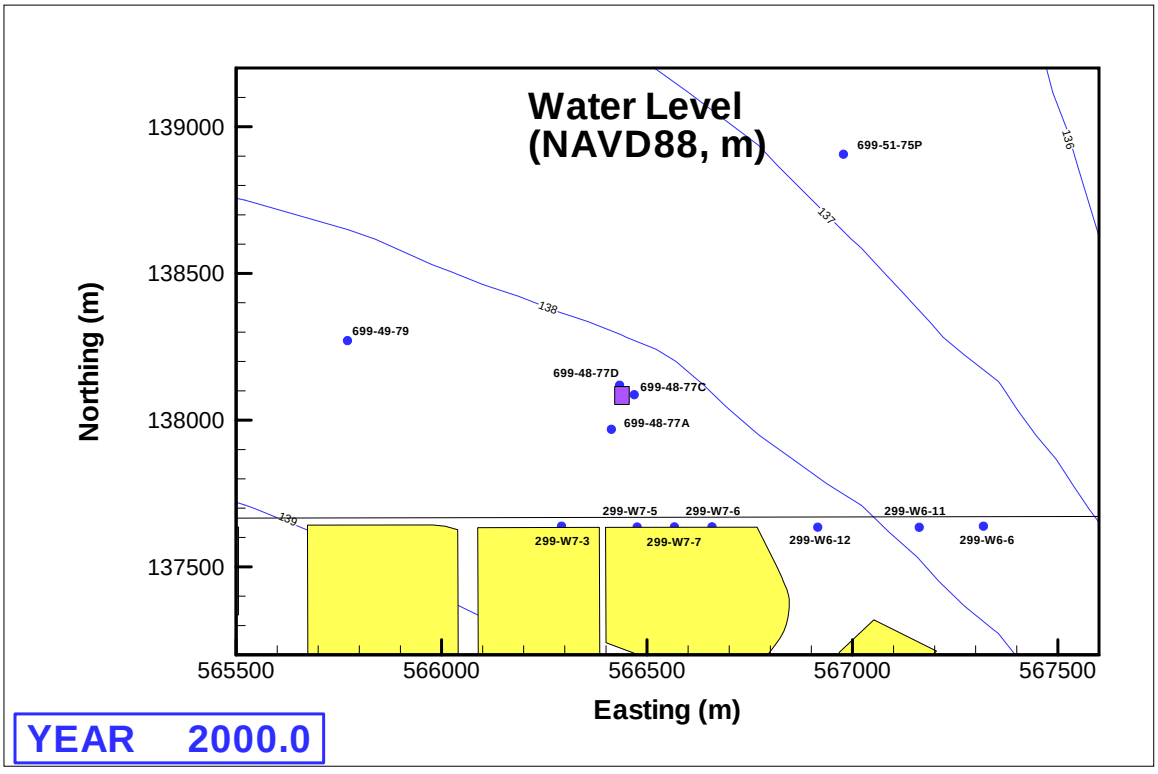
Water Level
(NAVD88, m)
699-51-75P
699-49-79
699-48-77D
699-48-77C
699-48-77A
299-W7-5
299-W7-6
299-W6-11
299-W7-3
299-W7-7
299-W6-12
299-W6-6
136
137
138
139
139000
138500
138000
137500
565500
566000
566500
567000
567500
Northing (m)
Easting (m)
YEAR 2000.0

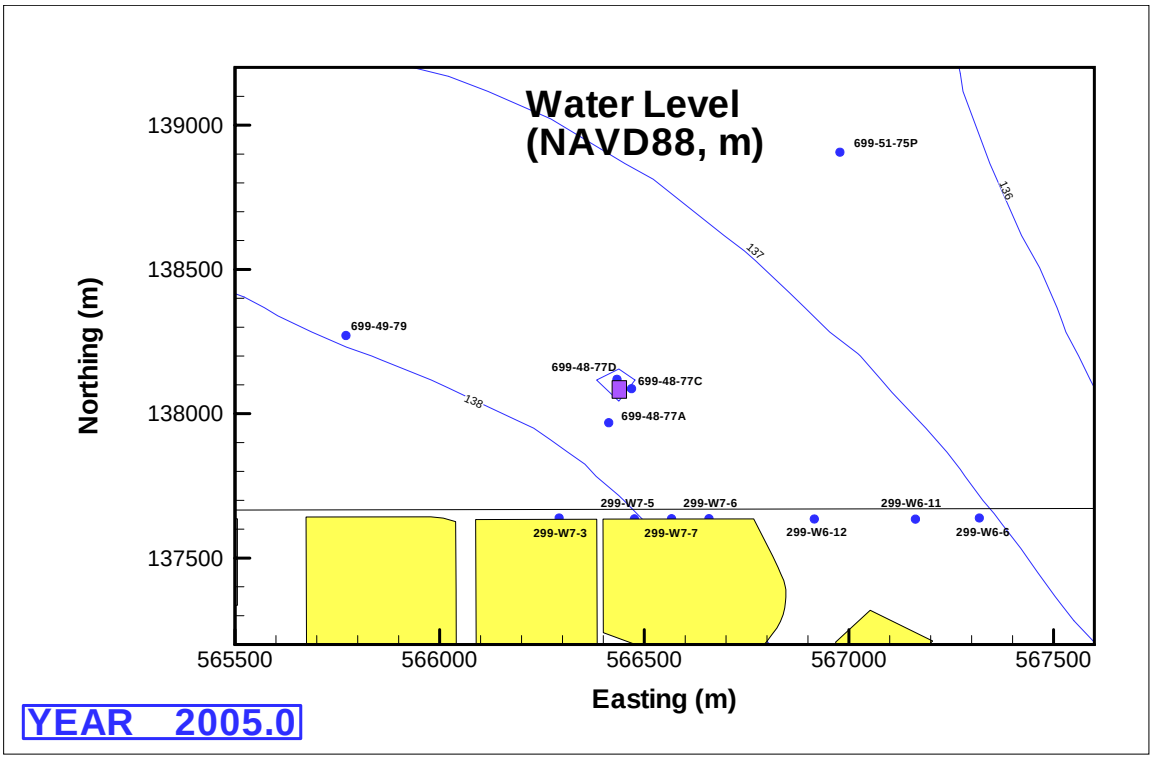
Water Level
(NAVD88, m)
699-51-75P
136
137
699-49-79
138
699-48-77D
699-48-77C
699-48-77A
299-W7-5
299-W7-6
299-W6-11
299-W7-3
299-W7-7
299-W6-12
299-W6-6
139000
138500
138000
137500
Northing (m)
565500
566000
566500
567000
567500
Easting (m)
YEAR 2005.0

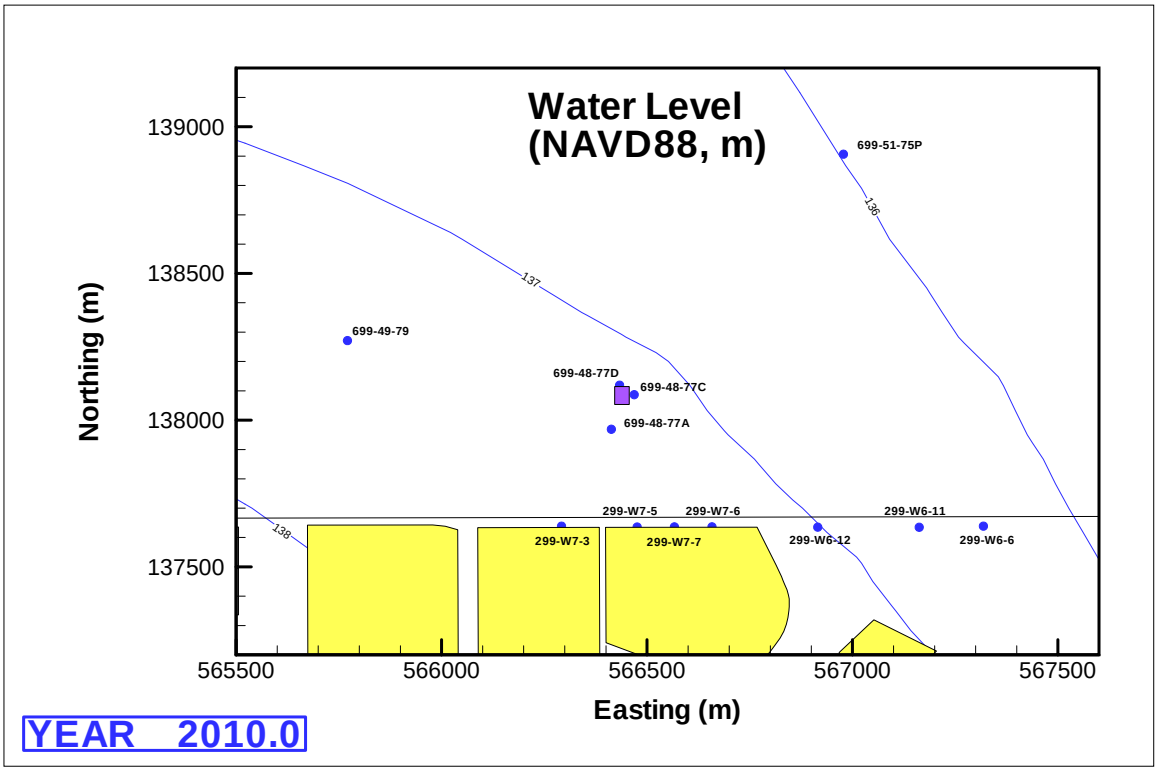
Water Level
(NAVD88, m)
699-51-75P
136
137
699-49-79
138
699-48-77D
699-48-77C
699-48-77A
299-W7-5
299-W7-6
299-W6-11
299-W7-3
299-W7-7
299-W6-12
299-W6-6
139000
138500
138000
137500
Northing (m)
565500
566000
566500
567000
567500
Easting (m)
YEAR 2010.0

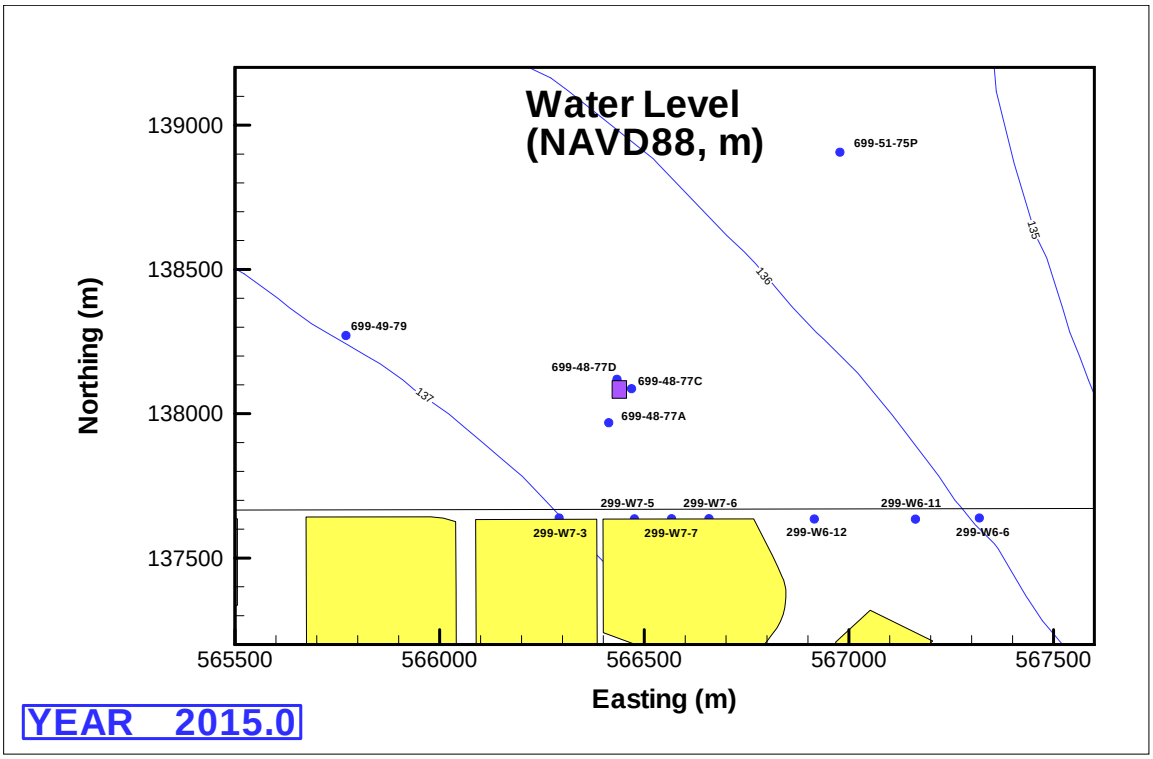
Water Level
(NAVD88, m)
699-51-75P
699-49-79
699-48-77D
699-48-77C
699-48-77A
299-W7-5
299-W7-6
299-W6-11
299-W7-3
299-W7-7
299-W6-12
299-W6-6
135
136
137
139000
138500
138000
137500
565500
566000
566500
567000
567500
Northing (m)
Easting (m)
YEAR 2015.0

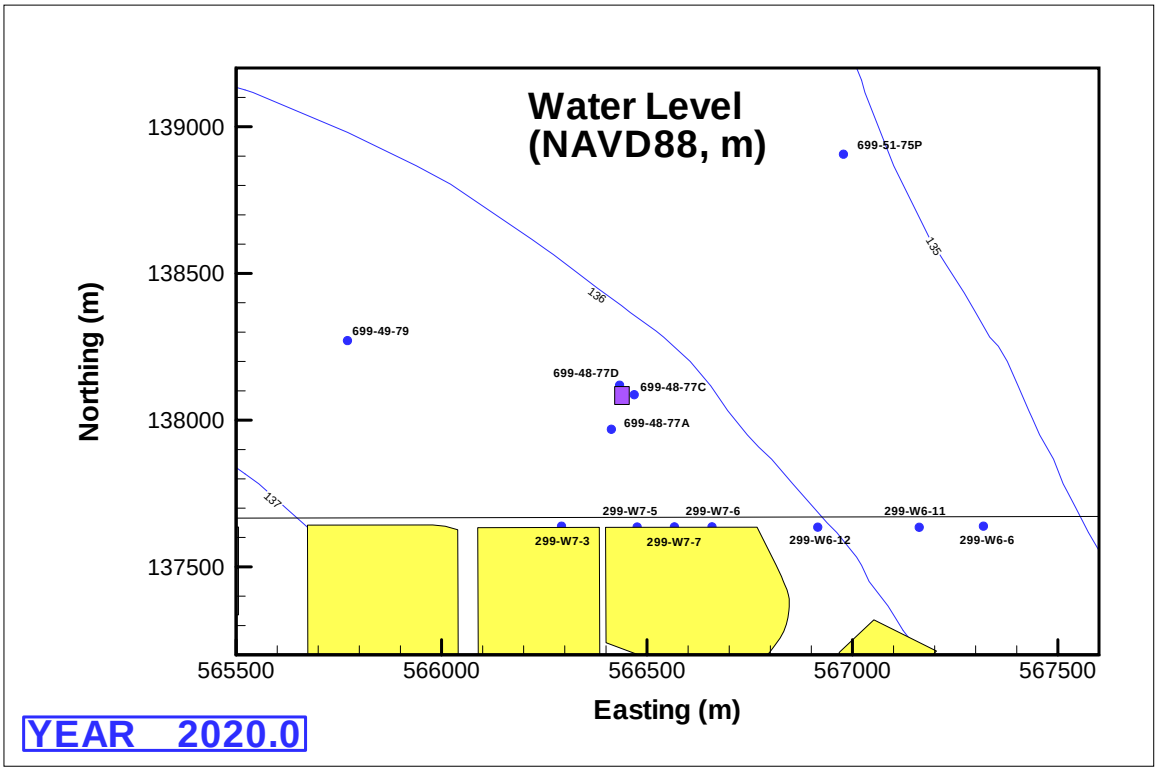
Water Level
(NAVD88, m)
699-51-75P
699-49-79
699-48-77D
699-48-77C
699-48-77A
299-W7-5
299-W7-6
299-W6-11
299-W7-3
299-W7-7
299-W6-12
299-W6-6
135
136
137
139000
138500
138000
137500
565500
566000
566500
567000
567500
Northing (m)
Easting (m)
YEAR 2020.0

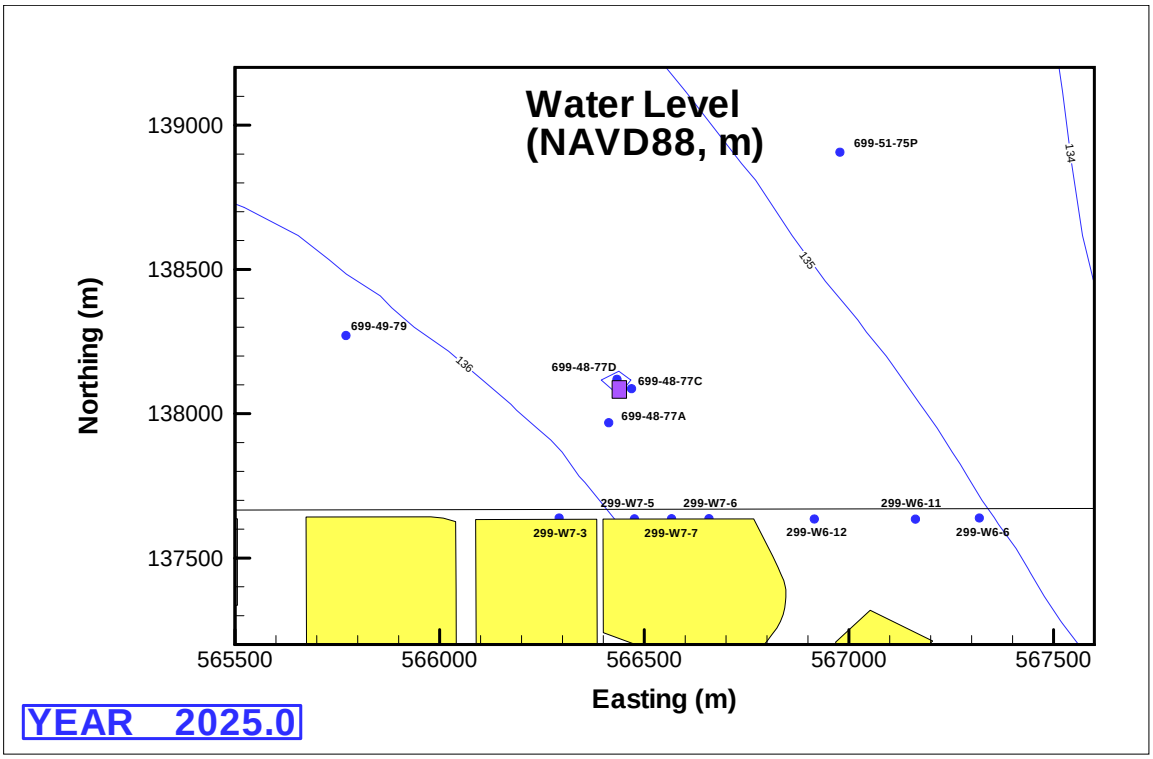
Water Level
(NAVD88, m)
699-51-75P
699-49-79
699-48-77D
699-48-77C
699-48-77A
299-W7-5
299-W7-6
299-W6-11
299-W7-3
299-W7-7
299-W6-12
299-W6-6
134
135
136
139000
138500
138000
137500
565500
566000
566500
567000
567500
Northing (m)
Easting (m)
YEAR 2025.0

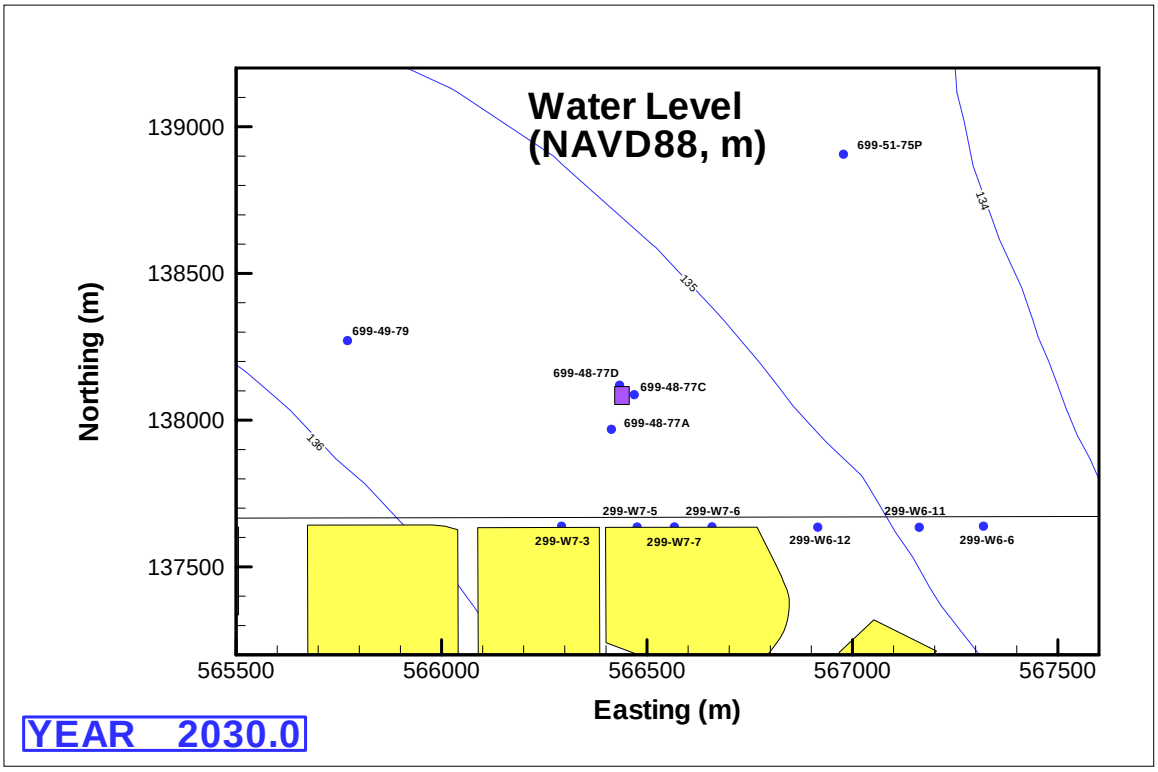
Water Level
(NAVD88, m)
699-51-75P
699-49-79
699-48-77D
699-48-77C
699-48-77A
299-W7-5
299-W7-6
299-W6-11
299-W7-3
299-W7-7
299-W6-12
299-W6-6
134
135
136
139000
138500
138000
137500
565500
566000
566500
567000
567500
Northing (m)
Easting (m)
YEAR 2030.0

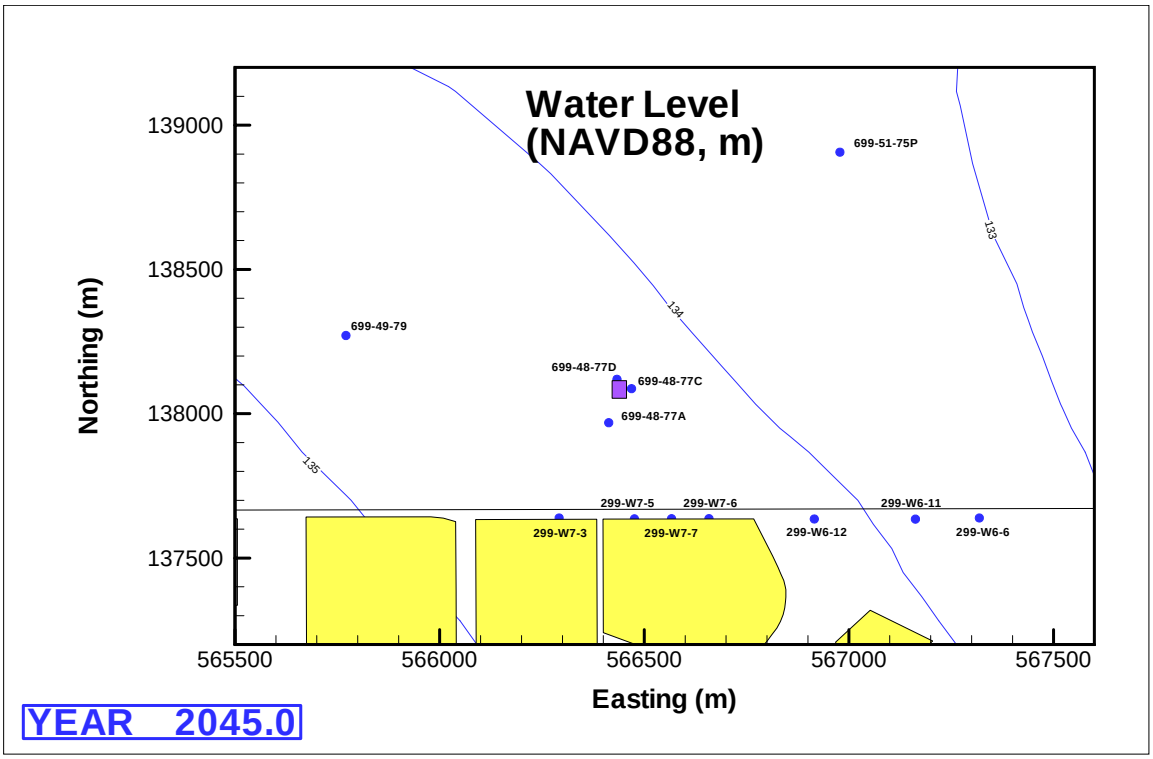
Water Level
(NAVD88, m)
699-51-75P
699-49-79
699-48-77D
699-48-77C
699-48-77A
299-W7-5
299-W7-6
299-W6-11
299-W7-3
299-W7-7
299-W6-12
299-W6-6
133
134
135
139000
138500
138000
137500
565500
566000
566500
567000
567500
Northing (m)
Easting (m)
YEAR 2045.0

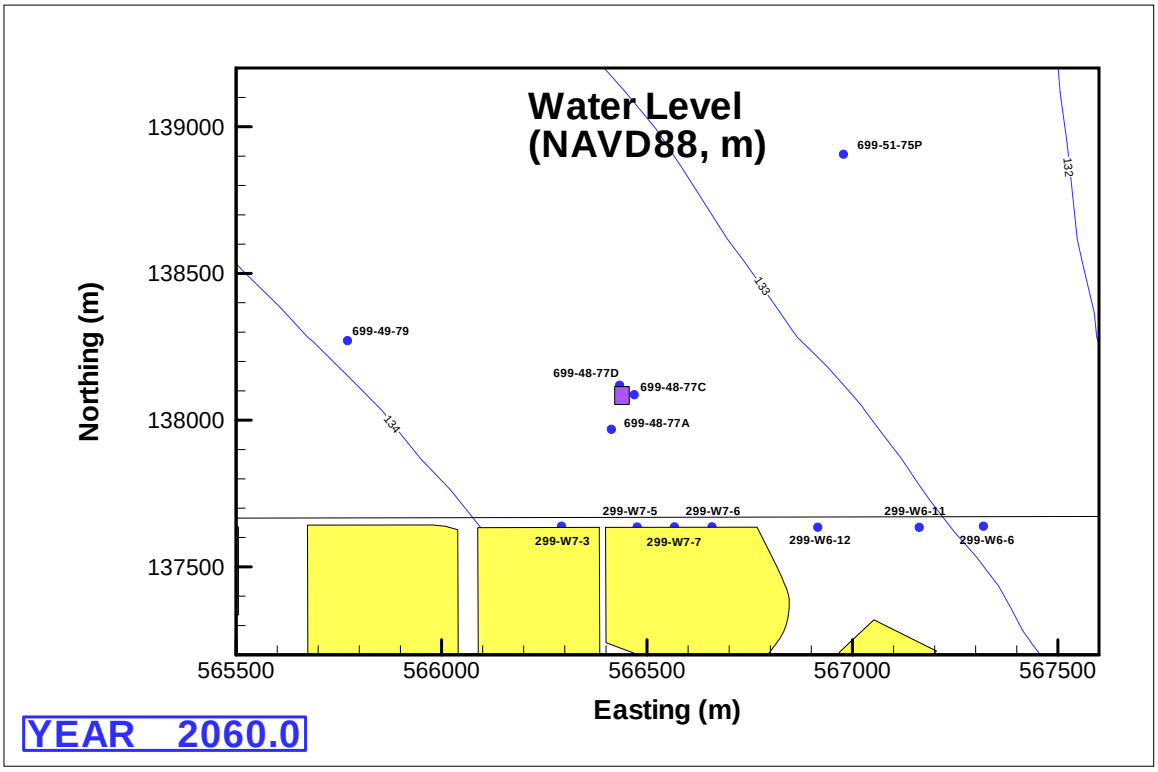
Water Level
(NAVD88, m)
699-51-75P
699-49-79
699-48-77D
699-48-77C
699-48-77A
299-W7-5
299-W7-6
299-W6-11
299-W7-3
299-W7-7
299-W6-12
299-W6-6
132
133
134
139000
138500
138000
137500
565500
566000
566500
567000
567500
Northing (m)
Easting (m)
YEAR 2060.0

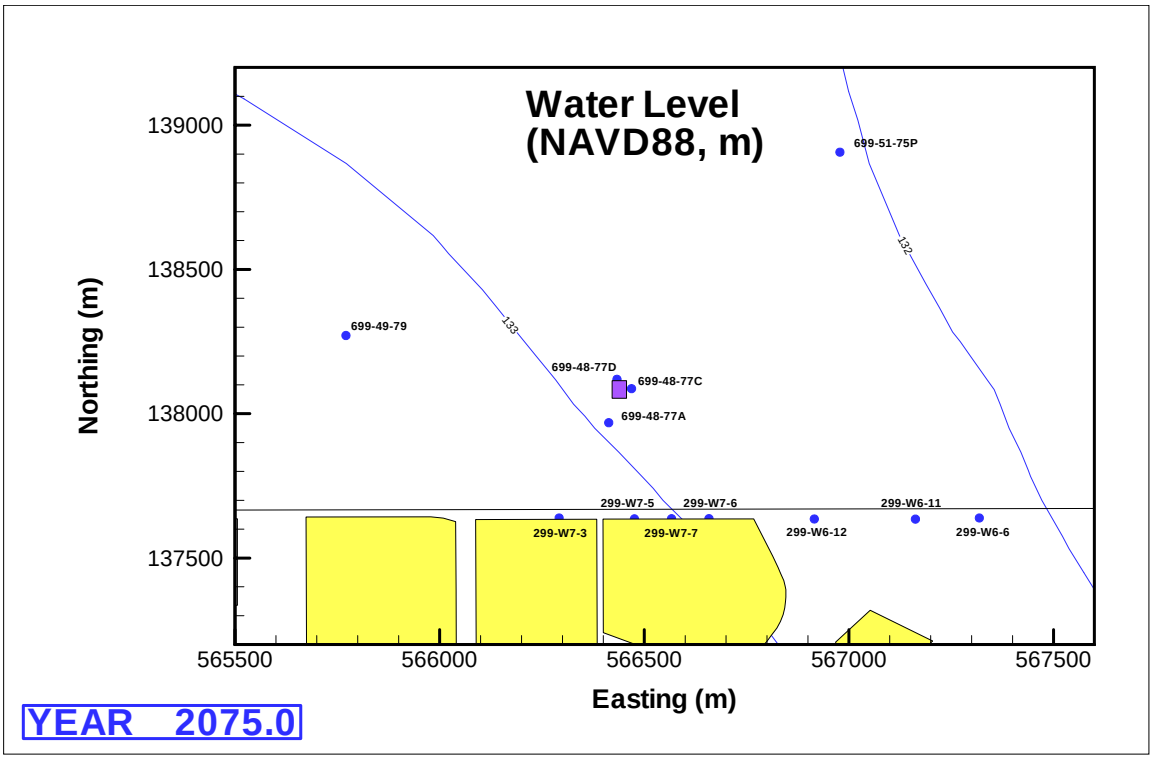
Water Level
(NAVD88, m)
699-51-75P
699-49-79
699-48-77D
699-48-77C
699-48-77A
299-W7-5
299-W7-6
299-W6-11
299-W7-3
299-W7-7
299-W6-12
299-W6-6
132
133
139000
138500
138000
137500
565500
566000
566500
567000
567500
Northing (m)
Easting (m)
YEAR 2075.0

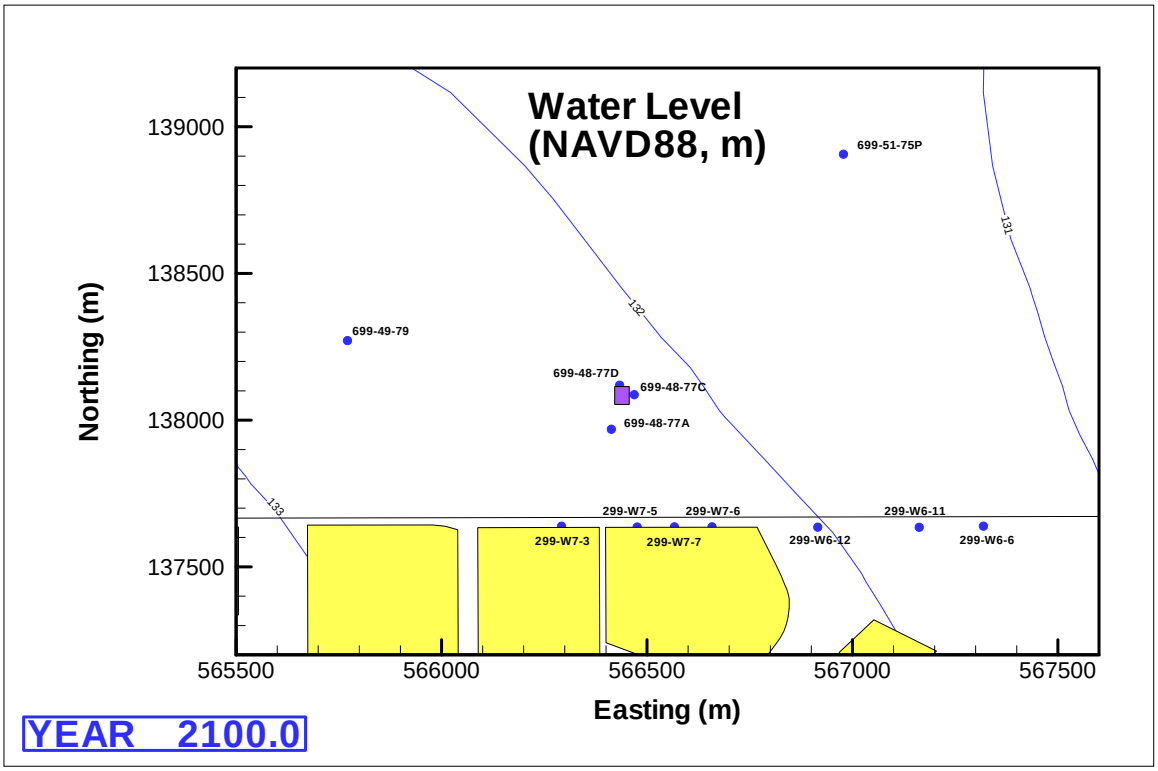
Water Level
(NAVD88, m)
699-51-75P
699-49-79
699-48-77D
699-48-77C
699-48-77A
299-W7-5
299-W7-6
299-W6-11
299-W7-3
299-W7-7
299-W6-12
299-W6-6
131
132
133
139000
138500
138000
137500
565500
566000
566500
567000
567500
Northing (m)
Easting (m)
YEAR 2100.0

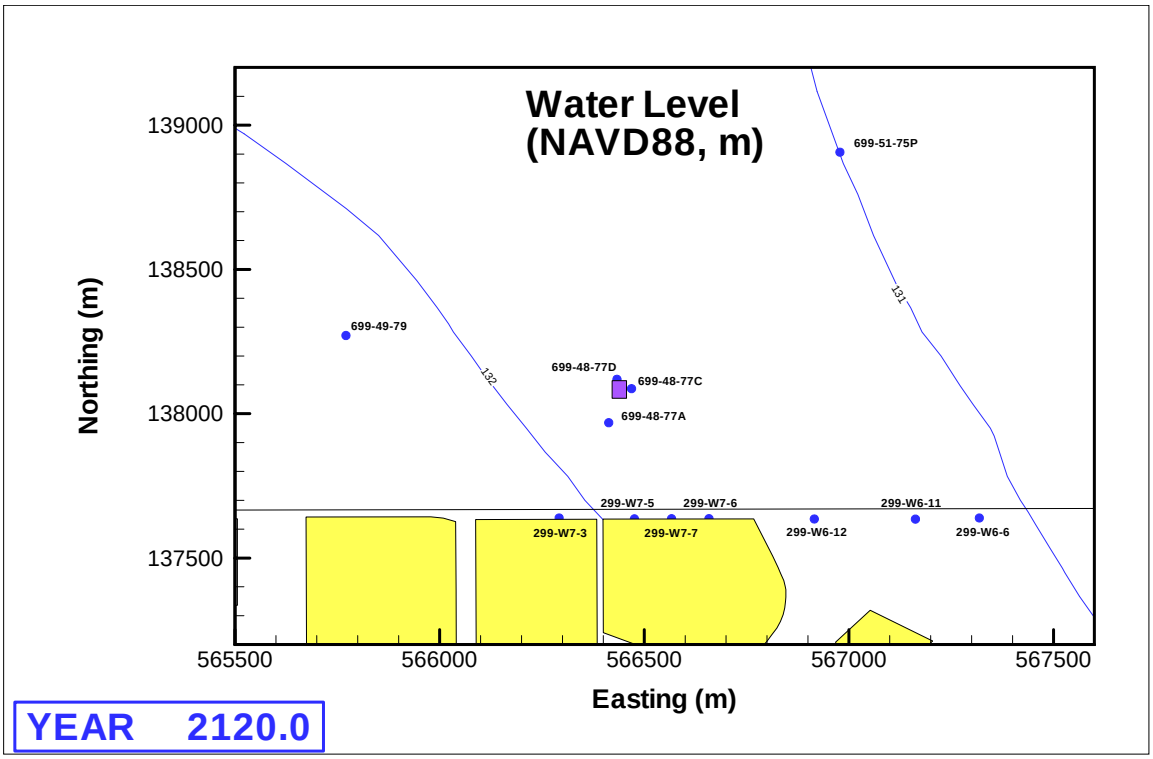
Water Level
(NAVD88, m)
699-51-75P
699-49-79
699-48-77D
699-48-77C
699-48-77A
299-W7-5
299-W7-6
299-W6-11
299-W7-3
299-W7-7
299-W6-12
299-W6-6
132
131
139000
138500
138000
137500
565500
566000
566500
567000
567500
Northing (m)
Easting (m)
YEAR 2120.0

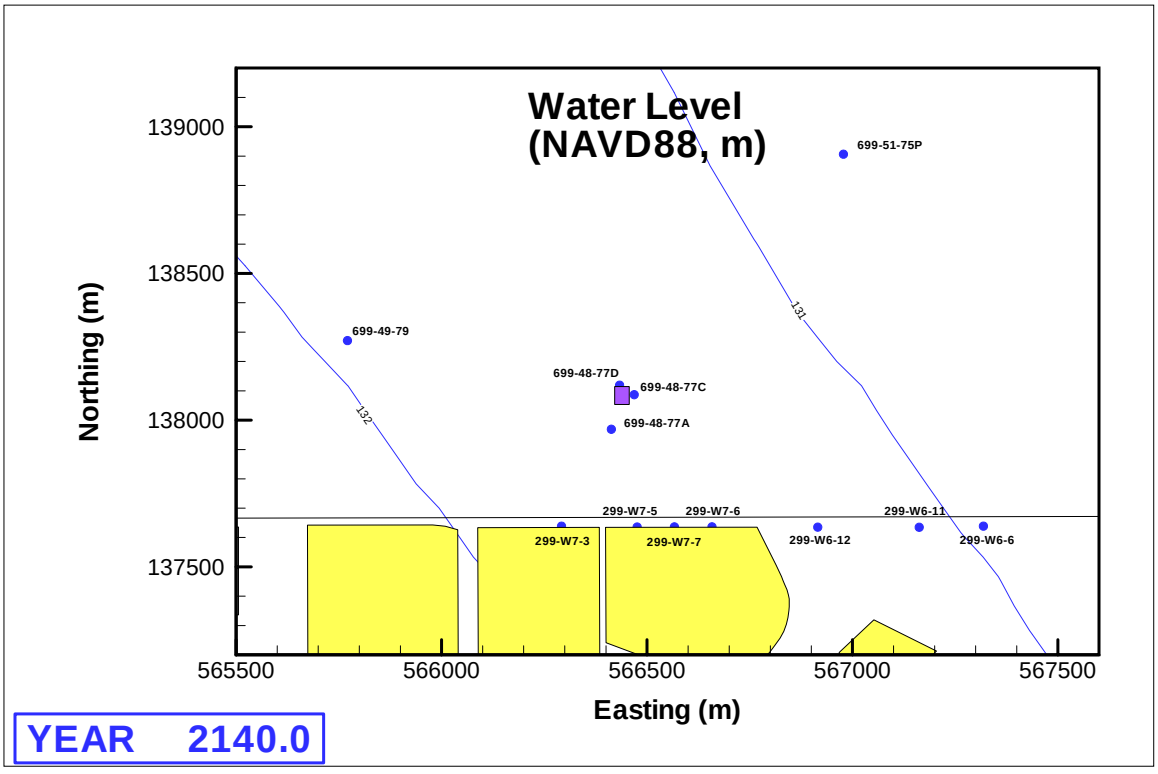
Water Level
(NAVD88, m)
699-51-75P
699-49-79
699-48-77D
699-48-77C
699-48-77A
299-W7-5
299-W7-6
299-W6-11
299-W7-3
299-W7-7
299-W6-12
299-W6-6
132
131
139000
138500
138000
137500
565500
566000
566500
567000
567500
Northing (m)
Easting (m)
YEAR 2140.0

Appendix C

Maps of Simulated Tritium Concentration Levels for Selected Time Planes between Years 1997 and 2140 in Vicinity of the SALDS Facility

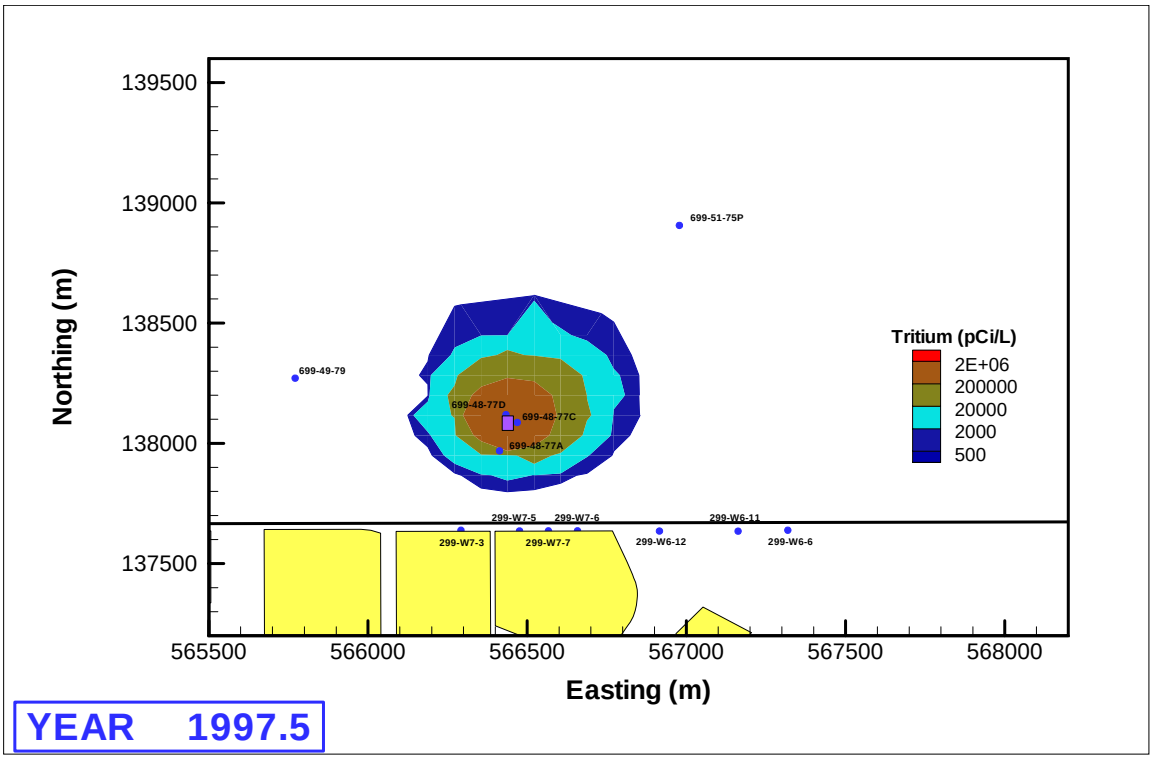
139500
139000
138500
138000
137500
Northing (m)
565500
566000
566500
567000
567500
568000
Easting (m)
699-51-75P
699-49-79
699-48-77D
699-48-77C
699-48-77A
299-W7-5
299-W7-6
299-W6-11
299-W7-3
299-W7-7
299-W6-12
299-W6-6
Tritium (pCi/L)
2E+06
200000
20000
2000
500
YEAR 1997.5

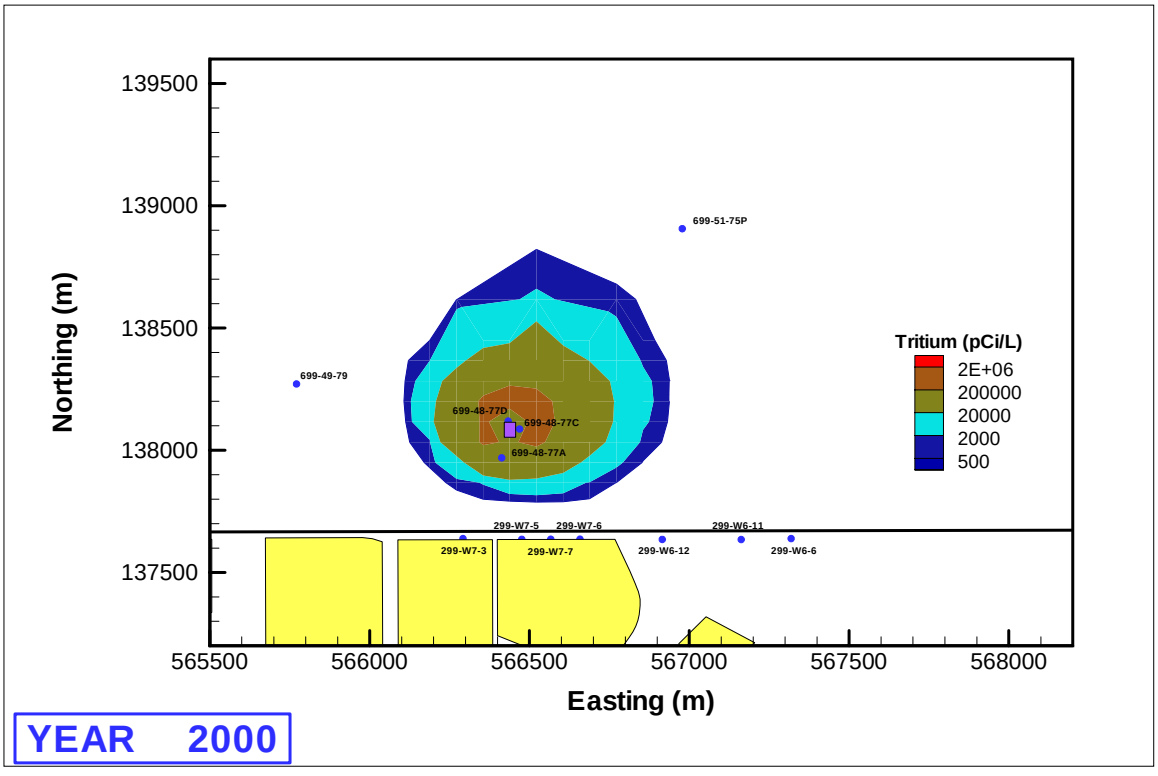
139500
139000
138500
138000
137500
Northing (m)
565500
566000
566500
567000
567500
568000
Easting (m)
699-51-75P
699-49-79
699-48-77D
699-48-77C
699-48-77A
299-W7-5
299-W7-6
299-W6-11
299-W7-3
299-W7-7
299-W6-12
299-W6-6
Tritium (pCi/L)
2E+06
200000
20000
2000
500
YEAR 2000

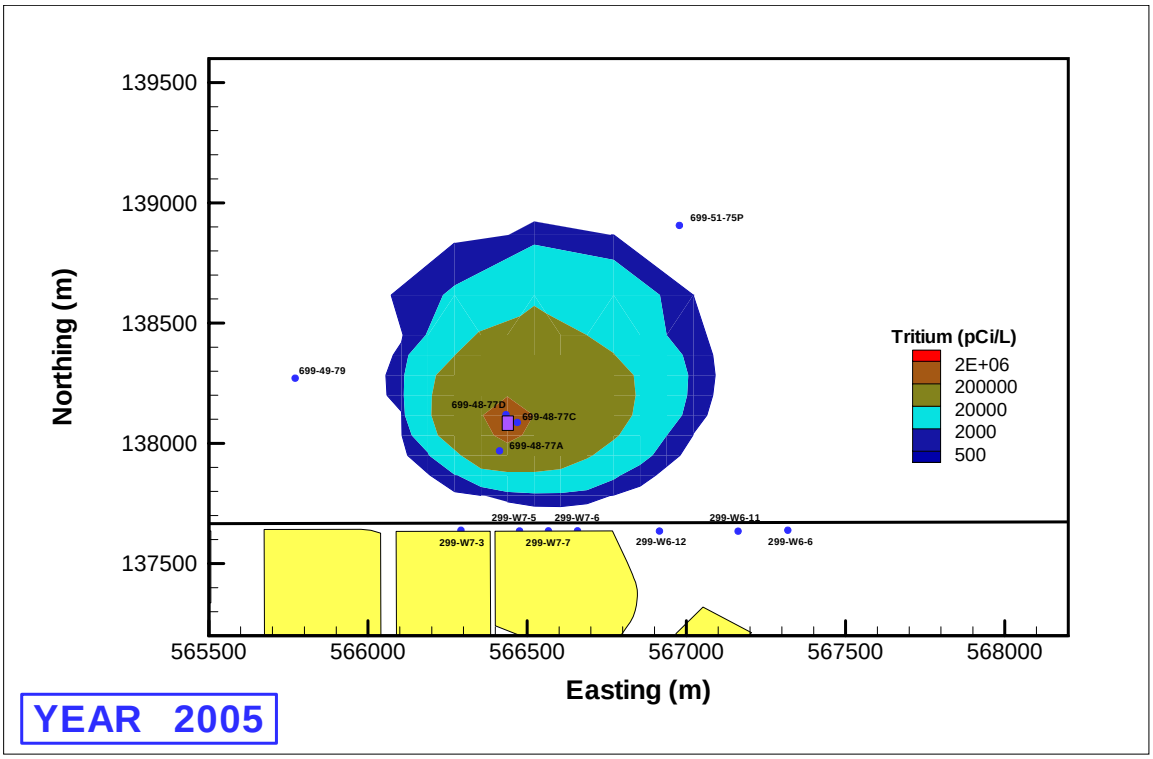
139500
139000
138500
138000
137500
Northing (m)
565500
566000
566500
567000
567500
568000
Easting (m)
699-51-75P
699-49-79
699-48-77D
699-48-77C
699-48-77A
299-W7-5
299-W7-6
299-W6-11
299-W7-3
299-W7-7
299-W6-12
299-W6-6
Tritium (pCi/L)
2E+06
200000
20000
2000
500
YEAR 2005

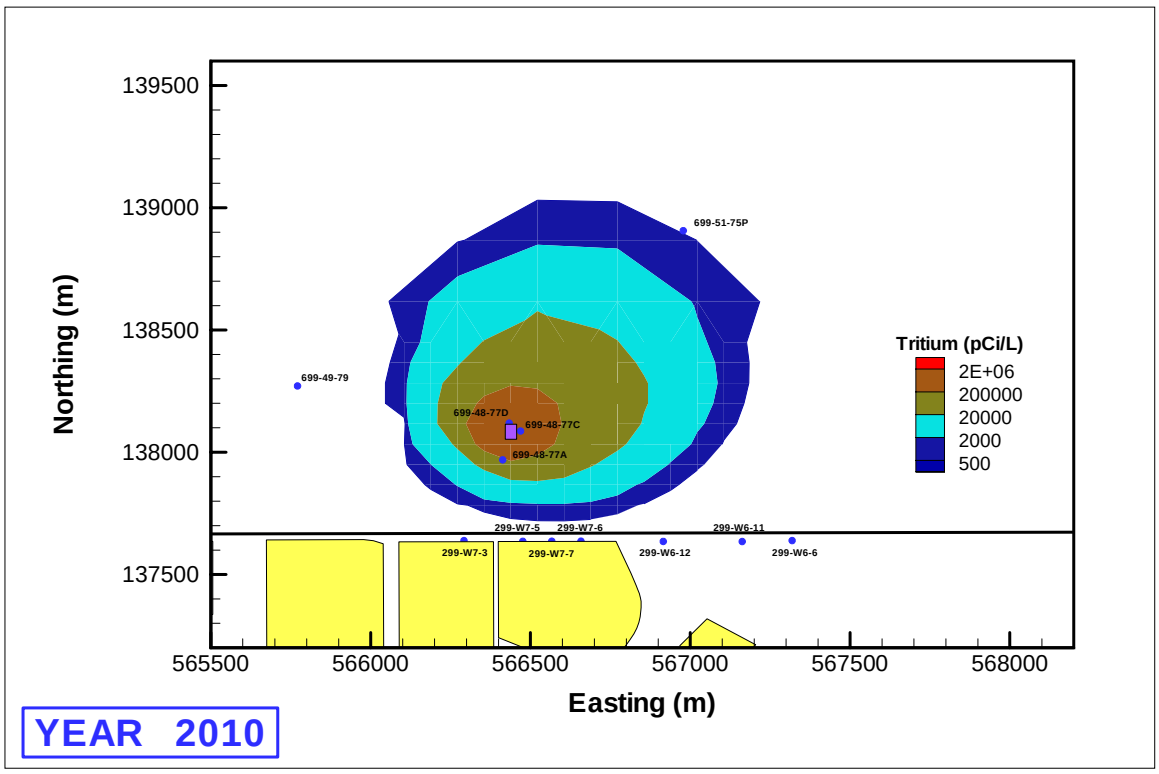
139500
139000
138500
138000
137500
Northing (m)
565500
566000
566500
567000
567500
568000
Easting (m)
699-51-75P
699-49-79
699-48-77D
699-48-77C
699-48-77A
299-W7-5
299-W7-6
299-W6-11
299-W7-3
299-W7-7
299-W6-12
299-W6-6
Tritium (pCi/L)
2E+06
200000
20000
2000
500
YEAR 2010

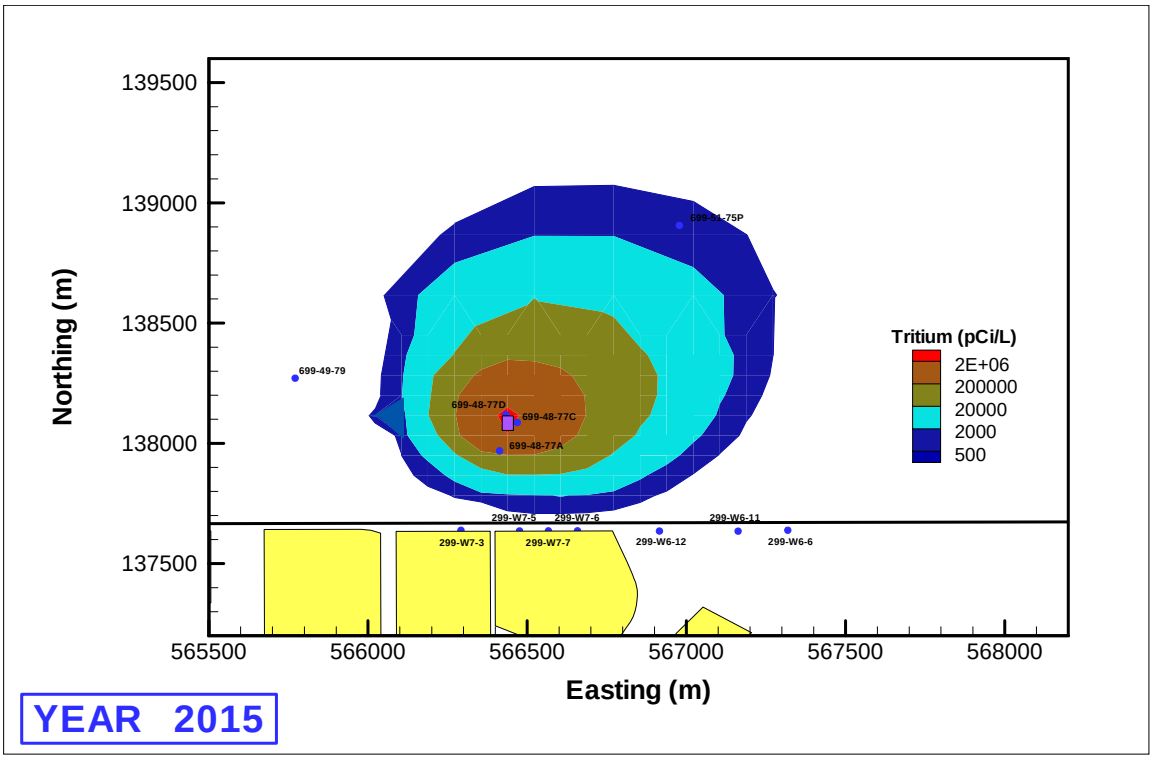
139500
139000
138500
138000
137500
Northing (m)
565500
566000
566500
567000
567500
568000
Easting (m)
699-51-75P
699-49-79
699-48-77D
699-48-77C
699-48-77A
299-W7-5
299-W7-6
299-W6-11
299-W7-3
299-W7-7
299-W6-12
299-W6-6
Tritium (pCi/L)
2E+06
200000
20000
2000
500
YEAR 2015

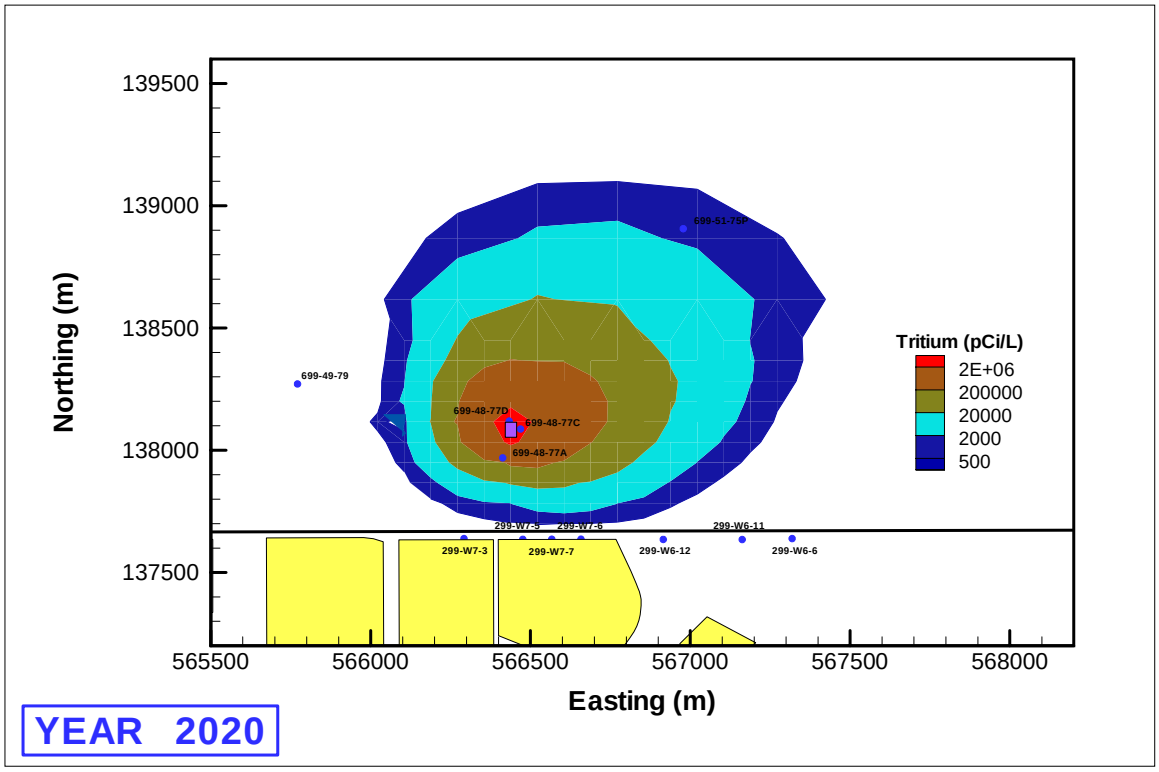
139500
139000
138500
138000
137500
Northing (m)
565500
566000
566500
567000
567500
568000
Easting (m)
699-51-75P
699-49-79
699-48-77D
699-48-77C
699-48-77A
299-W7-5
299-W7-6
299-W6-11
299-W7-3
299-W7-7
299-W6-12
299-W6-6
Tritium (pCi/L)
2E+06
200000
20000
2000
500
YEAR 2020

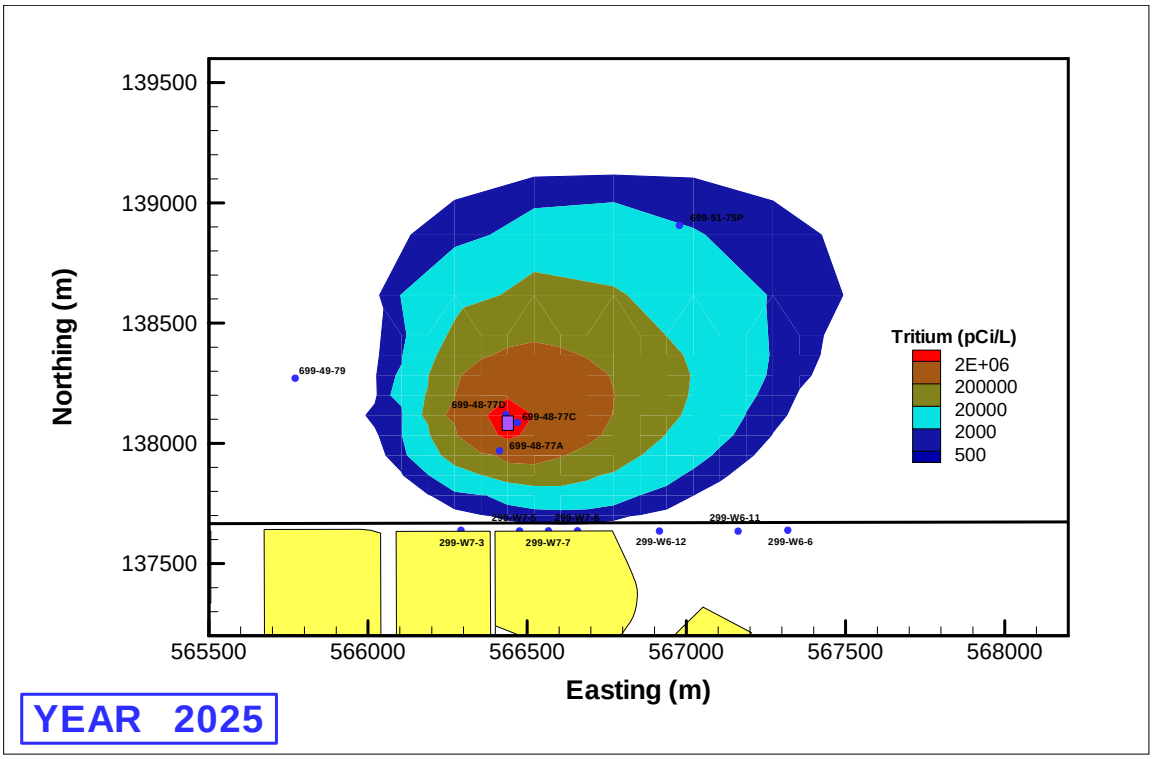
139500
139000
138500
138000
137500
Northing (m)
565500
566000
566500
567000
567500
568000
Easting (m)
699-51-75P
699-49-79
699-48-77D
699-48-77C
699-48-77A
299-W7-3
299-W7-7
299-W6-12
299-W6-11
299-W6-6
Tritium (pCi/L)
2E+06
200000
20000
2000
500
YEAR 2025

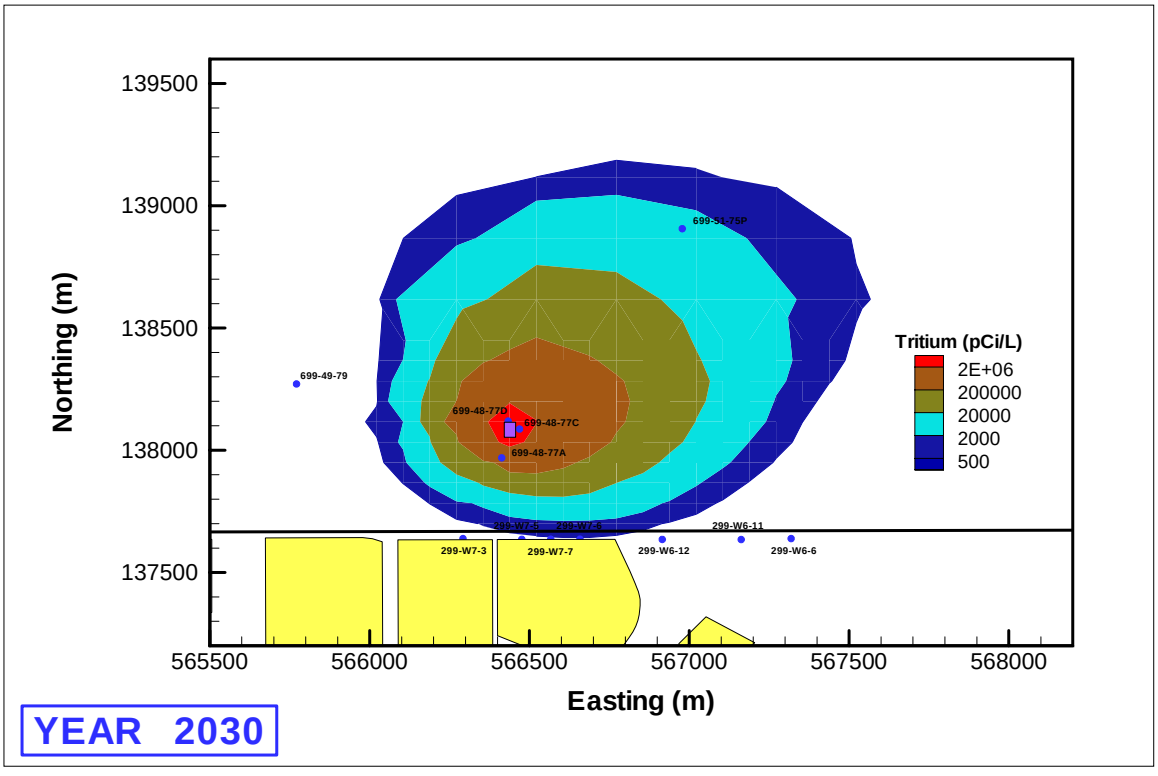
139500
139000
138500
138000
137500
Northing (m)
565500
566000
566500
567000
567500
568000
Easting (m)
699-51-75P
699-49-79
699-48-77D
699-48-77C
699-48-77A
299-W7-3
299-W7-7
299-W6-12
299-W6-11
299-W6-6
Tritium (pCi/L)
2E+06
200000
20000
2000
500
YEAR 2030

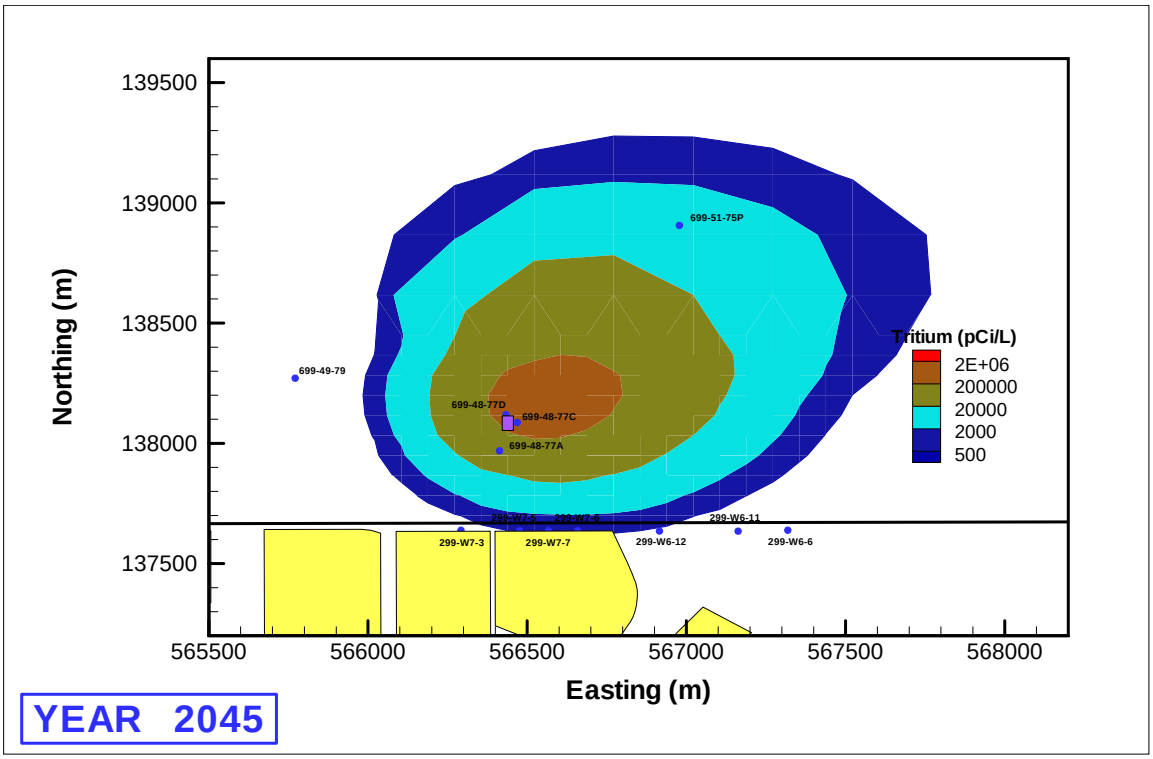
139500
139000
138500
138000
137500
Northing (m)
565500
566000
566500
567000
567500
568000
Easting (m)
699-51-75P
699-49-79
699-48-77D
699-48-77C
699-48-77A
299-W7-5
299-W7-6
299-W6-11
299-W7-3
299-W7-7
299-W6-12
299-W6-6
Tritium (pCi/L)
2E+06
200000
20000
2000
500
YEAR 2045

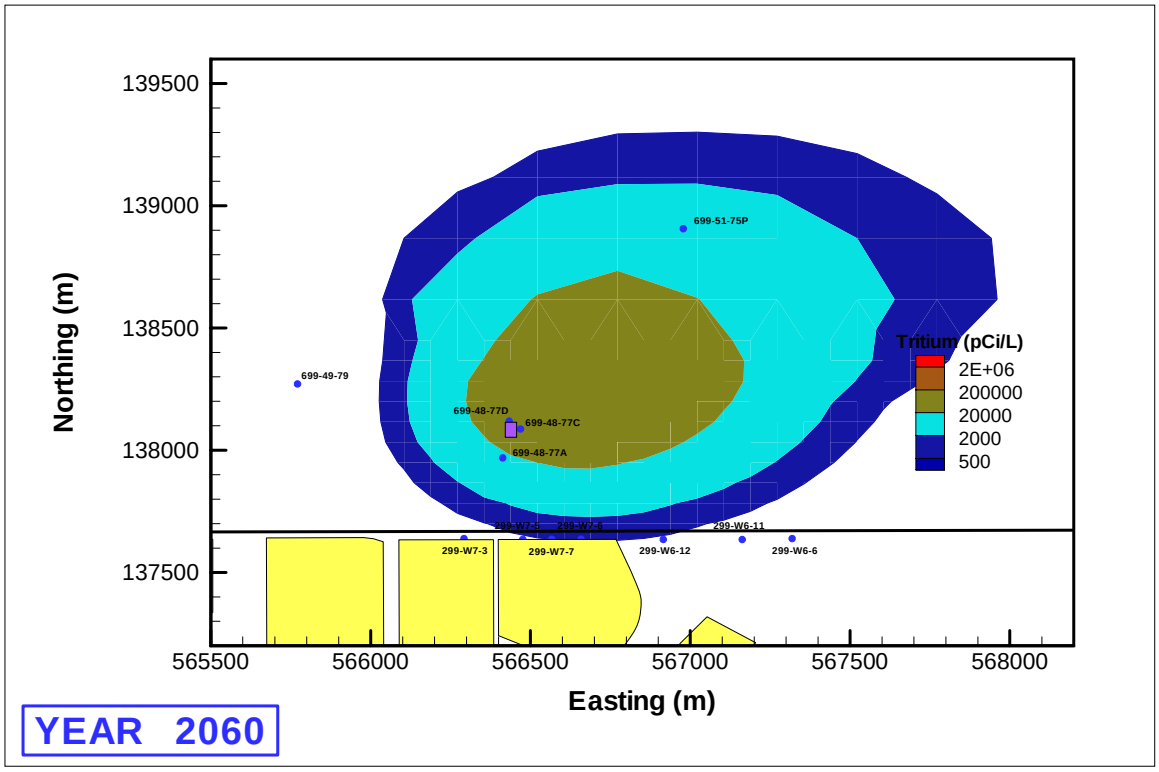
139500
139000
138500
138000
137500
Northing (m)
565500
566000
566500
567000
567500
568000
Easting (m)
699-51-75P
699-49-79
699-48-77D
699-48-77C
699-48-77A
299-W7-5
299-W7-6
299-W6-11
299-W7-3
299-W7-7
299-W6-12
299-W6-6
Tritium (pCi/L)
2E+06
200000
20000
2000
500
YEAR 2060

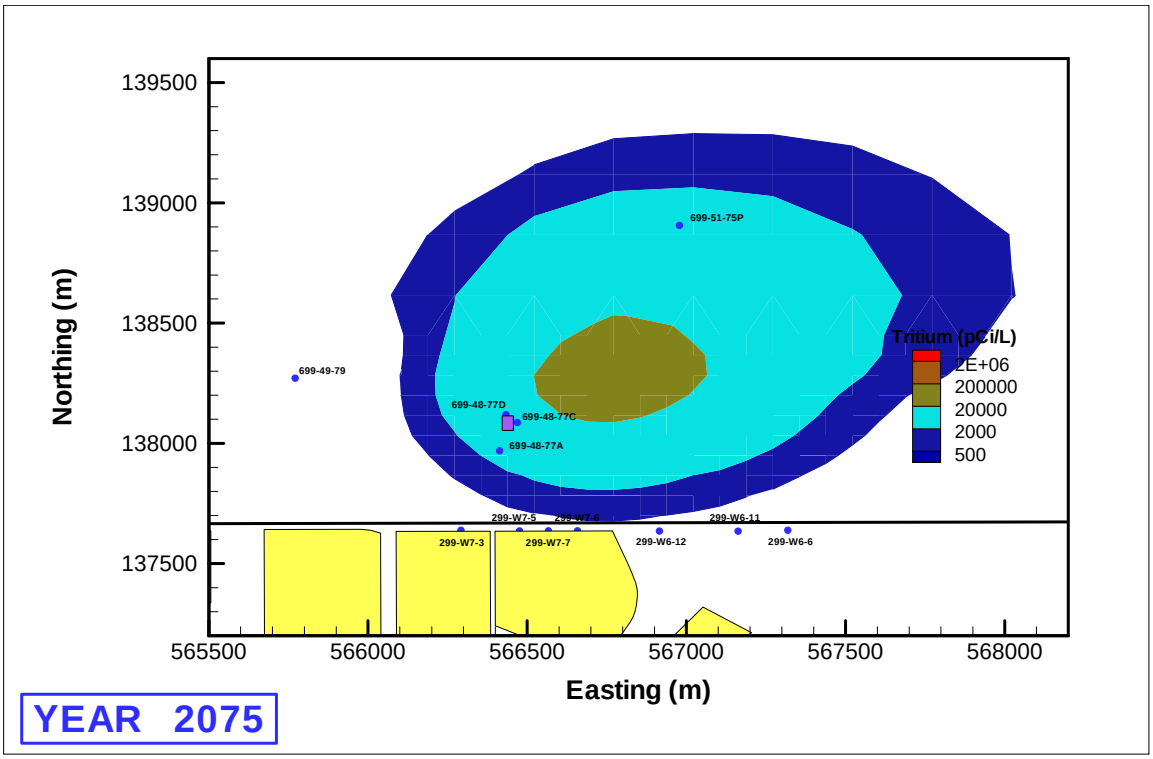
139500
139000
138500
138000
137500
Northing (m)
565500
566000
566500
567000
567500
568000
Easting (m)
699-51-75P
699-49-79
699-48-77D
699-48-77C
699-48-77A
299-W7-5
299-W7-6
299-W6-11
299-W7-3
299-W7-7
299-W6-12
299-W6-6
Tritium (pCi/L)
2E+06
200000
20000
2000
500
YEAR 2075

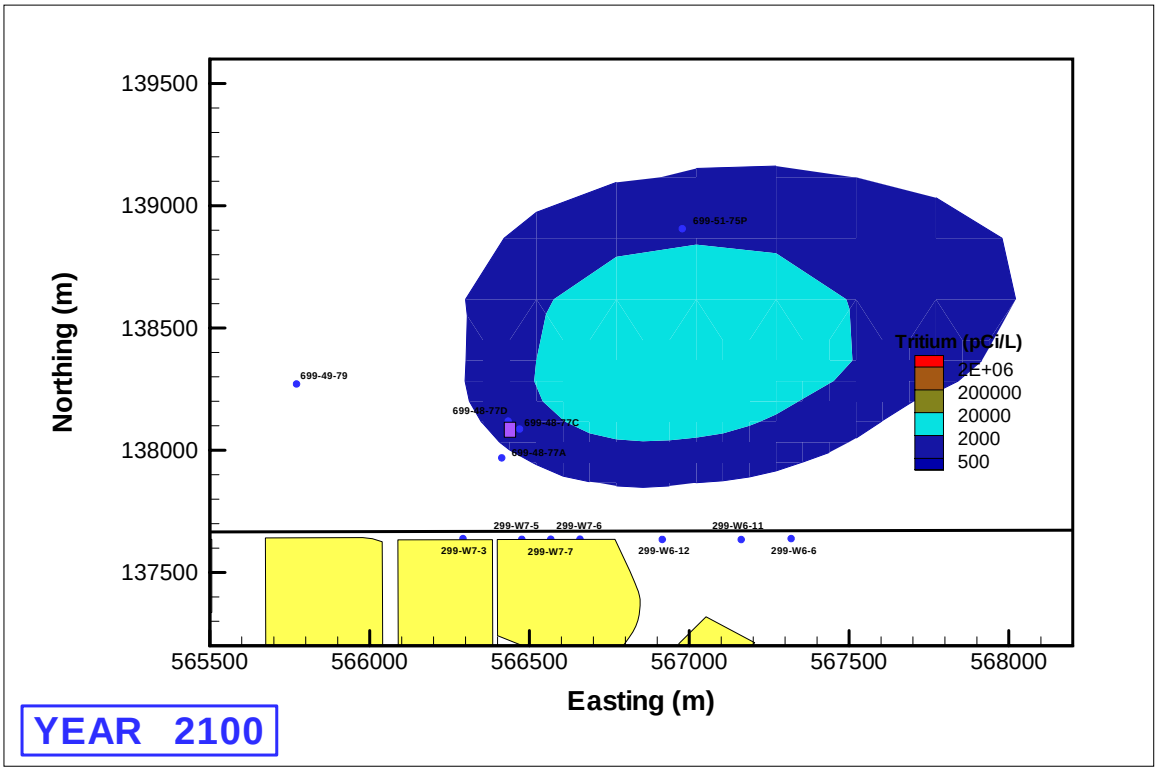
139500
139000
138500
138000
137500
Northing (m)
565500
566000
566500
567000
567500
568000
Easting (m)
699-51-75P
699-49-79
699-48-77D
699-48-77C
699-48-77A
299-W7-5
299-W7-6
299-W6-11
299-W7-3
299-W7-7
299-W6-12
299-W6-6
Tritium (pCi/L)
2E+06
200000
20000
2000
500
YEAR 2100

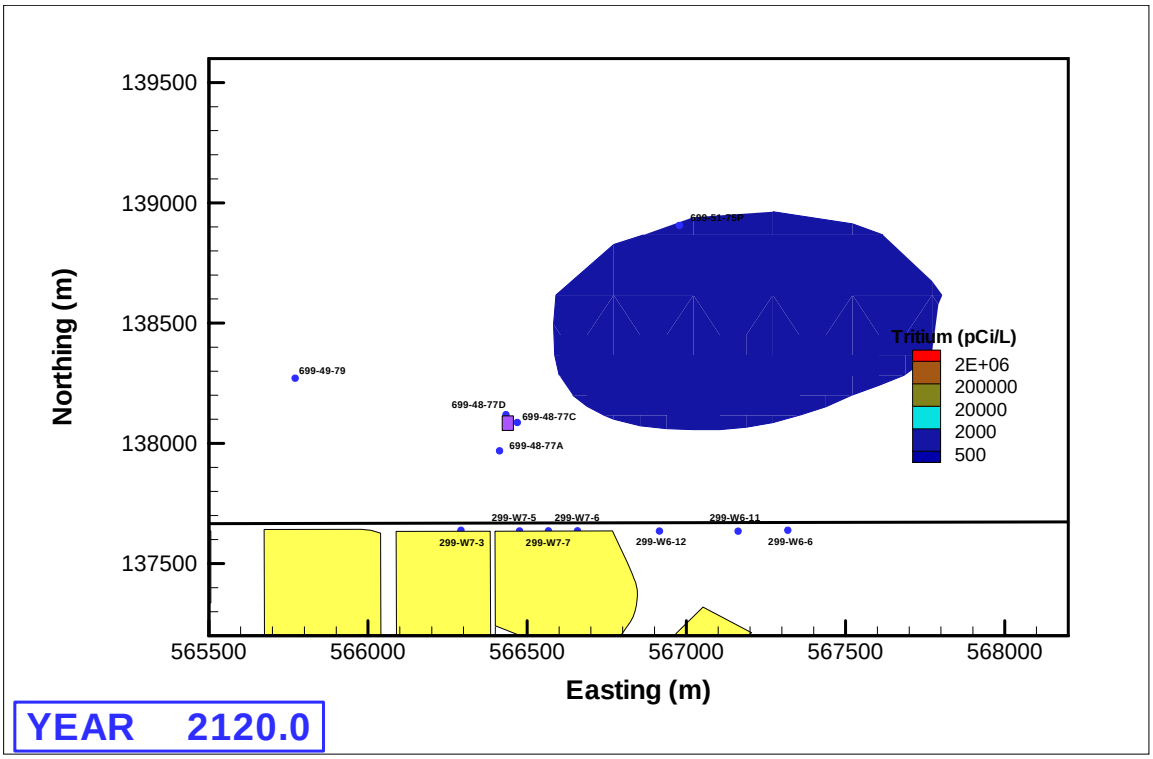
139500
139000
138500
138000
137500
Northing (m)
565500
566000
566500
567000
567500
568000
Easting (m)
699-51-75P
699-49-79
699-48-77D
699-48-77C
699-48-77A
299-W7-5
299-W7-6
299-W6-11
299-W7-3
299-W7-7
299-W6-12
299-W6-6
Tritium (pCi/L)
2E+06
200000
20000
2000
500
YEAR 2120.0

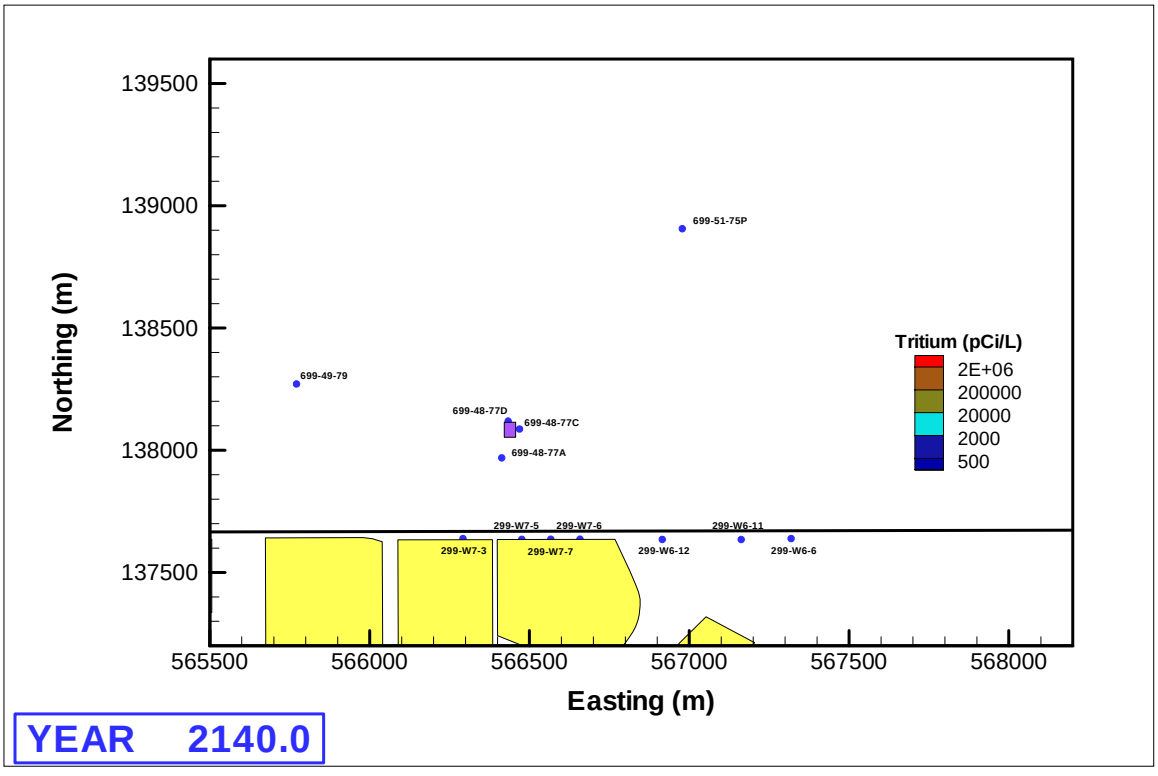
139500
139000
138500
138000
137500
Northing (m)
565500
566000
566500
567000
567500
568000
Easting (m)
699-51-75P
699-49-79
699-48-77D
699-48-77C
699-48-77A
299-W7-5
299-W7-6
299-W6-11
299-W7-3
299-W7-7
299-W6-12
299-W6-6
Tritium (pCi/L)
2E+06
200000
20000
2000
500
YEAR 2140.0

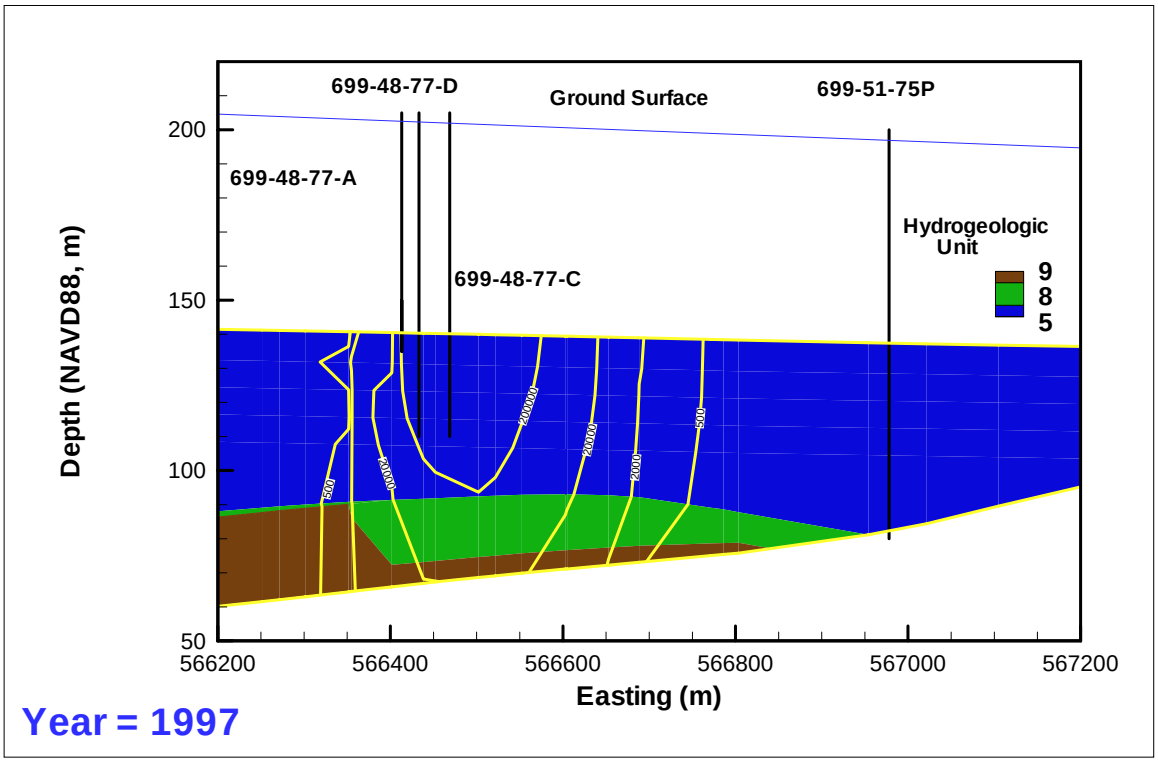
699-48-77-D
Ground Surface
699-51-75P
699-48-77-A
699-48-77-C
Hydrogeologic Unit
9
8
5
Depth (NAVD88, m)
200
150
100
50
566200
566400
566600
566800
567000
567200
Easting (m)
Year = 1997

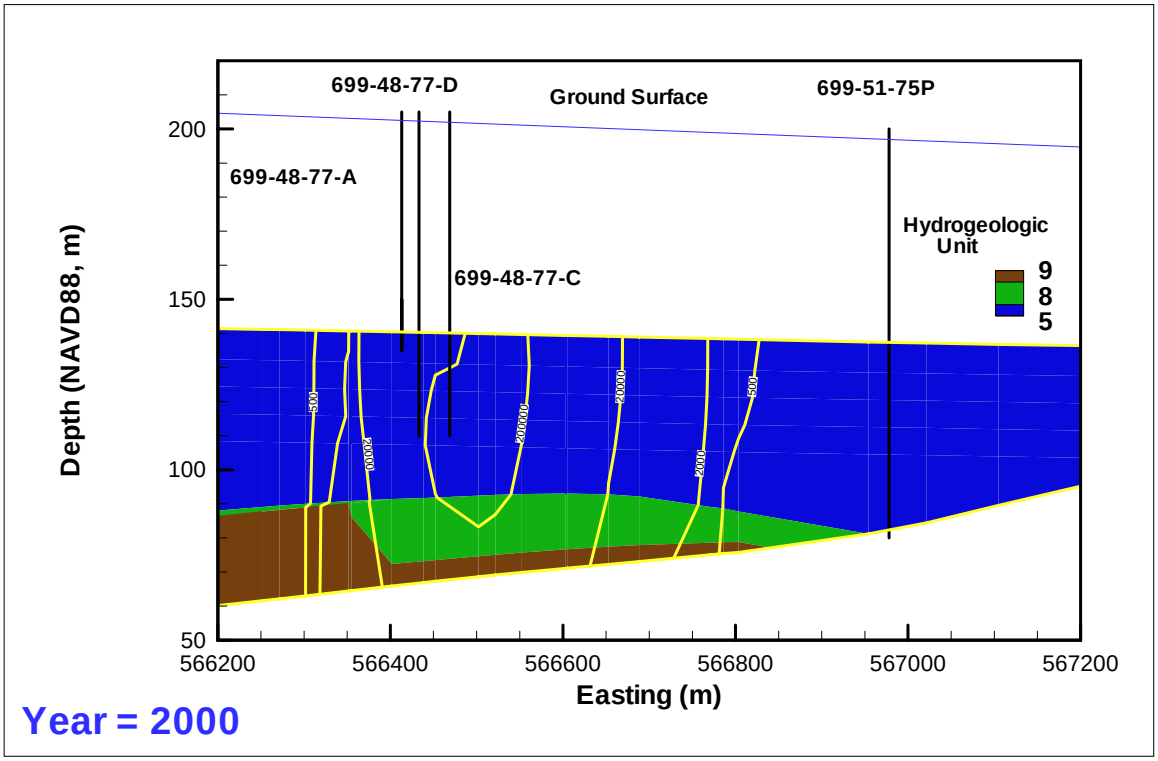
699-48-77-D
Ground Surface
699-51-75P
699-48-77-A
699-48-77-C
Hydrogeologic Unit
9
8
5
Depth (NAVD88, m)
200
150
100
50
566200
566400
566600
566800
567000
567200
Easting (m)
Year = 2000

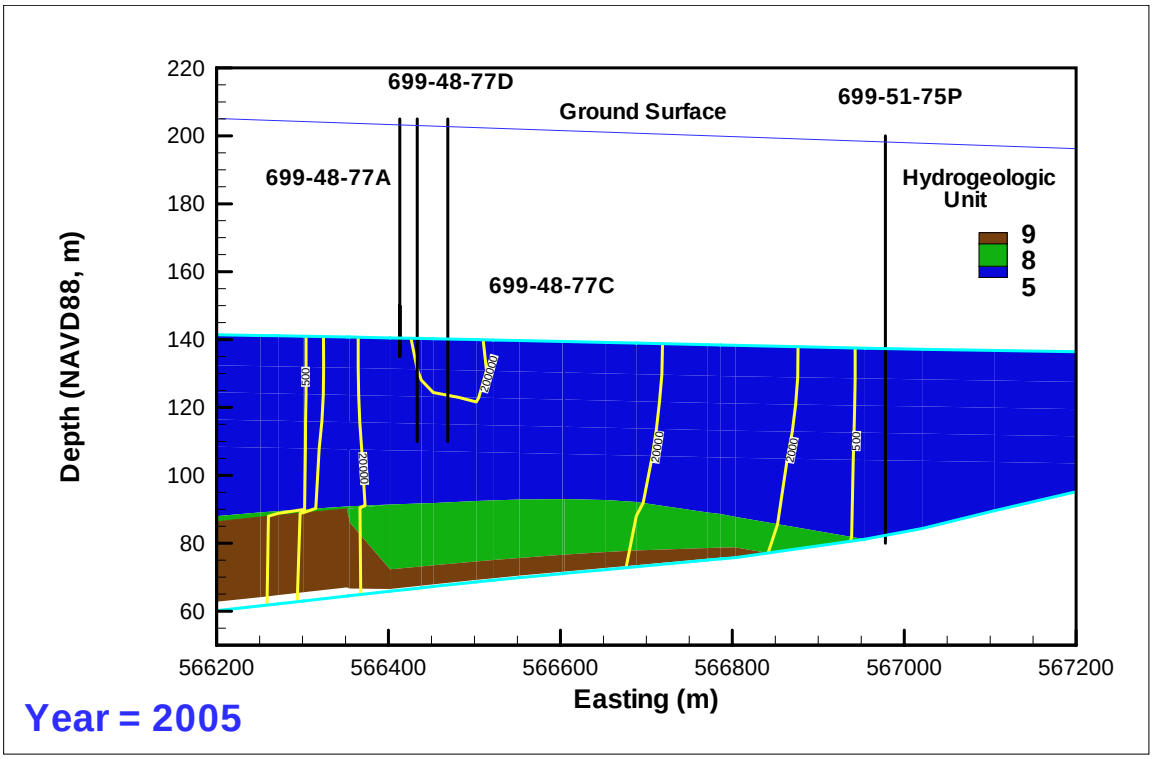
699-48-77D
Ground Surface
699-51-75P
699-48-77A
Hydrogeologic Unit
9
8
5
699-48-77C
Depth (NAVD88, m)
220
200
180
160
140
120
100
80
60
566200
566400
566600
566800
567000
567200
Easting (m)
Year = 2005

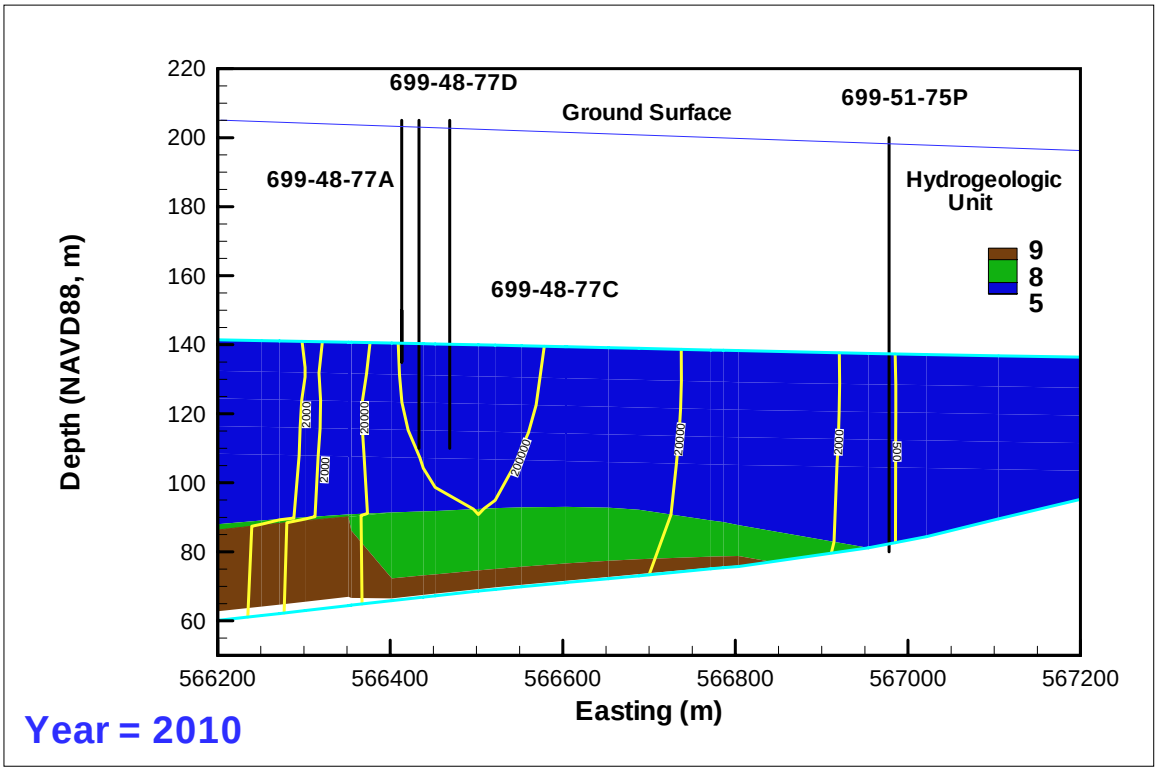
699-48-77D
Ground Surface
699-51-75P
699-48-77A
Hydrogeologic Unit
9
8
5
699-48-77C
Depth (NAVD88, m)
220
200
180
160
140
120
100
80
60
566200
566400
566600
566800
567000
567200
Easting (m)
Year = 2010

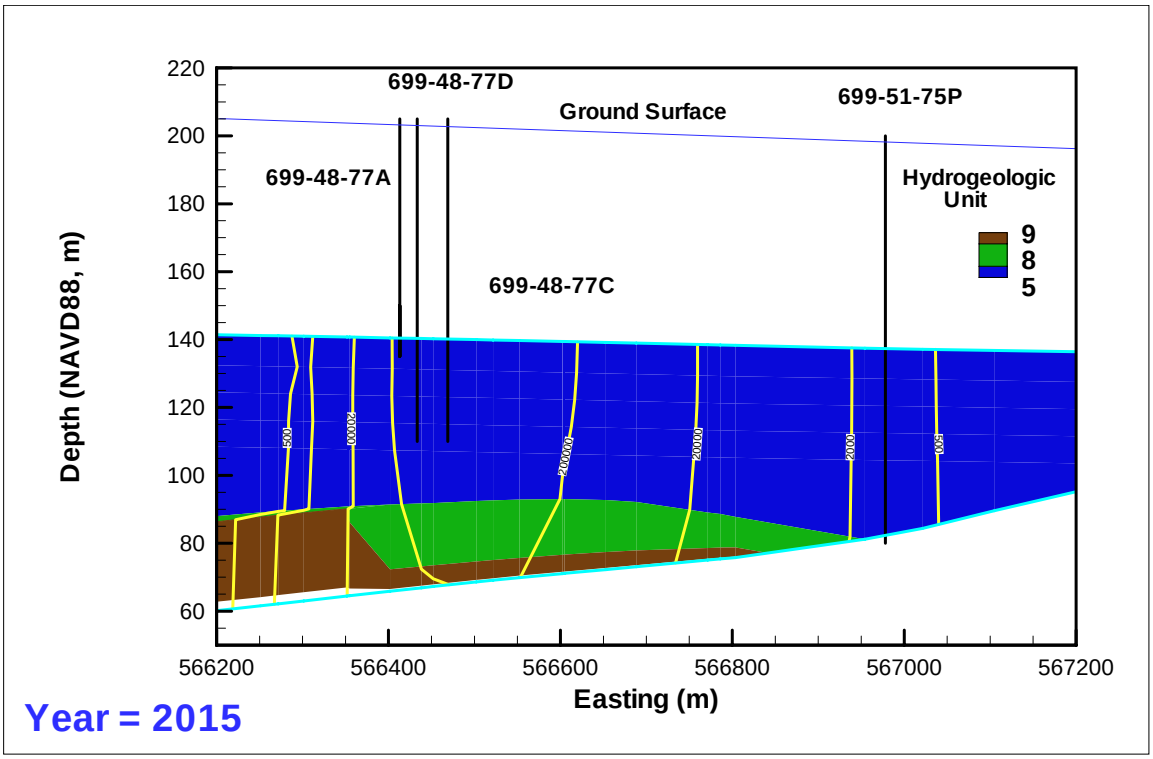
699-48-77D
Ground Surface
699-51-75P
699-48-77A
Hydrogeologic Unit
9
8
5
699-48-77C
Depth (NAVD88, m)
220
200
180
160
140
120
100
80
60
566200
566400
566600
566800
567000
567200
Easting (m)
Year = 2015

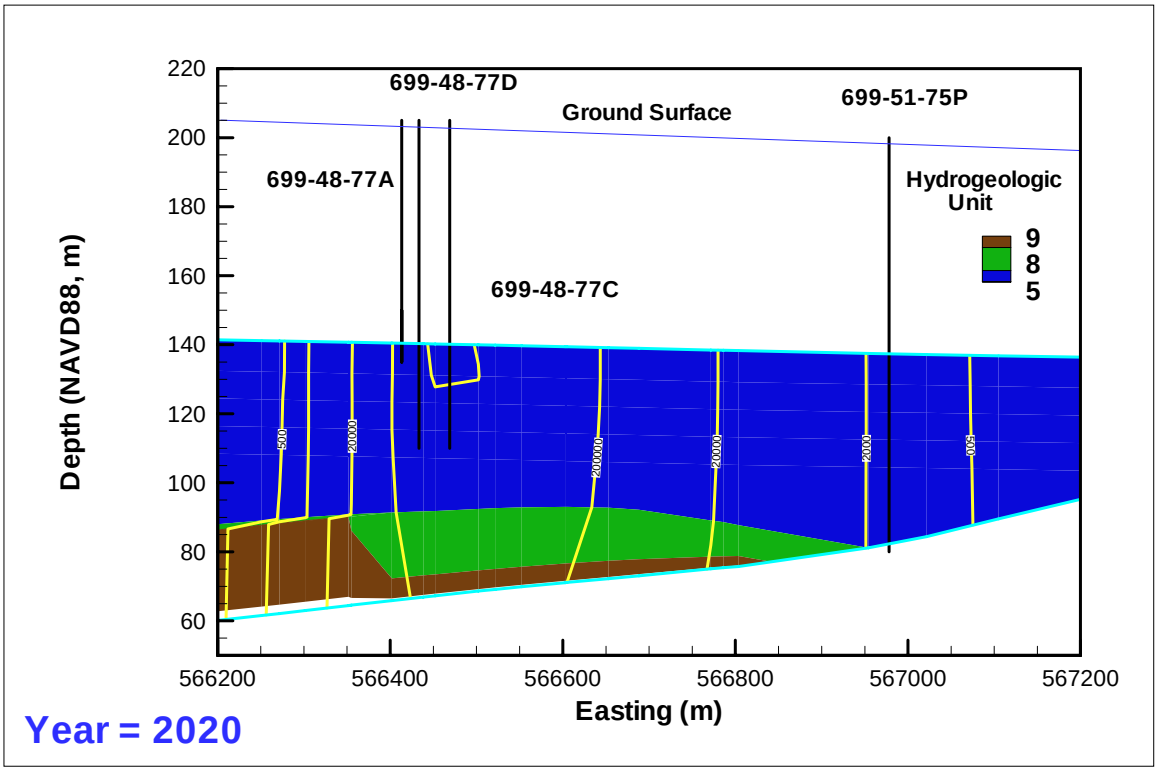
699-48-77D
Ground Surface
699-51-75P
699-48-77A
Hydrogeologic Unit
9
8
5
699-48-77C
Depth (NAVD88, m)
220
200
180
160
140
120
100
80
60
566200
566400
566600
566800
567000
567200
Easting (m)
Year = 2020

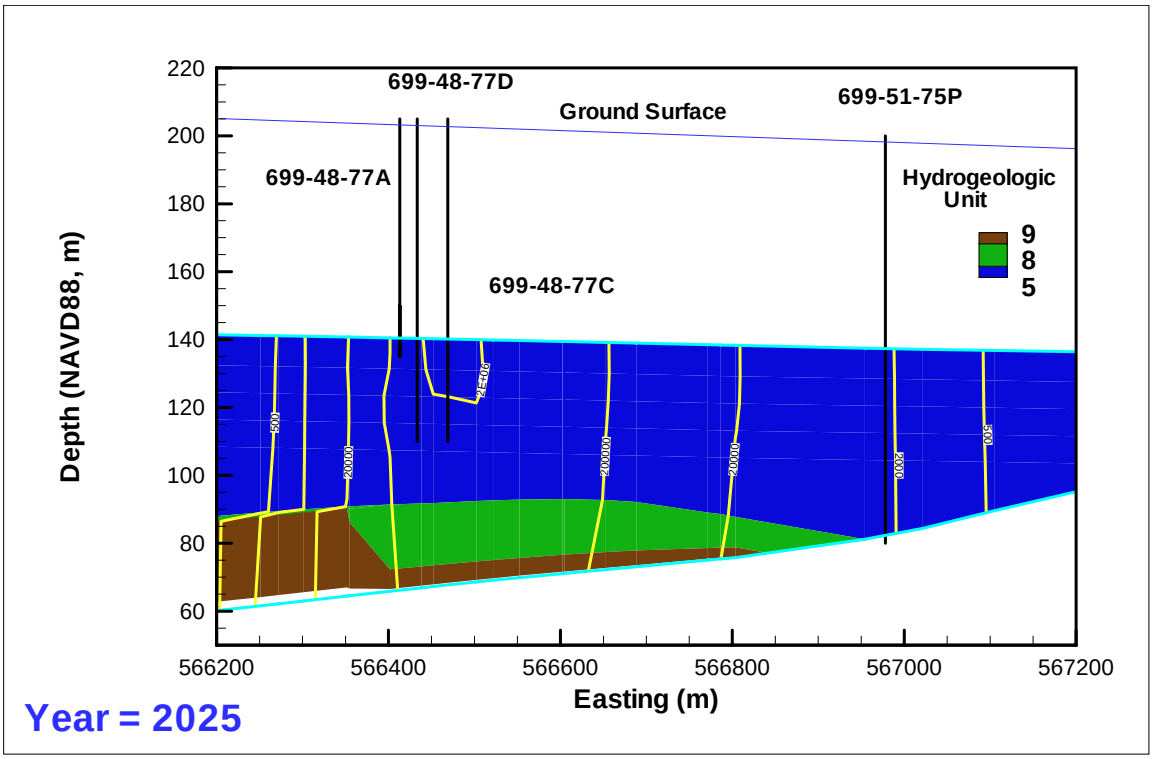
699-48-77D
Ground Surface
699-51-75P
699-48-77A
Hydrogeologic Unit
9
8
5
699-48-77C
Depth (NAVD88, m)
220
200
180
160
140
120
100
80
60
566200
566400
566600
566800
567000
567200
Easting (m)
Year = 2025

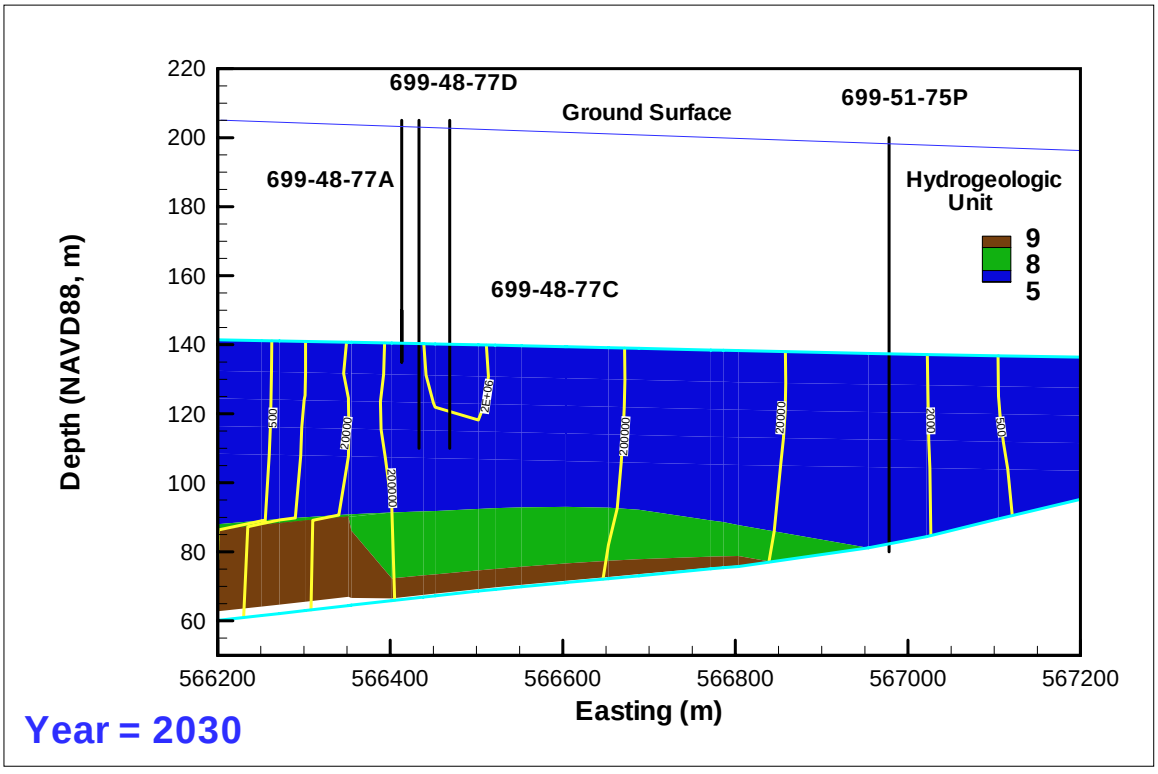
699-48-77D
Ground Surface
699-51-75P
699-48-77A
Hydrogeologic Unit
9
8
5
699-48-77C
Depth (NAVD88, m)
220
200
180
160
140
120
100
80
60
566200
566400
566600
566800
567000
567200
Easting (m)
Year = 2030

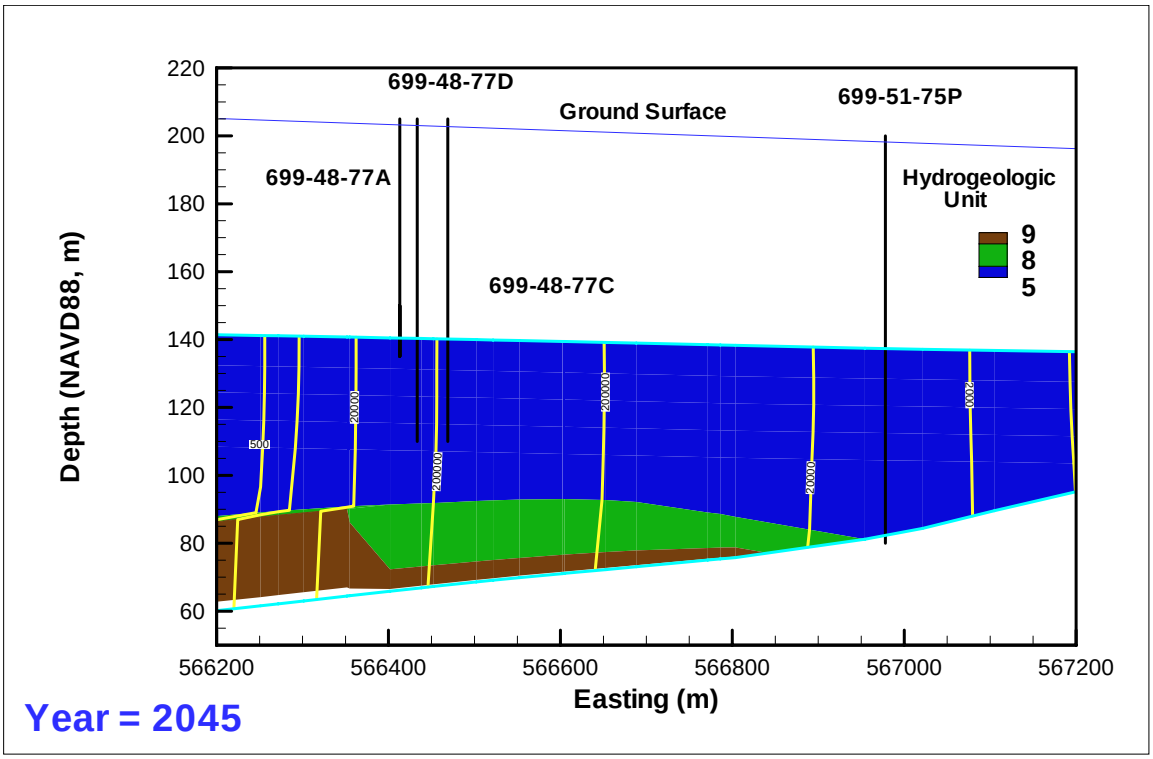
699-48-77D
Ground Surface
699-51-75P
699-48-77A
Hydrogeologic Unit
9
8
5
699-48-77C
Depth (NAVD88, m)
220
200
180
160
140
120
100
80
60
566200
566400
566600
566800
567000
567200
Easting (m)
Year = 2045

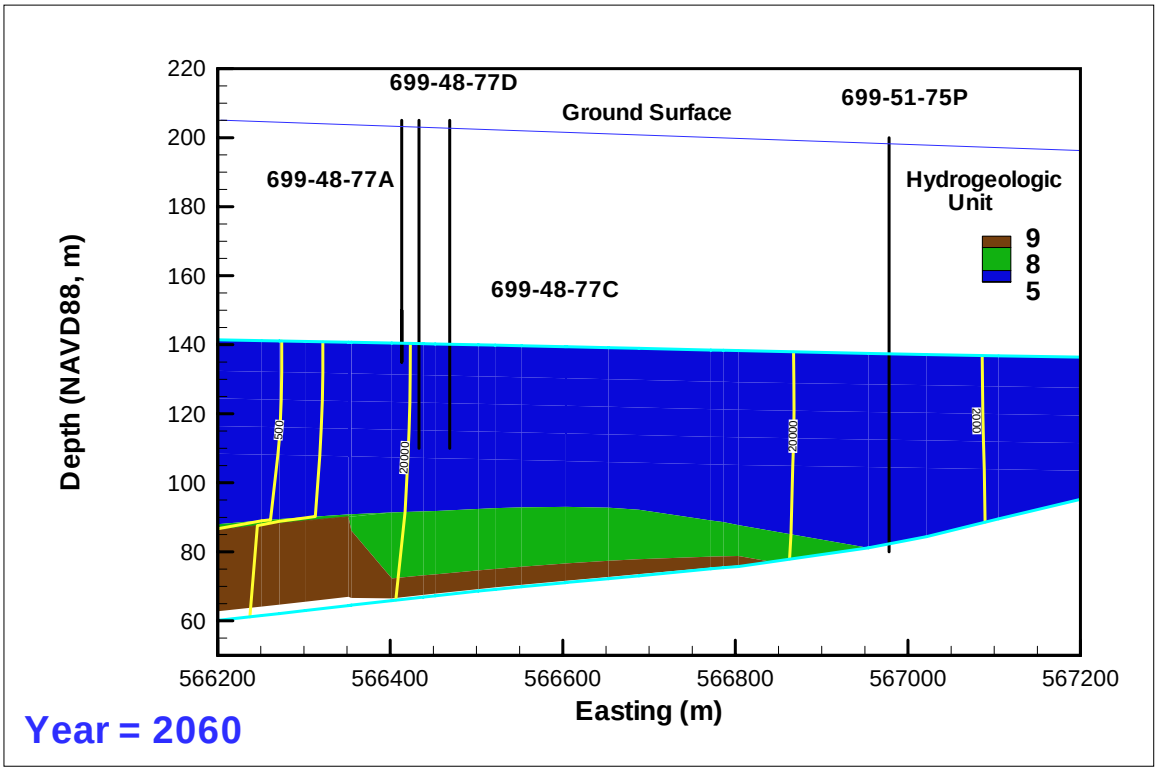
699-48-77D
Ground Surface
699-51-75P
699-48-77A
Hydrogeologic Unit
9
8
5
699-48-77C
Depth (NAVD88, m)
220
200
180
160
140
120
100
80
60
566200
566400
566600
566800
567000
567200
Easting (m)
Year = 2060

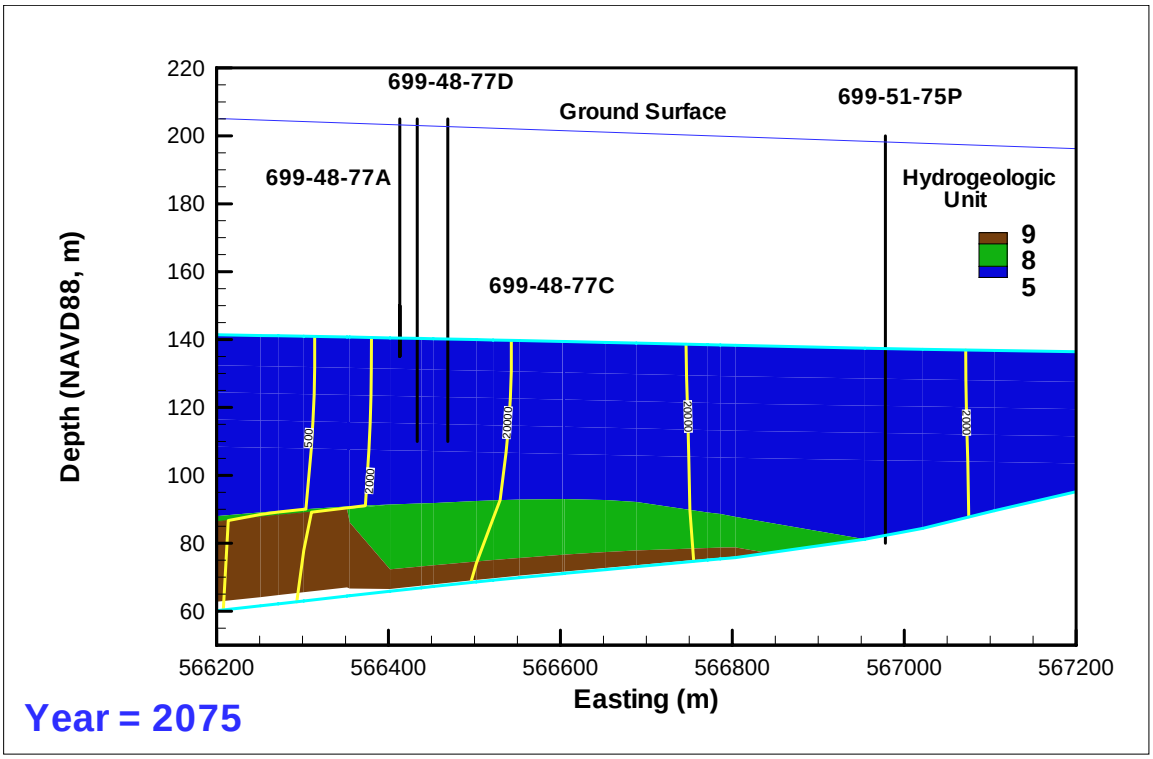
699-48-77D
Ground Surface
699-51-75P
699-48-77A
Hydrogeologic Unit
9
8
5
699-48-77C
Depth (NAVD88, m)
220
200
180
160
140
120
100
80
60
566200
566400
566600
566800
567000
567200
Easting (m)
500
2000
20000
40000
6000
Year = 2075

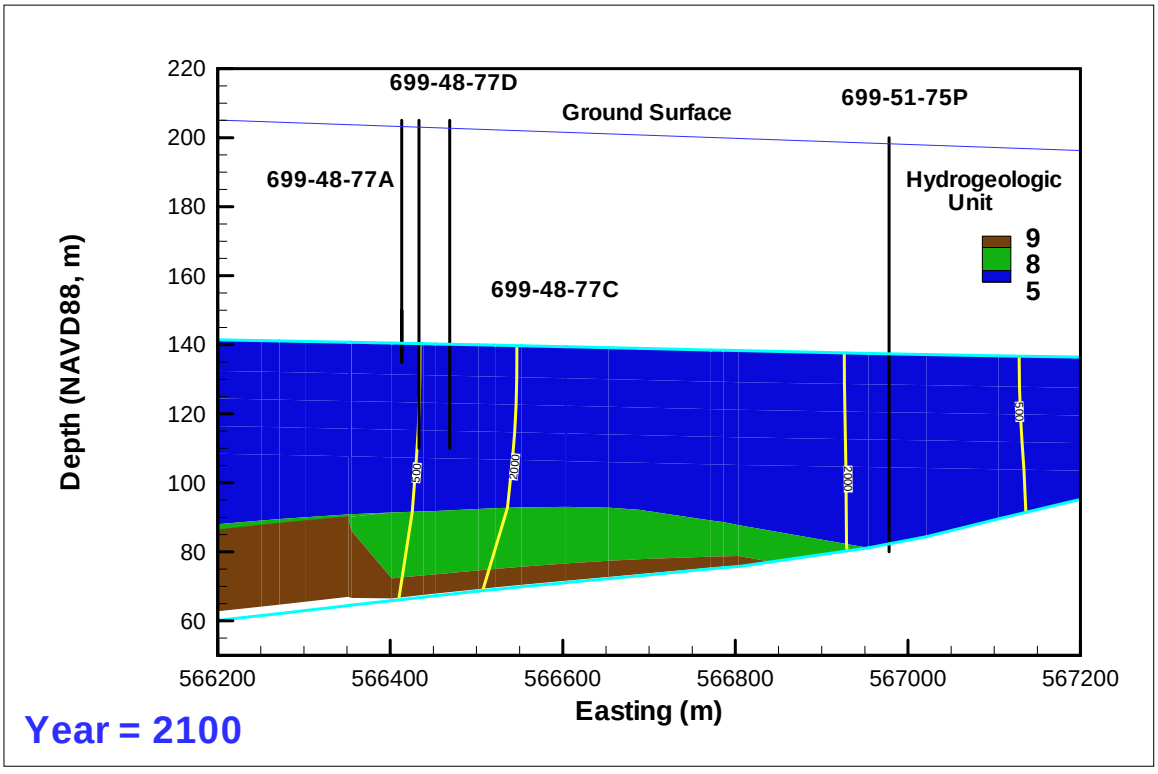
699-48-77D
Ground Surface
699-51-75P
699-48-77A
Hydrogeologic Unit
9
8
5
699-48-77C
Depth (NAVD88, m)
220
200
180
160
140
120
100
80
60
566200
566400
566600
566800
567000
567200
Easting (m)
500
2000
20000
40000
6000
Year = 2100

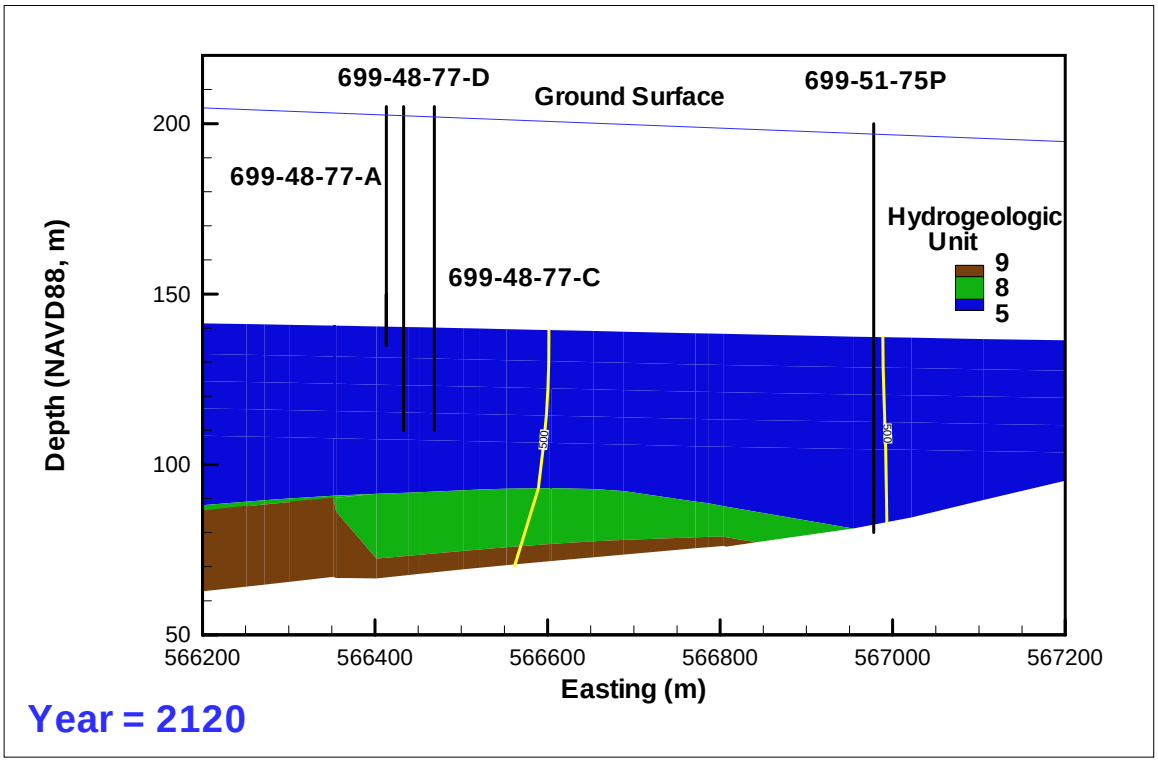
699-48-77-D
Ground Surface
699-51-75P
699-48-77-A
699-48-77-C
Hydrogeologic Unit
9
8
5
Depth (NAVD88, m)
200
150
100
50
566200
566400
566600
566800
567000
567200
Easting (m)
Year = 2120

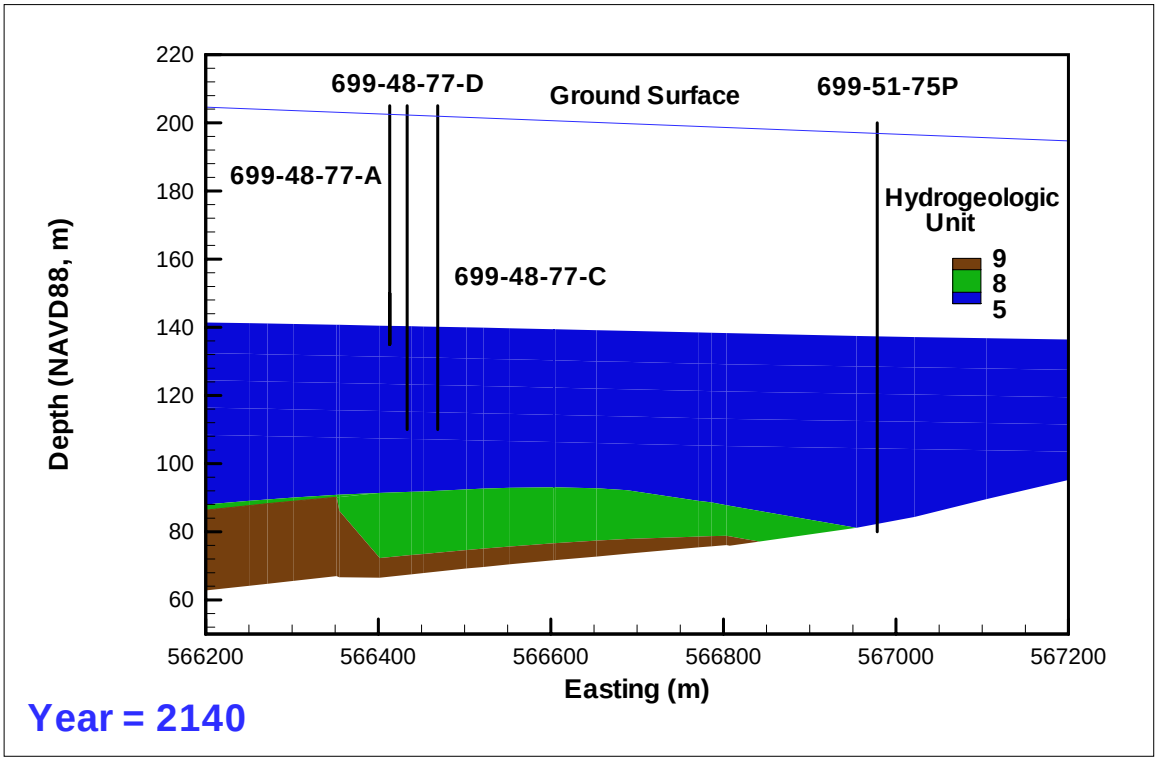
699-48-77-D
Ground Surface
699-51-75P
699-48-77-A
699-48-77-C
Hydrogeologic Unit
9
8
5
Depth (NAVD88, m)
220
200
180
160
140
120
100
80
60
566200
566400
566600
566800
567000
567200
Easting (m)
Year = 2140